4.0 REACTOR
TABLE OF CONTENTS

4.0 REACTOR
TABLE OF CONTENTS

4.0 REACTOR
TABLE OF CONTENTS

4.0 REACTOR
LIST OF TABLES

Table

4.0 REACTOR
LIST OF FIGURES

4.0 REACTOR
LIST OF FIGURES

Figure

DRAWINGS CITED IN THIS CHAPTER*

*The listed drawings are included as "General References" only; i.e., refer to the drawings to obtain additional detail or to obtain background information. These drawings are not part of the UFSAR. They are controlled by the Controlled Documents Program.

DRAWING*	SUBJECT
M-4	General Arrangement, Ground Floor Plan
M-34	Diagram of Control Rod Drive Hydraulic Piping Unit 2
M-365	Diagram of Control Rod Drive Hydraulic Piping Unit 3

4.0 REACTOR

This chapter includes the following sections:

Section	Description
4.1	Summary description
4.2	Fuel system design
4.3	Nuclear design
4.4	Thermal and hydraulic design
4.5	Reactor materials
4.6	Functional design of reactivity control systems

4.1 SUMMARY DESCRIPTION

The equipment and evaluations presented in this chapter are applicable to either Unit 2 or Unit 3.

Section 4.2 describes the design of fuel assemblies used in Dresden Units 2 and 3, including the SVEA-96 Optima2 fuel provided by Westinghouse Electric Company (WEC) and GE14 fuel provided by Global Nuclear Fuel (GNF). Section 4.2 also describes the use of Gadolinia (Gd_2O_3) as burnable neutron absorber in UO_2 fuel.

Section 4.3 presents a discussion of nuclear design and reactor stability, including discussions of reactivity coefficients and their contributions to stability.

Section 4.4 presents a summary of the thermal and hydraulic design of the reactor core and the reactor coolant system (including a description of the power-flow map). The presentation stresses the safety limit minimum critical power ratio (MCPR), the operating limit MCPR, and the maximum linear heat generation rate (MLHGR). The MCPR calculation methodology, the critical power correlations, and the associated uncertainties are discussed. In order to provide reference data for the Technical Specifications, the core thermal power limit at low-pressure/low-flow and the Reactor Protection System Instrumentation settings are discussed. The results of transient analyses show a high degree of effectiveness of the protection system in preventing the reactor from approaching conditions of safety concern.

The EPU analyses evaluated several Equipment Out-of-Service (EOOS) operating flexibility options (Reference 1). For a discussion of these EOOS options, see cycle specific reload documentation.

Steady operation can be at any power level which satisfies the following requirements:

A. Local MCPR, LHGR limits and the maximum average planar linear heat generation rate (MAPLHGR) limits are satisfied, and

B. Transient and accident analysis results have been shown to be valid for power levels up to the level in question.

By establishing approved local thermal limits for the fuel, it is possible to permit power outputs up to the licensed power level whenever the power distribution is favorable.

Principal core and fuel design data are summarized in Table 4.1-1. Principal nuclear design limits, targets, and typical values are summarized in Table 4.1-2. Principal thermal and hydraulic design values are summarized in Table 4.1-3.

Reactor vessel internals are described in Section 3.9.5. Reactor internals materials are described in Section 4.5.2.

Section 4.6 addresses the design of reactivity control systems, including the control rod drive system, and the design of the control rods.

4.1.1 References

1. "Dresden 2 and 3, Quad Cities 1 and 2 Equipment Out-of-Service and Legacy Fuel Transient Analysis," General Electric Company, GE-NE-J11-03912-00-01-R3, September 2005.

Table 4.1-1

CORE AND FUEL DESIGN

Core	
Equivalent core diameter, in.	182.2
Circumscribed core diameter, in.	189.7
Core lattice pitch (control cell), in.	12.0
Number of fuel assemblies in the core	724
Fuel Assembly*	
	*
Fuel rod array	*
Fuel rod pitch, in.	*
Channel material	Zircaloy-2 or Zircaloy-4
Approximate UO_2 weight per fuel assembly, lb.	*
Approximate Fuel assembly weight, lb	*
Number of fuel rods	*
Number of water rods	*
Water/$UO_{\{2\}}$ volume ratio (cold)	*
Heat transfer surface area/fuel assembly, ft^2	*
Fuel Rod, Cold*	
	*
Fuel pellet diameter, in.	*
Cladding thickness, in.	*
Cladding outside diameter, in.	*
Active fuel length, in.	*
Length of gas plenum, in.	*
Fuel material	*
Cladding material	*
Fill gas	He
Fill gas pressure, atm	*

* Values are GNF and Westinghouse proprietary. Values for GE14 fuel can be found in NFM-DIR-00-081. Values for SVEA-96 Optima2 fuel can be found in WCAP-15942-P-A.

Table 4.1-1 (Continued)

CORE AND FUEL DESIGN

Movable Control Rods	
Number of control rods in the core	177
Shape	Cruciform
Pitch, in.	12.0
Stroke, in.	144
Width, in.	9.8 (Nominal)
Control length, in.	143
Control material	$B_{\{4\}}C$ and hafnium
Burnable Neutron Absorber	
Control material	$Gd_{\{2\}}O_{\{3\}}$
Location	Mixed with $UO_{\{2\}}$ in several fuel rods per fuel assembly
Concentration	Location and reload dependent

Table 4.1-2

NUCLEAR DESIGN LIMITS, TARGETS, AND TYPICAL VALUES

Reactivity Control			
Cold shutdown k_{eff}, rod of maximum worth stuck out fully - design target	0.99		
Standby liquid control shutdown Δk_{eff}	0.01		
Approximate Reactivity Coefficients			
	Cold	Hot (no voids)	Operating
Moderator temperature coefficient, (Δk/k)/°F	-4×10^{-5}	-17.0×10^{-5}	
Moderator void coefficient, (Δk/k)/% void	$< -0.6 \times 10^{-3}$	-1.0×10^{-3}	-1.4×10^{-3}
Fuel temperature (Doppler) coefficient, (Δk/k)/°F	-1.2×10^{-5}	-1.2×10^{-5}	-1.2×10^{-5}
Power coefficient for xenon stability	More negative than -0.01 (Δk/k)/(ΔP/P)		
Typical Excursion Parameter Values			
Prompt neutron lifetime (λ^*)	48.9 μs		
Effective delayed neutron fraction ($-\beta$ 1) - at 0 MWd/t - at 10,000 MWd/t	 0.0072 0.0056		

Table 4.1-3

THERMAL AND HYDRAULIC DESIGN

Design Thermal Output, MWt		2957
Reactor pressure (dome), psia		1020
Steam flowrate, lb/hr		11.713x106
Recirculation flowrate, lb/hr		98x106
Fraction of power appearing as heat flux		0.971
Core subcooling, BTU/lb		24.1
Core average void fraction, active coolant		0.364
	GE-14	SVEA-96 Optima2
Safety Limit Minimum Critical Power Ratio (SLMCPR)	*	*
Maximum steady state LHGR (beginning of life), kW/ft	13.4	**

* Value is cycle-specific and can be found in cycle-specific reload licensing reports.
** Value is Westinghouse proprietary and can be found in WCAP-15942-P-A.

4.2 FUEL SYSTEM DESIGN

4.2.1 Design Bases

4.2.1.1 Fuel Assemblies

The fuel rods and assemblies are designed to assure, in conjunction with the core, nuclear, thermal, hydraulic, and unit equipment characteristics, the nuclear instrumentation, and the reactor protection system, that fuel damage will not occur during normal operation or during transients caused by any single equipment malfunction or any single operator error. Fuel damage is defined as perforation of the fuel cladding which would permit the release of fission products to the reactor coolant.

The mechanisms which can cause fuel damage in reactor transients are as follows:

A. Severe overheating of the fuel cladding caused by inadequate cooling. For design purposes, the critical heat flux, or equivalently, the critical power (the onset of the transition from nucleate boiling to film boiling), is conservatively defined as the limit. However, experimental data indicate that fuel damage will not occur until well into the film boiling regime.

B. Fracture of the fuel cladding due to strain caused by relative expansion of the UO_2 pellet. For design purposes, a value of 1% plastic strain of Zircaloy cladding is used as the limit. Below this value, fuel damage due to overstraining of the fuel cladding is not expected to occur.

Applicable Westinghouse CPR correlations that are NRC approved are applied to determine the MCPR Safety Limit (SLMCPR) for the Westinghouse fuel. In addition, Westinghouse applies the approved methodology in Reference 16 to establish CPR correlations and conservative factors, which are used to determine the Operating Limit MCPR (OLMCPR) for any co-resident non-Westinghouse fuel that may be present in the core during the cycle operation.

The effects of fuel densification are considered in the fuel performance analysis. A decrease in the length of pellets could result in the formation of axial gaps in the column of fuel pellets within a fuel rod. A decrease in pellet radius could result in the increase in the radial clearance between the fuel pellet and the fuel rod cladding. The following four principal effects are associated with the dimensional changes resulting from densification:

A. Axial gaps produce a local increase in the neutron flux and generate a local power spike;

B. A decrease in pellet length directly results in a proportional increase in the linear heat generation rate (LHGR);

C. If relatively large axial gaps form, creepdown of the cladding later in life may lead to the collapse of the cladding into the gaps; and

D. Decreased pellet radius results in decreased pellet-clad thermal conductance (gap conductance) which increases the fuel pellet temperature and stored energy and decreases the heat transfer capability of the fuel rod.

To account for these four effects, the analytic model for fuel densification consists of four parts: power spike model, linear heat generation model, cladding creep collapse model, and stored energy model. These models can be used to conservatively evaluate the effects of fuel densification.

The potential problems of channel bow in BWRs that could impact local peaking and reduce available minimum critical power ratio (MCPR) margin, as addressed in IE Bulletin 90-02, have been considered. Since IE Bulletin 90-02, analysis for reload fuel has included the effects of single bundle lifetime channel bow.

GNF includes the effects of single bundle lifetime channel bow by using a generic methodology which adjusts the bundle R-factors as a function of core-average channel bow. The bundle R-factors are weighted peaking factors used in the GEXL correlation for CPR determination and constitute an input to the online MCPR calculation. By adjusting the R-factor, the MCPR values calculated by the plant computer are adjusted accordingly to account for the effects of channel bow.

Similarly, the WEC reload analysis includes the effects of channel bow by adjusting the bundle R-factor.

EGC's current channel management strategy does not include the reuse of channels on new BWR fuel assemblies.

GNF and WEC have developed emergency core cooling system (ECCS) analytic codes for evaluating the effects of loss-of-coolant accidents (LOCA) in accordance with 10 CFR 50, Appendix K, to assure that the peak cladding temperature (PCT) of the hottest fuel rod in the core will not exceed the NRC-imposed PCT limit of 2200°F under postulated accident conditions. See Section 6.3 for ECCS discussions and Section 15.6.5 for LOCA analysis.

4.2.1.2 Control Rods

Design information for control rods is contained in Section 4.6.

4.2.1.3 Burnable Neutron Absorber

The primary design requirement for the reactivity effect of the burnable neutron absorber (gadolinia) is that it produces an adequate shutdown margin. Thus, for design goal purposes, the calculated k_{eff} does not exceed the design target (see Section 4.3.2.1.3) with the control rod of maximum worth fully withdrawn and all others fully inserted, for a core temperature and an exposure chosen to maximize core reactivity.

4.2.2 Description and Design Drawings

The fuel assemblies used at Dresden Unit 3 include GE14 fuel assemblies supplied by GNF and SVEA-96 Optima2 fuel assemblies supplied by WEC. A detailed description of the GE and WEC fuel designs is contained in References 13 and 17 respectively.

4.2.2.1 Fuel Assemblies

The SVEA-96 Optima2 fuel bundle consists of 96 rods, arranged in four 5x5-1 sub-bundles. The sub-bundles are separated by a cruciform internal structure (water cross) in the channel. Each sub-bundle is assembled as a separate unit with its own top and bottom tie plates. The sub-bundles are inserted into the channel from the top and are supported at the bottom by a stainless steel inlet piece bolted to the channel. The inlet piece consists of a transition piece and bottom support with an integrated debris filter. The water cross has a square central channel and smaller water channels in

each of the four wings to accommodate non-boiling water during operation. The design includes eight 2/3-length and four 1/3-length part-length rods. The positions of the part-length rods have been chosen to maximize shutdown margin and to optimize the critical power performance. The fuel assembly is lifted by a handle connected to the top end of the channel, and is supported against adjacent assemblies in the core by a double leaf spring.

Typical drawings of the SVEA-96 Optima2 fuel assembly and lattice arrangement are shown in Figures 4.2-6 and 4.2-7 respectively.

The SVEA-96 Optima2 fuel is designed for mechanical, nuclear, and thermal-hydraulic compatibility with other fuel designs. The design has a similar outer channel with four internal sub-channels and axial Gadolinia loading as in previous designs. In addition, Optima2 incorporates a debris filter that is cast into the lower tie plate.

The GE14C/GE14 fuel design consists of 92 fuel rods and two large central water rods contained in a 10 x 10 array. The 10 x 10 array provides more heat transfer surface area than the previous 8x8 and 9x9 designs. The two water rods encompass eight fuel rod positions. Fourteen of the fuel rods are designated as part length rods. Eight fuel rods are used as tie rods. The rods are spaced and supported by the upper and lower tie plates and eight spacers over the length of the fuel rods. This assembly is encased in a thick-thin walled fuel channel. Finger springs control the coolant flow between the lower tie plate and the channel. A schematic drawing of the bundle is shown in Figure 4.2-4. A typical core lattice unit is shown in Figure 4.2-5.

The fuel rods consist of high-density ceramic uranium dioxide or urania-gadolinia fuel pellets stacked within zirconium lined Zircaloy-2 cladding. The fuel rod is prepressurized with helium.

There are 78 full-length fuel rods in the GE14 lattice. Fourteen part length rods (PLRs) are selectively located in the lattice to reduce two-phase pressure drop. These PLRs enable this design to match the pressure drop and improve stability performance of currently operating fuel designs.

The GE14 fuel is designed for mechanical, nuclear, and thermal-hydraulic compatibility with the other fuel designs. The design includes similar thick corner/thin wall channel and axial Gd loading as present in the previous design. In addition, the GE14 incorporates a debris filter that is cast into the lower tie plate.

A more complete description of the GE14 fuel assembly design is contained in Reference 13.

The GE14 fuel was first introduced into the Dresden Unit 2 and 3 reactor cores beginning with Unit 2 Cycle 18. The specific name of the fuel assembly used at Dresden is GEl4C. This fuel assembly has minor design changes compared to the other GE14 designs. The GE14C fuel design will be referred to as either GE14 or GE14C in the UFSAR and Technical Specifications.

Zircaloy 2 or Zircaloy-4 channel encloses the fuel bundle and performs the following functions:

A. It provides a barrier to separate the two parallel flow paths: one to cool the fuel bundle and the other to suppress steam voids in the bypass region between channels;

B. It guides the control rods; and

C. It provides rigidity and protection for the fuel rods.

The channel makes a sliding seal fit on the lower tieplate surface and is attached to the upper tieplate by the channel fastener's cap screw (spring clip). The fuel channel provides a smooth surface with no protrusions as a bearing surface for the control rod rollers or pads.

An orifice, mounted in the fuel support casting upon which the fuel assembly rests, establishes the relative flow per channel.

Proper orientation of fuel assemblies in the reactor core is readily verified by visual observation and is assured by procedural requirements during core loading verification. There are several ways of confirming proper fuel assembly orientation:

A. All assembly serial numbers are readable from the center of the cell;

B. The channel fastener spring-clip assemblies are located adjacent to the center of the control rod;

C. The protrusions (lugs) on the assembly handles all point toward the adjacent control rod; (Optima 2 fuel does not have lugs on the assembly handle)

D. There is cell-to-cell symmetry; and

E. All channel spacing buttons are adjacent to the control rod blades.

4.2.2.2 Control Rods

Description and drawings of the control rods are contained in Section 4.6.

4.2.2.3 Burnable Neutron Absorber

4.2.2.3.1 Description of Design

The burnable neutron absorber, in the form of gadolinia (Gd_2O_3) may be present in all reload fuel assemblies.

The gadolinia is mixed uniformly with UO_2 in the fuel pellets in selected lengths of a few rods in the fuel assemblies. This burnable absorber is initially in a highly self-shielded configuration, leading to a near linear rate of change of control effect during the cycle.

4.2.2.3.2 Nuclear Analysis

GNF/GE methods and analysis for reloads are discussed in Section 4.3.3 and GESTAR II[14]. For SVEA-96 Optima2 reloads, both WEC nuclear methods, CASMO-4 and MICROBURN-B2 are used.

WEC nuclear methods and analysis for reloads with SVEA 96 Optima2 fuel are discussed in Reference 16. The burnup in a gadolinia rod is calculated using the WEC PHOENIX computer code. The lattice calculations including the effect of the gadolinia on power peaking and reactivity are performed with the PHOENIX[18] code. PHOENIX generates detailed pin-by-pin nuclear data, that is then averaged to obtain lattice physics constants for use in the core simulator code. Reactor core calculations are performed with the WEC POLCA7[18] code. POLCA is a three-dimensional code for simulating the neutronic, thermal, and hydraulic behavior of a reactor core under steady-state conditions. The code solves the two-group neutron diffusion equation and couples it to thermal-hydraulic equations.

The lattice calculations including the effect of the gadolinia on power peaking and reactivity are performed with CASMO-4[11]. CASMO-4 is a multigroup two-dimensional transport theory code. CASMO-4 generates lattice number densities and macroscopic two-group cross sections for the core simulator code.

Reactor core calculations are performed by Exelon with MICROBURN-B2, a three-dimensional core simulator code. MICROBURN-B2[11] performs a microscopic depletion of the gadolina and other key nuclear isotopes on a nodal basis with pin power reconstruction capability. The microscopic depletions is an accurate method of determining nodal reactivity and modeling the significant history and reactivity feedback effects. Additional information regarding these computer codes is given in Section 4.3.3.

The effective rate of depletion can be monitored by observation of the operating reactivity status.

Any tendency toward slower removal rates would affect only cycle length and would be an economic problem unrelated to safety.

In the event that burnable absorber removal occurs faster than expected, but within a reasonable uncertainty band based on past experience, the shutdown margin would continue to be acceptable throughout the cycle. Only if the rate of removal were more than 30% greater than expected could there be potentially an unacceptably small shutdown margin. A deviation of this magnitude would become evident during power operation, as substantial increments of control rod insertion would be required to maintain constant power output. In this highly improbable scenario, remedial action can be taken by shutting down the reactor and rearranging the fuel loading to place fuel assemblies with the highest absorber content in the regions of highest control rod worth.

Experience at Dresden and other BWRs with gadolinia-containing fuel confirms that gadolinia concentrations can be specified to satisfy specific shutdown margin requirements. Accuracy of the predicted behavior of the gadolinia control effect with exposure has been demonstrated.

4.2.2.3.3 Material Properties

In pellets containing gadolinia, the Gd_2O_3 is uniformly distributed in the UO_2 and forms a solid solution. During the initial fuel cycle, the presence of the high cross-section Gd isotopes and the position of the Gd_2O_3-containing fuel rods within the fuel assembly result in a relatively low heat generation in the fuel rods containing Gd_2O_3. At the start of irradiation, fuel rods which contain gadolinia produce relatively little power; however, as the gadolinia is depleted, the power in these rods increases relative to the lattice average. In later cycles, the power of the Gd_2O_3-containing fuel rods decreases as the fissile material is depleted.

The addition of small amounts of Gd_2O_3 to UO_2 affects both the thermal conductivity and melting temperature of the solid solution. Below 1800°C the conductivity is reduced relative to that of pure UO_2, but above 1800°C there is essentially no effect. At no temperature is the conductivity of the solid solution less than the minimum conductivity of pure UO_2. The melting temperature of the solid solution is also below that of pure UO_2. However, the combined effect of these changes is not large enough to cause melting in gadolinia-containing fuel rods at any core power output that does not cause melting in the highest powered pure UO_2 rods.

During postulated severe transients such as a control rod drop, there would be no melting of the Gd_2O_3-UO_2 solid solution at exposures low enough for the gadolinia to have any appreciable reduction in control effect. This phenomenon is a result of the very low relative power of the gadolinia-bearing rods. Because the severe transients are rapid and of short duration and because the fuel rods containing the control material do not sustain melting, changes in the control worth of the gadolinia due to migration inside the pellet would not occur. The performance of gadolinia-containing fuel in transients and excursions is also addressed in Section 4.2.3.3.3.

The axial and radial power peaking factors are determined primarily by the control rod pattern. The gadolinia distribution in the core is such that the effect on gross peaking is minor and is probably negligible at the end of cycle when maximum peaking is expected to occur.

The typical maximum local peaking in the limiting fuel assembly as a function of exposure is given in Table 4.2-1.[2]

In design, a conservative estimate of Gd_2O_3-UO_2 melting temperature based on available data is used. The melting temperature used is typically 4796°F for the maximum Gd_2O_3 concentration employed in WEC fuel and typically 4660°F for the maximum Gd_2O_3 concentration employed in GE fuel. The melting temperature is assumed to reduce at a rate of approximately 32°C/(10,000 MWd/MT) as with pure UO_2, since the effect of fission fragment buildup should be essentially unaffected by the addition of small amounts of Gd_2O_3.

The heat fluxes required to cause incipient fuel melting and fuel damage for gadolinia-bearing fuel rods are determined based on a conservative estimate of Gd_2O_3-UO_2 melting temperature for the maximum concentration of Gd_2O_3 to be employed. The values obtained indicate that the peak heat flux for the gadolinia-bearing fuel is substantially lower than either the incipient fuel melting limit or the overstrain fuel damage limit (i.e., the heat flux required to cause 1% plastic strain of the cladding) at any time during life. The effect of melting temperature reduction with burnup is offset by the increasing centerline flux depression (tending to reduce centerline temperature) due to plutonium buildup on the pellet periphery.

Note that a conservative estimate of Gd_2O_3-UO_2 melting temperature is used to make the above determinations. A limited amount of data obtained under strictly controlled and measured conditions indicates that the assumed reduction in fuel melting temperature due to Gd_2O_3 may be overly conservative.

WEC has designed, analyzed, licensed, and fabricated nuclear fuel containing Gadolinia burnable absorber for BWR and PWR applications.

4.2.2.3.4 Operating Experience

Prior to the adoption of gadolinia in the fuel, BWRs including Dresden Units 2 and 3 used temporary control curtains located in the water gaps between fuel channels to provide burnable neutron absorbers.

Since 1965, gadolinia-containing fuel has been used in BWRs. The substantial operating experience is documented in Quad Cities FSAR Amendment 9[3] and in NEDE-24343-P.[4]

4.2.2.3.5 Expected Performance

Temperature coefficients are virtually unaffected relative to nongadolinia cores with temporary control curtains (Note that the initial core loading for both Dresden units contained control curtains). The gadolinia-bearing pellets act as thermally gray or black absorbers. The effect of gadolinia on moderator coefficients in the lattice is indistinguishable from that of the control curtains. Doppler response is unaffected because the gadolinia has essentially no effect on the resonance group flux or on the U-238 content of the core.

The irradiation products of the gadolinia depletion process are other gadolinium isotopes having lower cross-sections (see Section 4.2.3.3.3). Thus, the reactivity control effect is caused to diminish on a predetermined schedule without changes in the chemical composition of the fuel or the physical makeup of the core.

The maximum fuel temperatures for Gd_2O_3-UO_2 fuel rods are less than the corresponding temperatures of the peak-power standard UO_2 fuel rod at any time during life.

The shift in thermal neutron spectrum as a result of coolant boiling is normal in a BWR. Addition of steam voids to the moderator produces a loss in reactivity not only as a result of spectrum and cross-section changes but also as a result of increases in the migration area leading to higher leakage and greater effectiveness of control materials. In order to develop specifications for BWR fuel, it is necessary to account for spectrum changes associated with moderator void fractions ranging from zero to those as large as, or larger than, what would be expected to exist at the exit of the highest powered assembly. The analysis methods account for the thermal neutron absorption characteristics of the gadolinia-bearing rods as a function of space and neutron energy over the entire range of moderator void fractions.

Examination of the analyses leads to the following conclusions:

A. The effect of spectrum changes caused by moderator density variation is essentially the same in the case of gadolinia absorber as it is in the case of curtain absorber; and

B. The absence of any sharp change in the gradient of the moderator void coefficient curve for the gadolinia design indicates that there are no steady-state or transient moderator void conditions at which unusual reactivity responses would occur.

4.2.3 Design Evaluation

The GE14 fuel bundle design has been evaluated against the Amendment 22 criteria described in Reference 15.

Westinghouse fuel designs are evaluated against mechanical design criteria described in Section 3 of Reference 17.

4.2.3.1 Fuel Assemblies

4.2.3.1.1 Mechanical Design Limits

The detailed mechanical design evaluations for the GE14 fuel are reported in Reference 15.

For Westinghouse fuel see Reference 17.

4.2.3.1.2 Operating Limit Linear Heat Generation Rate

The following information applies to reload cores licensed using GNF/GE methodology. The maximum linear heat generation rate (MLHGR) for normal operation (discussed in Section 4.4.1.3.1.3) is 13.4 kW/ft for GNF GE14 fuel at the beginning of bundle life and decreases with exposure. Detailed exposure based MLHGR values are specified in the Core Operating Limits Report.

The Thermal Mechanical Operating Limit (TMOL) for Westinghouse SVEA-96 Optima2 fuel decreases with exposure. The exposure-based TMOL is specified in the Core Operating Limits Report.

4.2.3.1.3 Fuel Design Analysis

For Westinghouse SVEA-96 Optima2 fuel, see Reference 17.

For GE14 fuel, see Reference 15.

Flow-induced fuel rod vibrations depend primarily on flow velocity and fuel rod geometry. The maximum vibrational amplitude occurs midway between spacers due to the constraint of the spacer contact points.

It is recognized that when enrichment variation between rods in a fuel assembly is employed to reduce local power peaking due to core water gaps, it is important to eliminate possible errors in the manufacture and installation of the assembly to assure that the various enrichments are in the specified locations relative to the water gaps. In addition, cycle-specific analyses are performed to determine the impact of a misloaded fuel assembly on thermal margin. Fuel loading error analyses are discussed in Section 4.2.3.3.4.

Fuel element design and manufacturing procedures have been developed to prevent errors in enrichment location within the fuel assembly. This includes the unique marking of fuel rods so that fuel type and enrichment can be traced during the fabrication of fuel assemblies.

4.2.3.1.4 Fuel Damage Limit (Historical Information)

4.2.3.1.4.1 Relationship Between Operating Limit and Fuel Damage

For reload cores licensed using WEC and GNF methodology with ARTS limits, the TLHGR fuel limits are not applicable.

4.2.3.1.4.2 Experimental Basis for Operating Limit and Fuel Damage Limit

The fuel operating limit and the fuel damage limit are established based on operating experience and experimental tests covering the complete range of design power and exposure levels. This experience is used in establishing design features and in analyzing performance characteristics.

A number of Zircaloy-clad fuel rods with 0.56-inch diameter, 0.030-inch thickness cladding have been operated in the Vallecitos BWR to exposures in excess of 8,000 MWd/t at an LHGR greater than 18.5 kW/ft. A large number of other fuel rods of smaller diameter have been operated in the Vallecitos BWR at lower LHGRs but to higher heat fluxes and exposures.

Dresden Unit 1 provides the largest body of operating experience on Zircaloy-clad fuel. Maximum Dresden-type assembly average exposures have reached 17,000 MWd/t with peak fuel rod segments having attained 27,000 MWd/t. Special irradiations in Dresden Unit 1 with peak segment exposures of 31,000 MWd/t have been attained at a peak LHGR of 10 kW/ft. The Dresden Unit 1 Type III fuel provides experience with the through-rod-and-spring-spacer design. Type III assembly average exposures up to 12,000 MWd/t, with a peak local exposure of 16,000 MWd/t and a peak LGHR of 15 kW/ft have been attained.

Data for determining the fuel damage limit of 1% plastic strain have been obtained in tensile tests of cladding irradiated in the Vallecitos BWR (see GEAP 4597[6]), in Dresden Unit 1 (Type I fuel), and in the General Electric Test Reactor. To better determine the effects of exposure at high power generation, several capsules containing Zircaloy-clad fuel specimens have been irradiated in the General Electric Test Reactor to exposures as high as 40,000 MWd/t and peak LGHRs up to 24 kW/ft.

The GE fuel rod tests applicable to the design of the core, including 18.5 kW/ft, 21 to 22 kW/ft, and 28 kW/ft tests, have verified that the calculational methods adequately predict the cladding strain associated with a particular LHGR. In addition to tests performed by GE, tests in the range of 12 to 24 kW/ft have been performed by others.

These programs, combined with extensive BWR operating experience, have demonstrated that fuel integrity can be maintained in the core.

4.2.3.1.5 Experimental Data on Cladding Fragmentation After LOCA (Historical Information)

The results of experimental simulations of the environment of Zircaloy-clad UO_2 core fuel rods following a loss-of-coolant accident performed at Argonne National Laboratory (ANL) have been published in ANL-7438.[7] It was shown that if Zircaloy-clad rods were heated to near the melting point under conditions of unlimited oxidation and then quenched, gross fragmentation would occur. With significant oxidation of the Zircaloy, oxygen diffuses into the unreacted portion of the metal causing it to lose ductility at the lower temperatures. Upon quenching, thermal stresses are induced; when sufficient lowering of the temperature occurs, brittle failure of the cladding takes place.

Although there are other metallurgical considerations, there is general agreement that the degree of oxidation appears to be the predominant factor governing fragmentation after quenching. The combination of variables (temperature, time, and the presence of oxidant) which determine the degree of oxidation determine when fragmentation occurs. Hence, by comparing the peak degree of oxidation calculated to occur in the reactor to the degree of oxidation which causes fragmentation, some measure of the margin to fragmentation can be obtained. A thorough analysis of these experimental tests has been completed with the following conclusions:

A. Zircaloy fuel rod cladding failure did not occur for any rod with less than 5 mils (i.e., approximately 17%) reaction of the cladding;

B. Zircaloy fuel rod cladding fragmentation did not occur for any rod with less than approximately 7.5 mils (i.e., 24%) reaction of the cladding; and

C. Zircaloy fuel rod cladding failure did not occur for any rod with peak cladding temperatures below 1600°C (2910°F).

In comparing these results to their counterparts in the reactor, it is first noted that when comparing peak temperatures alone, although an oversimplification, the reactor temperatures for the large break are 900°F less than those for which

cladding failure occurred. For breaks smaller than the design break, the differences are even larger.

Next, the degree of cladding oxidation under actual reactor conditions can be compared with that under test conditions. The calculation of the core heatup following the design LOCA resulted in less than 0.2% metal-water reaction for the peak (i.e., maximum-oxidation) bundle and approximately 0.02% metal-water reaction for the average bundle. Therefore, the overall metal-water reaction is very small compared to what is required for gross cladding fragmentation. Assuming an unlimited steam supply, the maximum local oxidation of the peak fuel rod cladding would occur for the case of low pressure coolant injection (LPCI) system operation alone and would be less than 0.5 mils (approximately 0.3 mils for the design break which is the worst case). It is seen that a very large margin with respect to the degree of oxidation exists between the test (5-7.5 mils) and what is expected to occur in the reactor (0.5 mils). It is concluded, therefore, that except for local rod perforations due to internal gas pressure, gross cladding fragmentation would not occur in the core following a LOCA. A detailed description of the ANL test data can be found in the FSAR Amendment 7/8 for Unit 2/3, Answer to AEC Question 5.1.

4.2.3.2 Control Rods

Design evaluation for control rods is contained in Section 4.6.

4.2.3.3 Safeguard Aspects of Burnable Neutron Absorber

4.2.3.3.1 Thermal Margin

The fuel assembly nuclear design, including the gadolinia design and the reactor core design, is developed to maintain adequate thermal margin during the operating cycle.

The reactivity available for power shaping by control rods is more than adequate, and there should be no difficulty in satisfying the established local limits throughout the cycle at the maximum power level anticipated. Therefore, the use of gadolinia in the fuel leads to adequate thermal margins.

4.2.3.3.2 Shutdown Margin

The shutdown margin requirement on gadolinia design is addressed in Section 4.2.1.3. and 4.3.2.1.3.

The shutdown margin for each reload cycle is calculated using the analytical methods described in Section 4.3.3 and is verified in accordance with the Technical Specifications.

4.2.3.3.3 Transients and Excursions

Results of transients and excursions remain unchanged with the replacement of absorber curtains by the gadolinia burnable absorber. Of primary importance in the rapid excursions is the presence of a strong Doppler effect to compensate for the excess reactivity input. For slower transients, the moderator void coefficient assumes a major role. None of the reactivity coefficients associated with the fuel lattice are materially affected by the change in control augmentation method from absorber curtains to gadolinia absorber.

Gadolinia is held in solid solution by the UO_2. The initially chemically uniform gadolinia-bearing pellets remain so at all exposures, because neutron absorption in Gd-155 and Gd-157 produces stable isotopes Gd-156 and Gd-158, respectively. Initially, the gadolinia is highly self-shielded. During irradiation, the isotopic distribution varies radially in the pellet, nearly as a step function with an essentially zero concentration of Gd-155 and Gd-157 outside a certain radius and a natural percentage of these isotopes inside that radius. Because no chemical concentration gradients exist in the pellet, net migration of gadolinia in normal temperature gradients has not been detected in any of the postirradiation examinations to date. Either the migration does not occur, or it is limited to amounts below the detection threshold. Any dispersal of the solid solution into the moderator caused by an excursion would only reduce the self-shielding, causing an increase in the local neutron absorption and producing a loss in reactivity. There seems to be no mechanism which could cause the control effectiveness of the gadolinia to vary in such a way as to compromise safety.

4.2.3.3.4 Absorber Omission and Fuel Loading Errors

The safety effect of the omission of gadolinia during fuel fabrication and the consequences of fuel assembly misorientation or mislocation during fuel loading are considered.

Quality contol procedures assure production of fuel in conformance with design. For initial cores, even if gadolinia were omitted from all fuel assemblies, no safety problem would result. The fuel storage facilities were designed for fuel reactivity in excess of that which would exist in the initial fuel designs with gadolinia omitted. For the GNF GE14C and Westinghouse SVEA-96 Optima2 assemblies, residual gadolinia is credited in the fuel storage criticality analyses. Extensive experience with the use of gadolinia has justified the confidence in crediting the presence of the gadolinia. This confidence is based upon precise quality control measures which are utilized during the manufacture of gadolinia bearing UO_2 pellets and during the assembly of these fuel pellets into fuel rods. Fuel fabrication procedures also assure accurate placement of gadolinia bearing fuel rods.

Core loading procedures also provide control in the event that the fuel reactivity was higher than expected. For initial cores, frequent shutdown margin checks would expose the abnormal condition before sufficient fuel could be loaded to exceed the capability of the control rod system. After extensive experience with the construction of gadolinia bearing fuel bundles and the computer modeling of the depletion of the gadolinia during power operation, the shutdown margin checks during the core loading process have been replaced with close monitoring of the Source Range Monitor (SRM) count rates.

The effects of fuel misloading errors for Dresden Units 2 and 3 are analyzed. Misloading errors include both misrotation error and mislocation error. Results show that the lowest MCPR resulting from operation with a misloaded fuel assembly is well above the Fuel Cladding Integrity Safety Limit MCPR (defined in Section 4.4). The fuel misloading errors are addressed in greater detail in UFSAR Sections 15.4.7 and 15.4.8.

4.2.4 Testing and Inspection Plan

4.2.4.1 Fuel Assemblies

Rigid quality control requirements are enforced at every stage of fuel manufacturing to ensure that design specifications are met. Written manufacturing procedures and quality control plans define the steps in the manufacturing process. Fuel cladding is subjected to 100% dimensional inspection and ultrasonic inspection to reveal any defects in the cladding wall. Destructive tests are performed on representative samples from each lot of tubing, including chemical analysis and tensile, bond, and burst tests. A representative sample of tubes are subjected to a corrosion resistance test. The integrity of end plug welds is assured by the standardization of weld processes based on radiographic and metallographic inspection of welds, and by the helium leak test of completed fuel rods. The UO_2 powder characteristics and the densities, composition, and surface finish of the pellets are controlled by regular sampling inspections. The UO_2 weights are recorded at various stages of manufacturing. Dimensional measurements and visual inspections of critical areas such as fuel rod-to-rod clearances are performed after assembly. After arrival at the reactor site a receipt inspection is performed.

Flow tests were conducted using prototype reactor hardware in which the single-phase and two-phase flow characteristics were determined for core and vessel internal components which contribute to the core pressure drop. Fuel assembly handling tests were done to verify structural integrity. Mechanical tests and corrosion tests of the Zircaloy spacers were performed to identify design and specification requirements. Critical heat flux tests were performed using prototype multi-rod configurations, minimum allowable coolant clearance gaps, and prototype Zircaloy spacers.

4.2.4.2 Control Rods

Testing and inspection for control rods are described in Section 4.6.

4.2.4.3 Burnable Neutron Absorber Bearing Rods

The same rigid quality control requirements observed for standard UO_2 fuel are employed in the manufacture of Gd_2O_3-UO_2 fuel. Gadolinia-bearing UO_2 fuel pellets of a given enrichment and gadolinia concentration are maintained in separate groups throughout the manufacturing process.

Fuel rods are individually numbered prior to the loading of fuel pellets. This is done to:

A. Identify which pellet group is to be loaded in each fuel rod;

B. Identify which position in the fuel assembly each fuel rod is to be loaded; and

C. Facilitate total fuel material accountability for a given project.

The following quality control inspections are made:

A. Gadolinia concentration in the Gd_2O_3-UO_2 powder blend is verified;

B. Sintered pellet Gd_2O_3-UO_2 solid-solution homogeneity across a fuel pellet is verified by examination of metallographic specimens;

C. Gadolinia-UO_2 fuel rod loading is verified.

Finally, an inspection is made of all assemblies and rods of a given project to assure overall accountability of fuel quantity and placement for the project.

4.2.5 References

1. Deleted.

2. "Dresden 2 ANF-5 Design Report - Mechanical, Thermal, and Neutronic Design for ANF 9x9 Fuel Assemblies," Siemens Power Corporation, ANF-90-057(P), April 1990.

3. Commonwealth Edison Company Quad Cities Station, Units 1 and 2, FSAR Amendment 9, "Contained Burnable Neutron Absorber as Supplementary Control."

4. "Experience with BWR Fuel Through January 1981," General Electric Company, NEDE P, 24343-P, May 1981.

5. "RODEX2: Fuel Rod Thermal-Mechanical Response Evaluation Model," Siemens Power Corporation, XN-NF-81-58(P)(A), Supplements 1 and 2, Rev. 2, March 1984.

6. Williamson, H.E., et al., "Examination of Zircaloy Clad UO_2 Fuel Rods Operated in the VBWR to 10,000 MWD/TU," General Electric Company, GEAP 4597, March 1965.

7. "Argonne National Laboratory Reactor Development Program Progress Report, March 1968," Argonne National Laboratory, ANL-7438, April 26, 1968.

8. "Advanced Nuclear Fuels Corporation Generic Mechanical Design for Advanced Nuclear Fuels 9x9-IX and 9x9-9X Reload Fuel," ANF-89-014(P)(A), Revision 1 and Supplements 1 and 2, Advanced Nuclear Fuels Corporation, October 1991.

9. "Generic Mechanical Design Criteria for BWR Fuel Designs," ANF-89-98(P)(A), Revision 1 and Supplements, Advanced Nuclear Fuels Corporation, May 1995.

10. "Generic Mechanical Design for Exxon Nuclear Jet Pump BWR Reload Fuel", XN-NF-85-67(P)(A) Revision 1, Exxon Nuclear Company, September 1986.

11. Siemens Power Corporation Methodology for Boiling Water Reactors Evaluation and Validation of CASMO-4/ MICROBURN-B2", EMF-2158(P), Revision 0, October 1999.

12. "Advanced Nuclear Fuels Corporation BWR 3/4p-Lattice Symmetrization with Advanced Fuel Channels, Mechanical Design for Normal Operation," ANF-91-064(P), March 1991.

13. "General Electric Fuel Bundle Designs," NEDE-31152P.

14. Licensing Topical report, "General Electric Standard Application for Reactor Fuel," NEDE-24011-P-A-14, June 2000.

15. "GE14 Compliance with Amendment 22 of NEDE-24011-P-A (GESTARII)," NEDE-32868P, Revision 1, September 2000.

16. "Reference Safety Report for Boiling Water Reactor Reload Fuel," Westinghouse Topical Report CENPD-300-P-A, July 1996.

17. "Fuel Assembly Mechanical Design Methodology for Boiling Water Reactors, Supplement 1 to CENPD-287-P-A," Westinghouse Topical Report WCAP-15942-P-A, March 2006.

18. "The Advanced PHOENIX and POLCA Codes for Nuclear Design of Boiling Water Reactors", CENPD-390-P-A, December 2000.

Table 4.2-1

THIS TABLE HAS BEEN INTENTIONALLY DELETED.

Table 4.2-2

THIS TABLE HAS BEEN INTENTIONALLY DELETED.

4.3 NUCLEAR DESIGN

This section discusses the nuclear design bases (Section 4.3.1), steady-state and dynamic nuclear characteristics of the core (Sections 4.3.2.1 and 4.3.2.2, respectively), stability (Section 4.3.2.3), nuclear design analytical methods (Section 4.3.3), and new changes in stability criteria (Section 4.3.4).

4.3.1 Design Bases

The bases for nuclear design include the nuclear design basis for the reactor and the design basis for system stability, which are discussed in Section 4.3.1.1 and 4.3.1.2, respectively.

4.3.1.1 Reactor

A summary of the nuclear design bases is presented below:

A. The neutronic design shall be compatible with all reactivity control requirements specified in the Technical Specifications.

B. The average enrichment of the reload fuel design shall be selected so as to achieve the target equilibrium batch average discharge exposure.

C. The enrichment distribution within an assembly shall be designed with consideration of the following:

   1. Fuel performance criteria, i.e., limits on plastic strain;

   2. Fuel assembly thermal limits, i.e., limits on minimum critical power ratio (MCPR); and

   3. Operating limits associated with the postulated loss-of-coolant accident (LOCA), i.e., limits on maximum average planar linear heat generation rate (MAPLHGR).

D. The core shall be capable of being made subcritical at any time or at any core condition with the highest worth control rod fully withdrawn. A cold shutdown margin of 1% Δk is used as a design target in the core loading plan.

E. A value of 1% Δk is used as a design objective for hot excess reactivity at the beginning of cycle (BOC). The minimum value considers the existence of an equilibrium-xenon core at BOC and provides a balance of reactivity attributed to gadolinia and control blades to allow fixing of acceptable margins to operating limits.

F. The moderator void coefficient is negative over the entire operating range.

G. Reactivity coefficients generally shall:

1. Provide a strong negative reactivity feedback under conditions of rapid power increase; and

2. Regulate slower changes in core power level and spatial distribution consistent with the requirement of overall plant hydrodynamic stability.

4.3.1.2 System Stability

Stability criteria are established to demonstrate compliance with 10 CFR 50, Appendix A, General Design Criterion (GDC) 12. The requirement of this GDC is that one of the following alternatives be satisfied:

A. Power oscillations which can result in conditions exceeding specified acceptable fuel design limits are not possible; or

B. Such power oscillations can be reliably and readily detected and suppressed.

Dresden Units 2 and 3 were originally designed to satisfy the first alternative; they were expected to be stable during all procedurally possible modes of operation, i.e., they would have no inherent tendency toward oscillations of power and channel flow, either divergent or of limited amplitude. The units were also designed to be well damped over all normal modes of power and flow.

However, since 1988, industry experience indicates that BWRs similar to Dresden Units 2 and 3 may not be stable under all operating conditions during a fuel cycle as originally expected. Core design and operating criteria have been modified to concentrate on satisfying the latter alternative of 10 CFR 50, Appendix A, GDC 12 (see Section 4.3.4).

4.3.2 Description

The reactors at Dresden Units 2 and 3 are light-water moderated BWRs, fueled with slightly enriched uranium dioxide (UO_2). At operating conditions, the moderator is permitted to boil, producing a spatially varying density of steam voids within the core. The use of water as moderator produces a neutron energy spectrum such that the fissions are induced principally by thermal neutrons. Gadolinia (Gd_2O_3) is used as a burnable neutron absorber in the fuel, as discussed in Section 4.2.

The presence of U-238 in the uranium dioxide fuel has several major effects. First, it leads to the production of significant quantities of plutonium during core operation. This plutonium contributes both to fuel reactivity and to power production in the reactor and changes the delayed neutron fraction with exposure.

In addition, the direct fissioning of U-238 by fast neutrons yields approximately 7% of the total power. Finally, the U-238 contributes a strong negative Doppler coefficient of reactivity, which improves the inherent or self-regulating response of the reactor and limits the peak power in excursions.

The strong negative moderator void reactivity effect contributes to the overall plant stability and to the damping of xenon oscillations.

4.3.2.1 Core Steady State Characteristics

The design of the BWR core and fuel is based on a combination of design variables, such as moderator-to-fuel volume ratio, core power density, thermal-hydraulic characteristics, fuel exposure level, nuclear characteristics of the core and fuel, heat transfer parameters, flow distribution, moderator void content, heat flux, and operating pressure. These variables are dynamic functions of operating conditions. However, design analyses and calculations verified by comparison with data from operating plants are usually performed for specific steady-state conditions. This section addresses steady-state analyses for the fuel cycle, local power peaking, reactivity control, and control rod worths.

4.3.2.1.1 Fuel Cycle

The fuel cycle is designed to meet the required cycle energy, which varies from cycle to cycle.

The enrichments in the fuel assemblies are chosen to provide excess reactivity sufficient to overcome the negative reactivity effects of core neutron leakage, moderator heating and boiling, fuel temperature rise, xenon and samarium poisoning, and fuel depletion. During fuel burnup, control rods are used in part to counteract the power distribution effect of steam voids. The combined use of both the control rod and moderator void distributions provides the BWR design with considerable flexibility to control power distribution. Power distributions during the course of the cycle cause changes in fuel burnup and isotopic composition throughout the core, which in turn affect the reactivity and power distributions later in the cycle. This phenomenon permits using the control rods to shape the fuel burnup and isotopic composition early in the fuel cycle to counteract the effect of moderator voids on the axial distribution toward the end of a fuel cycle, when few control rods remain in the core.

4.3.2.1.2 Local Power Peaking

The local power peaking in each assembly is a function of the fuel rod and gadolinia (Gd_2O_3) bearing rod enrichments. Several different enrichments and mixtures are utilized in each fuel design to flatten the local power peaking, the relative peak-to-average fuel rod powers. The fuel is designed to balance the performance of the fuel relative to thermal limits.

4.3.2.1.3 Reactivity Control

The excess reactivity designed into the core is controlled by a control rod system supplemented by gadolinia in the fuel. Control rod design is discussed in Section 4.6. The use of gadolinia as a burnable neutron absorber is discussed in Section 4.2.

The control rod system is designed to provide adequate control of the maximum excess reactivity anticipated during the fuel cycle operation. Shutdown capability is evaluated assuming a xenon-free core at ambient temperature, which represents the condition of maximum fuel reactivity.

The basic design criterion for reactivity control is that the core, in its maximum reactivity condition, be subcritical with the control rod of highest worth fully withdrawn and all other rods fully inserted. The criterion provides a substantial shutdown margin with all rods in.

In accordance with this basic design criterion, the core loading is limited to that which can be made subcritical (i.e., effective neutron multiplication factor k_{eff} less than 1) in the most reactive condition during the operating cycle with the highest worth operable control rod in its full-out position and all other operable rods fully inserted.

According to the Technical Specification Limiting Conditions for Operation the shutdown margin (SDM) shall be equal to or greater than:

1. 0.38% $\Delta k/k$ with the highest worth control rod analytically determined, or

2. 0.28% $\Delta k/k$ with the highest worth control rod determined by test.

The shutdown margin is defined as the amount of reactivity by which the reactor is subcritical or would be subcritical assuming all control rods are fully inserted except for the single control rod of highest reactivity worth which is assumed to be fully withdrawn and the reactor is in the shutdown condition; cold; i.e. 68 °F and xenon free.

Since satisfaction of the limitation is demonstrated at the time of core loading and applied to the entire fuel cycle, the generalized requirement is that the reactivity of the loaded core be limited so the core can be made subcritical by at least R + 0.38% $\Delta k/k$ or R + 0.28% $\Delta k/k$, as appropriate, with the strongest control rod fully withdrawn and all others fully inserted. The quantity R is the difference between the calculated shutdown margin at the beginning of the cycle and the minimum calculated shutdown margin at any time later in the cycle when it would be less than at the beginning. The value of R is always positive or zero, and it includes the potential shutdown margin loss assuming full settling of boron carbide (B_4C) in all inverted control rod poison tubes in the core. A new value of R is determined for each fuel cycle.

In order to assure that the basic design criterion and the LCO (k_{eff} less than 1) are always satisfied, a 0.01 Δk design margin was adopted as the design goal. Thus, the design target is calculated k_{eff} less than or equal to 0.99 (after normalizing eigen values such that the critical Keff=1.000), with the control rod of highest worth fully withdrawn. This design target assures that the unit can be shut down

by control rods alone. In addition to the control rod shutdown requirements, the standby liquid control system (Section 9.3.5) provides sufficient reactivity control to shut down the unit at any time independent of control rod action.

Current fuel designs incorporate gadolinia, which is taken into account for shutdown requirement calculations. Gadolinia is used to control the reacitivity of the reload fuel (see Section 4.2.2.3.5)

Analyses of shutdown margin are performed as a function of cycle exposure to demonstrate conformance to cold shutdown margin requirements.

4.3.2.1.4 Control Rod Worth

In an operating reactor there is a spectrum of possible control rod worths, depending on the reactor state and on the control rod patterns chosen for operation. Control rod withdrawal sequences and patterns are selected prior to reactor startup to achieve optimal core performance and, simultaneously, low individual rod worths.

Distributed control rod patterns are used. The operating procedures to establish such patterns are supplemented by the rod worth minimizer (RWM) which prevents rod withdrawals that would yield a rod worth greater than that permitted by the prescribed rod withdrawal sequence. The RWM is described in Section 7.7.

The beginning of life (BOL) control rod worth and fuel assembly reactivity ($k\infty$) are presented in the reload specific fuel design reports. An example fuel design report is EDB No. 2483[15] for GE14 fuel. Typical data computed at six specific moderator and fuel conditions expected during reactor operation are presented in Table 4.3-1. The control rod worths at these conditions are also show.

At any specified reactor state, control rod worths have a direct impact on the peak fuel enthalpy that would result from a control rod drop accident (CRDA), i.e., the free fall of any rod to the position of its drive (see Section 15.4.10). The peak fuel enthalpy, i.e., the maximum calculated radial average energy density at any axial fuel location in any fuel rod, is a measure of the severeness of the consequences of a reactivity accident.

The UO_2 vapor pressure data obtained by Ackermann[2] and the test data obtained at the TREAT facility of Argonne National Laboratory indicate that the sudden fuel pin rupture threshold is about 425 cal/g. Analyses indicate that prompt dispersal of finely fragmented fuel into the coolant with subsequent large pressure rise rates will not occur at excursion energy densities below 425 cal/g. Excursion energies above this level can cause pressure surges which may endanger the primary coolant system.

In general, failure consequences for UO_2 fuel are insignificant below 300 cal/g for both irradiated and unirradiated fuel rods. Therefore, a limit of 280 cal/g on the peak fuel enthalpy ensures that core damage resulting from any postulated reactivity excursion would be minimal and that both short-term and long-term core cooling capability would not be impaired.

To implement the preceding limitation, control rod withdrawal sequences are designed to limit rod worths, so that a CRDA would result in a peak fuel enthalpy of not more than 280 cal/g. Conformance to this peak fuel enthalpy is demonstrated by analysis for each operating cycle (See Section 15.4.10).

For current control rod types the rod velocity limiter (see Section 4.6) restricts rod removal to rates of 3.11 ft/s or less, and the RWM enforces rod withdrawal in sequences preselected to maintain low rod worths. Above 10% power, the control rod worths are not high enough to produce a peak fuel enthalpy of 280 cal/g if a rod were removed at 5 ft/s. Therefore, the RWM is not required to be operable when the reactor is above 10% power.

4.3.2.2 Core Nuclear Dynamic Characteristics

The performance characteristics of the core provide a nuclear dynamic response which:

A. Has a strong negative reactivity feedback under severe transient conditions;

B. Contributes negative reactivity feedback consistent with the requirements of overall plant nuclear-hydrodynamic stability; and

C. Regulates or dampens changes in core power level and spatial distribution in a manner consistent with safe and efficient plant operation.

Characteristic A, through the Doppler and moderator reactivity coefficients which are negative during power operation, provides shutdown mechanisms in the event of a power excursion. Characteristics B and C assure that there are no inherent tendencies for undamped oscillations during normal modes of operation.

4.3.2.2.1 Reactivity Coefficients

The dynamic behavior of the core is characterized in terms of the following reactivity coefficients:

A. The fuel temperature or Doppler coefficient,

B. The moderator void coefficient, and

C. The moderator temperature coefficient.

The Doppler and void coefficients are collectively termed the power coefficient.

4.3.2.2.2 Doppler Coefficient

In UO_2 fuel, the Doppler coefficient provides an inherent mechanism for terminating nuclear transients. It provides instantaneous negative reactivity feedback to any fuel temperature rise, either gross or local. The magnitude of the Doppler coefficient is inherent in the fuel design and does not vary significantly among light-water-moderated UO_2 fuel designs.

The effectiveness of the Doppler coefficient in terminating rapid reactivity transients can be seen in the analyses of the cold water insertion incidents in Sections 15.1.1 and 15.5.1 and the CRDA in Section 15.4.10.

Figure 4.3-1 shows the Doppler coefficient (calculated by GE) as a function of fuel temperature and steam voids for unirradiated fuel. The beginning-of-life or zero-exposure Doppler coefficients are used in analyzing all accidents; although, in fact, contributions from plutonium, particularly Pu-240, will increase the magnitude of the Doppler coefficient by 10 to 15% at the end of the first cycle (see Figure 4.3-2).

Figure 4.3-3 illustrates the Doppler reactivity defect existing in the core under normal steady-state operating conditions up to 110% of rated power, as analyzed by GE. The analysis includes the effects of steam voids characteristic of normal operation.

Figure 4.3-4 shows the total Doppler reactivity defect available for any maximum fuel temperature during a transient. Doppler defects are shown for adiabatic fuel heating transients starting from cold, hot standby, and rated-power fuel temperatures. Fuel temperatures on the abscissa represent effective average fuel temperatures in the core. This figure shows that substantially more Doppler reactivity defect is available than is required to terminate an excursion caused by removal of any single control rod from a normal pattern.

Uncertainties in the design calculations of Doppler effects in BWRs have been assessed. The GE analyses are compared with the analyses of Pettus[3] and Hellstrand[4] which represent carefully performed work applicable to UO_2-fueled BWRs. The equations involved are summarized below:

A. Pettus

$$I = I_o \left[1 + \alpha \left(\sqrt{T} - \sqrt{T_o}\right)\right]$$

$$I_o = 3.0 + 28.0 \sqrt{S/M}$$

$$\alpha = 0.0075 \text{ @ } (S/M) = 0.449$$

$$\alpha = 0.0063 \text{ @ } (S/M) = 0.206$$

B. Hellstrand

$$I = I_o \left[1 + \alpha \left(\sqrt{T} - \sqrt{T_o}\right)\right]$$

$$I_o = 4.15 + 26.6 \sqrt{S/M}$$

$$\alpha = 0.0058 + 0.005 (S/M)$$

C. General Electric

$$I = I_o \exp\left[\alpha \left(\sqrt{T} - \sqrt{T_o}\right)\right]$$

$$I_o = 30 \sqrt{S/M + 0.077}$$

$$\alpha = 0.00696 - 0.000262 (M/S)$$

where:

I = U-238 resonance integral

T = effective fuel temperature (ΔK)

S/M = effective surface to mass ratio for fuel rod (cm^2/g).

Figure 4.3-5 shows the Doppler reactivity defect as a function of fuel temperature for a typical BWR with fuel and moderator initially at 547°F. The GE curve is conservative relative to Pettus and Hellstrand throughout the temperature range of the original data (below 1800°F). At 5000°F the GE model is 5% less conservative that the Pettus model extrapolation but is about 5% more conservative than Hellstrand.

However, the exponential, temperature-dependent form of the GE resonance integral equation is better justified theoretically than the simple-square-root dependence on temperature used by Pettus and Hellstrand. Furthermore, high temperature Doppler measurements at Hanford lend additional support to the exponential form.[5] There is no significance, therefore, to the crossover of the GE extrapolation by the Pettus curve in Figure 4.3-5.

For a given excursion in which the Pettus and Hellstrand forms of the Doppler reactivity defect yield a fuel enthalpy of 221 cal/g, the GE model, for the same conditions, predicts a fuel enthalpy of 220 cal/g, about 0.5% more conservative. Since the extrapolation to elevated temperatures using the GE model is more

theoretically sound than using Pettus or Hellstrand models, it is expected that this 0.5% conservatism will persist into the high temperature range.

4.3.2.2.3 Moderator Temperature and Moderator Void Coefficients

The moderator void coefficient contributes to nuclear-hydrodynamic stability. Since a number of plant parameters including the moderator void coefficient contribute to stability requirements, no specific coefficient value can be used as a design basis. In general, to assure stability, the moderator void coefficient during power operation must not become too negative.

The moderator temperature and moderator void coefficients include temperature and void effects of the moderator interior to the fuel assemblies and the moderator in the gaps between flow channels.

In Doppler-terminated or Doppler-controlled transients, the component of the moderator coefficient interior to the fuel assembly is relatively slow-acting due to the long heat transfer time constant of the fuel. Nevertheless, there should not be a significant positive reactivity contribution to the core as heat transfers from fuel to coolant. This condition is satisfied if the moderator coefficients interior to the fuel assemblies are designed to be zero or slightly negative. The void component of the coefficient internal to the fuel is held negative at all times.

The component of the moderator temperature coefficient external to the fuel channel is slower acting than the in-channel density or temperature coefficient since it takes on the order of minutes for the water gaps to reach temperature equilibrium with the circulating coolant. Because of the relative slowness of the water gap temperature to respond in the time domain of transients, the reactivity feedback due to the external moderator temperature coefficient is negligible for any transient. The negative reactivity feedback effects of the interior and exterior moderator void coefficients and the interior moderator temperature coefficient contribute to the inherent tendency to avoid undamped oscillations.

The moderator temperature coefficient of reactivity is negative for most of the operating cycle; however, near the end-of-cycle the overall moderator temperature coefficient may become slightly positive. This is due to the fact that the uncontrolled BWR-D lattice is slightly overmoderated near the end-of-cycle; this, combined with the obvious requirement that more control rods must be withdrawn from the reactor core near the end-of-cycle to establish criticality, may result in a slightly positive moderator temperature coefficient. These conditions are the principal causes of the positive trend of the total moderator temperature coefficient with core life.

The moderator void coefficient of reactivity becomes less negative with fuel depletion. However, unlike the moderator temperature coefficient which may become slightly positive towards the end of cycle, the moderator void coefficient remains negative during the entire fuel cycle.

The moderator temperature and moderator void coefficients are mathematically represented by the following:

A. Moderator temperature coefficient

$$\frac{1}{k_{eff}}\frac{dk_{eff}}{dT} = \frac{1}{k_\infty}\frac{dk_\infty}{dT} - \frac{\frac{dL}{CdT}}{1 - CL} - \frac{M^2\frac{dB_g^2}{dT} + B_g^2\frac{dM^2}{dT}}{1 + M^2B_g^2}$$

B. Moderator void coefficient

$$\frac{1}{k_{eff}}\frac{dk_{eff}}{dV} = \frac{1}{k_\infty}\frac{dk_\infty}{dV} - \frac{\frac{dL}{CdV}}{1 - CL} - \frac{M^2\frac{dB_g^2}{dV} + B_g^2\frac{dM^2}{dV}}{1 + M^2B_g^2}$$

where:

T = average moderator temperature

V = in-channel void fraction

C = lattice constant

L = diffusion length

M^2 = migration area

B_g^2 = geometric buckling

The terms on the right side of the equation represent the contributions of fuel multiplication, control rods, and leakage, respectively, to the coefficients.

Any decrease in moderator density or increase in moderator voids increases neutron leakage from the region of the disturbance and also enhances the strength of the control rods. These two contributions, therefore, are always negative everywhere in the core and monotonically increase in magnitude with moderator density reduction.

The k_∞contribution has a local spatial dependence. Undermoderation exists within the fuel channel under all conditions, and the local moderator temperature coefficient is negative. External to the fuel element, in the surrounding water gaps, the local coefficient is slightly positive from the cold ambient condition through the lower part of the heatup range. In the power range, the local coefficients are everywhere negative. Early in core life, the control rod density is high and the control rod term contributes a strong negative effect to the coefficient. At high fuel exposures, this term approaches zero due to removal of control rods. While the k_∞ term has a slight positive trend with exposure, the control rod term is by far the major factor in the reduction of magnitude of the coefficient with fuel exposure. In a gross core power disturbance, the k_∞ and control rod terms dominate since leakage is small. In a disturbance such as a control rod withdrawal, the control rod term in the region of disturbance is zero, but the material buckling and, therefore, the leakage from the disturbed zone are large.

Near the end of core life when control rod density is at a minimum, a gross core transient that is sufficiently slow to allow water gaps to equilibrate with the flowing coolant (tenths of a second) may, below operating temperature, cause a

slightly positive moderator reactivity effect. If, however, the transient accelerates so that steam voids are produced inside the channel, an immediate negative k_∞ contribution would result such that the total moderator coefficient would be negative. There are no potentially severe transients in which a positive moderator reactivity effect plays a major role.

In summary, in those regions of the core where rapid moderator density changes can occur, the effect of the moderator temperature and moderator void coefficients together is negative. Overall, the moderator temperature and moderator void coefficient are negative in the power range.

Figures 4.3-6 and 4.3-7 show typical moderator temperature and moderator void coefficients for beginning of life and at 10,000 MWD/t fuel exposure. Because refueling is done utilizing symmetrical loadings which avoid concentrations of the most exposed fuel, the 10,000 MWD/t points are representative of the high exposure effects. As shown in Figure 4.3-7, the moderator void coefficient satisfies the design basis that it remains negative throughout core life.

4.3.2.3 Stability

The current design and operating criteria since IE Bulletin 88-07 are based on detection and suppression of oscillations as addressed in 10 CFR 50, Appendix A, GDC 12 (see Section 4.3.1.2). This GDC is satisfied by implementing the option III long-term solution options discussed in NEDO-31960 (see Section 4.3.4).

The new stability concerns resulting from the LaSalle Unit 2 instability event of March 9, 1988, are addressed in Section 4.3.4.

4.3.3 Analytical Methods

Depending on the aspect of the reload in question, WEC methodology, CASMO-4 and MICROBURN-B2, or GNF methodology is used.

CASMO-4 is a multigroup two-dimensional transport theory code for burnup calculations on BWR assemblies or simple pin cells. The code handles a geometry consisting of cylindrical fuels rods of varying composition in a square pitch array with allowance for fuel rods with burnable absorber, burnable absorber rods, incore instrument channels, water gaps, cluster control rods, and cruciform control rods in the regions separating fuel assemblies.

MICROBURN-B2 is a three-dimensional, two-group, course-mesh diffusion theory reactor simulator program for the analysis of BWR cores. The simulator code models the reactor core in three-dimensional geometry, and the reactor calculations can be performed in one-quarter, one-half, or full core geometry. The code calculates the reactor core reactivity, core flow distribution, nodal power distribution, reactor thermal limit values, and incore detector responses. The code includes special treatment of moderator void and control rod history and a more accurate treatment of plutonium production and depletion. CASMO-4 and MICRBURN-B2 are codes developed by AREVA (formerly SPC) [19]

GNF currently uses the GEMINI methods for determining the nuclear characteristics of reload fuel. The analytic models and computer codes are described in NEDO-30130-A[16] and Reference 17.

Westinghouse nuclear evaluations are performed using an NRC approved lattice physics code (PHOENIX4) and core simulator (POLCA7). See Reference 26 for a detailed description of the WEC nuclear design codes.

Since the BWR core contains hundreds of fuel assemblies of various designs and in various control states, moderator void conditions, and accumulated exposures, the nuclear evaluations are best addressed as two parts: lattice analysis and core analysis.

Most of the lattice analyses are performed during the fuel assembly design process. The fuel assembly modeling is further divided into two stages: the fuel rod cell and external region modeling using transport theory methods, and the coarse-mesh fuel assembly modeling based on cell homogenization and diffusion theory methods. The results of these single assembly calculations are reduced to "libraries" of lattice reactivities, relative rod powers, and few-group cross-sections as functions of instantaneous moderator void fraction, exposure, exposure-void history, control state, and fuel and moderator temperatures for use in the core analysis. These analyses are dependent upon fuel lattice parameters only, and therefore, are valid for all plants and cycles to which they are applied.

For GNF methods, the lattice analyses are performed using the TGBLA advanced physics model described in NEDO-3O13O-AU6I and Reference 17.

The core analysis is unique for each cycle. It is performed prior to cycle loading to demonstrate that the core meets all applicable safety limits. The principal tool used in the core analysis is a three-dimensional BWR simulator code. This code performs coupled nuclear and thermal-hydraulic calculations based on a coarse-mesh nodal approximation to the one-group, steady-state neutron diffusion equation. Neutron parameters are obtained from the lattice analysis output, parametrically fitted as a function of moderator temperature density, exposure, control, and moderator density history for each fuel type. The BWR simulator computes core power distributions, exposure, and reactor thermal-hydraulic characteristics as a function of spatially varying moderator voids, control rod positions, fuel loading patterns, burnable poisons, coolant flow, and other design and operational variables. The BWR simulator code includes the Doppler reactivity effect as a function of effective average fuel temperature and the effect of xenon poisoning.

For GNF methods, the core analysis is performed using the PANACEA advanced core physics model described in NEDO-3013O-A[16] and Reference 17.

4.3.4 Protection Against Instabilities

BWR cores may exhibit thermal-hydraulic instabilities in certain portions of the core power and recirculation flow operating domain.

On March 9, 1988, LaSalle County Station Unit 2 experienced a dual recirculation pump trip event. After the pump trip, while on natural circulation, the unit experienced an excessive neutron flux oscillation. The event was described in NRC Information Notice No. 88-39, "LaSalle Unit 2 Loss of Recirculation Pumps With Power Oscillation Event," dated June 15, 1988.

The NRC has been concerned with generic questions that this event raised and has issued IE Bulletin No. 88-07 which requests that holders of operating licenses for BWRs ensure that adequate operating procedures and instrumentation are available and adequate operator training is provided to prevent the occurrence of uncontrolled power oscillations during all modes of operation.

In IE Bulletin No 88-07, Supplement 1, the NRC provides additional information concerning power oscillations in BWRs and requests that addressees take action to ensure that the safety limit for the plant minimum critical power ratio is not violated.

In Generic Letter 94-02, the NRC requested that manual operator actions be implemented until permanent hardware was installed as a solution to the issue of detection and suppression of neutron flux oscillations. These interim corrective actions were implemented by Commonwealth Edison Company (ComEd).

ComEd joined the BWR Owners' Group (BWROG) program to develop generic long-term solutions to the stability issue. The BWROG program developed a design and evaluation methodology to analyze thermal-hydraulic stability and identified several viable approaches to the long-term resolution of the stability issue. Details of this methodology, and the Option III solution adopted by EGC, are discussed in NEDO-31960-A[10], NEDO-31960-A Supplement 1[12], and CENPD-400-P-A,[27].

The solution to the instability problem implemented at Dresden is the installation of the ABB-designed Oscillation Power Range Monitor (OPRM), see also Section 7.6.1.6. The OPRM system is designed to initiate a reactor scram via RPS trip logic and provide alarm indication upon detection of core power oscillations prior to exceeding the Minimum Critical Power Ratio (MCPR) safety limit. The OPRM augments the original Reactor Protection System (RPS) functions by adding the suppress function of thermal-hydraulic oscillations in the reactor core and does not remove or replace any existing RPS functions. The OPRM utilizes the Local Power Range Monitor (LPRM) signals to detect core instabilities using a period-based algorithm. Also, the OPRM uses amplitude and growth rate algorithms, which are implemented for defense-in-depth but are not relied upon for detecting instabilities. If an unacceptable oscillation is detected by any of these algorithms, a trip signal is generated by the OPRM. However, during the interim tune-up period, the OPRM was installed in a detect-and-alarm only mode and the RPS trip logic was disabled.

Details of the licensing basis and related licensing methodology to demonstrate the adequacy of the Option III hardware is described in NEDO-32465-A[13]. The methodology consists of three major components:

A. A determination of the MCPR margin that exists prior to the onset of the oscillation.

B. A statistical treatment of various parameters that influence the magnitude of the peak fuel bundle power oscillation.

C. A conservative relationship between the change in CPR and hot bundle oscillation magnitude.

A 10CFR Part 21 notification delayed implementation of the Option III solution since the generic relationship between the change in CPR and hot bundle oscillation magnitude did not bound all cycle designs. Subsequently, the BWROG developed a plant-specific procedure [Reference 23] to replace the generic relationship in NEDO-32465-A between the change in CPR and hot bundle oscillation magnitude. The OPRM setpoint is established or confirmed on a cycle-specific basis.

A Backup Stability Protection (BSP) procedure is also available for situations when the OPRM hardware is out of service. The methodology for developing the exclusion regions in the power / flow map is described in Reference 24, and it illustrates regions where the Dresden procedures specify controlled entry into the region or an immediate scram. The exclusion regions are also established or confirmed on a cycle-specific basis.

4.3.4.1 Solution Description

The instabilities and the solutions devised to detect and suppress them are discussed in References 10 and 12. Dresden has adopted the solution Option III designated as the Oscillation Power Range Monitor (OPRM). The OPRM complies with GDC-12, as discussed in Section 3.1.2.2.3.

The overall design philosophy of the OPRM is to generate an alarm in the control room if it detects core instabilities (based on period-based algorithm only), and when it is armed, to generate an automatic suppression system trip if the instabilities reach an amplitude that could threaten the fuel safety limits. The OPRM augments the existing RPS functions by adding a detect and suppress function and does not remove or replace any of the existing RPS functions or hardware.

The OPRM consists of a microprocessor that takes and analyzes signals from LPRMs. Since LPRMs are evenly distributed throughout the reactor core, they are capable of responding to any neutron flux oscillations that can create an MCPR concern. Individual LPRMs readily respond to a wide variety of normal operating maneuvers and expected events, and are also subject to electrical interference. For these reasons, each OPRM may use multiple LPRMs as a means of maintaining a strong response to a neutron flux oscillation while minimizing the susceptibility to false signals associated with a single LPRM, or may utilize a detection algorithm designed to achieve the same objective. The OPRM is automatically bypassed at high flow or low power conditions, where core instabilities are unlikely to occur, to avoid spurious actuation.

4.3.4.2 Licensing Basis

The licensing basis is to generate a trip signal during oscillations of sufficiently low amplitude to provide margin to the MCPR safety limits for all expected modes of BWR oscillations. The OPRM oscillation recognition algorithm is intended to discriminate between true stability-related neutron flux oscillations and other flux variations that may be expected during plant operation. Extensive evaluation of operating plant data is done to determine the combination of algorithm and OPRM setpoints, which meet the design objectives. The final algorithm/setpoint design is subjected to in-plant testing with the trip function disabled.

The OPRM assures that for BWR fuel designs, this operating mode does not result in specified acceptable fuel design limits being exceeded. The onset of power oscillations for which corrective actions are necessary is reliably and readily detected and suppressed by operator actions and/or automatic system functions, when OPRM is armed.

4.3.4.3 Expected Oscillation Modes

The OPRM is capable of responding to the expected modes of BWR stability-related oscillations. The expected oscillation modes are as follows (Reference 10, Section 6.1):

- Core-wide, in which the average neutron flux in all fuel assemblies oscillates in phase.
- First Order Side-by-Side or a regional oscillation where the neutron flux on one side of the reactor oscillates 180° out of phase with the flux on the other side.
- First Order Processing, a regional oscillation where the axis of zero oscillation amplitude rotates azimuthally, or the two reactor regions of peak oscillation amplitude shift from one location to another at a frequency lower than the oscillation frequency.

Other modes of oscillation are not expected in a BWR.

4.3.4.4 Analysis Approach

The overall objective of the oscillation detection algorithm is to reliably detect expected instabilities at a low magnitude such that mitigation can occur well before the MCPR Safety Limit is exceeded, while avoiding spurious trips during expected neutron flux transients. The algorithm is based on the detection of the three known characteristics that BWR neutron flux oscillations exhibit. These characteristics are the amplitude or absolute magnitude, growth rate, and periodic behavior. Only the period based detection algorithm is used in the safety analysis. The other algorithms provide defense in depth and additional protection against unanticipated oscillations. Details of the algorithm can be found in References 10 and 12.

References 13 describes the process used to calculate a conservative final MCPR value for an anticipated stability-related oscillation. It involves the determination of initial MCPR by a cycle-specific evaluation and the calculation of hot bundle oscillation magnitude. The licensing criterion is met when the final MCPR is greater than the MCPR safety limit. Appropriate reload parameters are checked every cycle to determine the initial MCPR. This methodology provides a conservative means of demonstrating with a high probability and confidence that the MCPR safety limits will not be violated for anticipated oscillations. The use of the MCPR safety limit to provide protection against possible fuel damage is exceedingly conservative (Reference 13, Section 4.5.2).

4.3.4.5 Testing and Verification

The OPRM, which is installed to detect and suppress thermal-hydraulic instabilities, is extensively tested using available data from several BWR plants. After installation, the plant will be operated for one fuel cycle, and until the OPRM Technical Specifications are approved, with the OPRM trip function disabled and the OPRM operation being monitored and tested.

4.3.4.6 Stability Analyses

Stability analyses continue to be performed for the reload cores and fuel designs to validate the boundaries of the administratively controlled regions of the Power-Flow map during operation with and without the OPRM system.

4.3.4.6.1 GNF/GE Stability Model

ODYSY is a best-estimate General Electric (GE) proprietary Engineering Computer Program (ECP) which incorporates a linearized, small perturbation, frequency domain model of the reactor core and associated coolant circulation system. ODYSY has been approved by the NRC for use in all reload validation analyses (Reference 18). The program is used to predict hydrodynamic stability for a single channel and the coupled thermal-hydraulic reactivity stability of a full reactor core.

ODYSY defines an open loop transfer function of the reactor that can be used to evaluate stability characteristics. The major reactor components are modeled using first— principles governing equations. A small perturbation from steady—state is assumed and the effect on each component model is evaluated by linearizing the governing equations. A Laplace Transform of each

linearization is performed and transfer functions are constructed to relate model output to the input variables. Once the open loop transfer function is assembled, its frequency response is calculated and the decay ratio of the system is determined. In addition to the core decay ratio, the thermal-hydraulic stability of individual channels is evaluated. The channel decay ratio is calculated assuming a constant pressure drop across the channel and constant fuel rod heat flux. ODYSY is based on the approved ODYN transient model, including an axial one-dimensional (l-D) kinetics model extended to multiple channel groups. Each channel group represents a collection of individual channels. Channel grouping is based on bundle geometry and power level. ODYSY consists of a reactor kinetics model, a channel thermal-hydraulic model, a recirculation (ex-core) hydraulics model, and a fuel heat transfer model:

- Reactor kinetics model — neutronic parameters are collapsed from a three-dimensional core simulator (PANACEA) wrap-up and evaluated using a 1-D kinetics model which includes void and Doppler reactivity feedback. The power distribution for each channel group is based on the PANACEA conditions.

- Channel thermal-hydraulics model — consistent with other GE design methods, it has a drift flux correlation including subcooled void modeling. The channel model will accommodate axial variation in fuel bundle geometry. The bypass region is also simulated using this model. Pressure drop balancing yields the flow distribution between parallel channel groups.

- Recirculation system model — the upper plenum, steam separators, steam dome, downcomer, and recirculation system are modeled as hydraulic regions. The steam lines and control system are not included in the simulation.

- Fuel heat transfer model — consists of a 1-D radial conduction model for the fuel rod cladding, gap and fuel pellet at each axial node in the channel.

ODYSY has been qualified by comparisons with analytical solutions, alternate approved design codes, plant data from stability testing, and plant data from instability events. Steady—state results have been compared to results from the ISCOR design code for steady—state conditions. Component transfer functions (i.e., fuel heat transfer, channel thermal—hydraulics, ex—core

hydraulics, and kinetics) have been compared with analytical solutions and the results from time domain codes. Integral code tests have been performed to compare ODYSY predictions with the results from licensing basis frequency domain codes, best—estimate time domain codes (i.e., TRACG), and actual plant data from both testing and events. The code uncertainty as well as uncertainties in input and core state have been factored into the accepted ODYSY stability criterion map.

The use of ODYSY calculated core and channel decay ratios is described in Reference 18. The ODYSY application procedure includes an exposure-dependent calculation, with exposure-dependent inputs such as void coefficient, Doppler coefficient, and axial power shape.

4.3.4.6.2 Westinghouse Stability Model

The Westinghouse stability methodology, which is described in References 20 through 22, is based on the RAMONA-3 computer code. The code is used to predict hydrodynamic channel instability and coupled neutronic and thermal-hydraulic instability for a full reactor core.

RAMONA-3 is a three-dimensional, transient, coupled neutronic and thermal-hydraulic code that explicitly models each fuel type in the reactor core. the code is comprised of a neutron kinetics model, a thermal-hydraulic model, a steam line model, and several special models to represent the recirculation loop, the jet pumps, the steam separator, the feedwater sparger, and various plant control and protections systems.

RAMONA has been validated by comparison to plant data from stability testing and from instability events. The application of the methodologies for implementing BWROG long-term solution Option III (detect and suppress), and the backup stability protection in the event the Option III OPRM hardware is unavailable, are described in References 13, 22, 23 and 24.

4.3.5 References

1. Deleted.

2. Ackermann, et al., "High Temperature Vapor Pressure of UO_2," Journal of Chemical Physics, Vol. 25, No. 6, December 1956.

3. Pettus, W.G., and Baldwin, M.N., "Resonance Absorption in U-238 Metal and Oxide Rods", BAW-1244.

4. Hellstrand, E., Nuclear Science and Engineering, No. 8, p. 497, 1960.

5. Engesser, F.C., et al., "PCTR Measurements of the EGCR Fuel Temperature Coefficient," HW-67766, February 1960.

6. Deleted.

7. Deleted.

8. Deleted.

9. Deleted.

10. "BWR Owner's Group Long-Term Stability Solutions Licensing Methodology," General Electric Company, NEDO-31960-A, November 1995.

11. John C. Brons to William T. Russell, "Dresden Stations 2 and 3, Quad Cities Station Units 1 and 2, LaSalle County Station Units 1 and 2, Response to Generic Letter 94-02 (BWR Stability), NRC Dockets 50-237 and 50-249, NRC Dockets 50-254 and 50-265, NRC Dockets 50-373 and 50-374," Commonwealth Edison Company, September 9,1994.

12. NEDO 31960-A, “BWR Owners Group Long-Term Stability Solutions Licensing Methodology,” Supplement 1, November 1995.

13. NEDO-32465-A, “BWR Owners’ Group Reactor Stability Detect and Suppress Solution Licensing Basis Methodology and Reload Application,” August 1996.

14. Deleted.

15. “Fuel Bundle Design Report GE14-P10HNAB408-16GZ-100T-145-T6-2483,” EDB No. 2483, Global Nuclear Fuel, February 2001.

16. “Steady State Nuclear Methods,” General Electric Company, April 1987, Licensing Topical Report, NEDO-30130-A.

17. Letter from Ralph J. Reda to R. C. Jones, Jr., "Implementation of Improved GE Steady-State Nuclear Methods," Letter No. MFN-198-96, July 2, 1996.

18. Licensing Topical Report, "ODYSY Application for Stability Licensing Calculation," NEDC-32992P-A, July 2001.

19. "Siemens Power Corporation Methodology for Boiling Water Reactors: Evaluations and Validation of CASMO-4/MICROBURN-B2," EMF-2158(P), Revision 0, October 1999.

20. "Reference Safety Report for Boiling Water Reactor Reload Fuel," Westinghouse Topical Report CENPD-300-P-A, July 1996.

21. "Thermal-Hydraulic Stability Methods for Boiling Water Reactors," Westinghouse Topical Report CENPD-294-P-A, July 1996.

22. "Thermal-Hydraulic Stability Methodology for Boiling Water Reactors, Westinghouse Topical Report CENPD-295-P-A, July 1996."

23. "Plant-Specific Regional Mode DIVOM Procedure Guideline," GENE Letter OG 04-0153-260, June 15, 2004.

24. "Backup Stability Protection (BSP) for Inoperable Option III Solution," OG 02-0119-260, July 17, 2002.

25. "Fuel Assembly Mechanical Design Methodology for Boiling Water Reactors Supplement 1 to CENP-287," WCAP-15942-P-A, March 2006.

26. "The Advanced PHOENIX and POLCA Codes for Nuclear Design of Boiling Water Reactors," Westinghouse Topical Report CENPD-390-P-A, December 2000.

27. "Generic Topical Report for the ABB Option III Oscillation Power Range Monitor (OPRM)," Licensing Topical Report CENPD-400-P-A, Rev. 001, May 1995.

Table 4.3-1

FUEL ASSEMBLY k_∞ AT VARIOUS BOL CONDITIONS
FOR TYPICAL ENRICHED FUEL

	Assembly k_∞		Control Rod Worth
	Uncontrolled	Controlled	Δ-k_∞/k_∞
Cold (68°F)	1.1282	0.9716	-0.1388
Intermediate (170°F)	1.1227	0.9584	-0.1463
Hot Standby (546°F)	1.1060	0.8932	-0.1924
Hot Operating - 0% Void	1.1024	0.8903	-0.1924
Hot Operating - 40% Void	1.0853	0.8294	-0.2358
Hot Operating - 70% Void	1.0709	0.7654	-0.2853

Tables 4.3-2 through 4.3-6

THESE TABLES HAVE BEEN DELETED INTENTIONALLY

4.4 THERMAL AND HYDRAULIC DESIGN

4.4.1 Design Bases, Criteria, and Operating Limits

4.4.1.1 Design Bases

The design basis for the thermal and hydraulic characteristics of the core is to ensure, in conjunction with the fuel system design, the plant equipment characteristics, the nuclear instrumentation, and the reactor protection system, that no fuel damage will occur during normal or operational transients caused by any reasonably expected single operator error or single equipment malfunction. Fuel damage is defined in Section 4.2.1.1.

The above design basis is used both for core design and for determination of operating limits.

4.4.1.2 Fuel Damage Limits

Two principal mechanisms could cause fuel damage during reactor transients: cladding overheating due to inadequate cooling and excess cladding strain due to UO_2 pellet expansion. Each of these mechanisms has a corresponding design limit to ensure that fuel damage will not occur. The fuel damage limit to prevent cladding overheating is conservatively defined as the onset of transition boiling. The fuel damage limit to prevent excess cladding strain is defined as 1% plastic strain of the Zircaloy cladding. A further discussion of these limits is provided in Section 4.2.1.1. These fuel damage limits are also employed in the development of operating limits to control reactor operation.

4.4.1.3 Design Criteria, Operating Basis, and Operating Limits

4.4.1.3.1 Design Criteria

The design criteria developed to implement the preceding design bases are discussed in Sections 4.4.1.3.1.1 through 4.4.1.3.1.3. The conditions addressed in these sections correspond to reactor pressures above 800 psia and core flows above 10% of rated. The cases of reactor pressures at or below 800 psia or core flows at or below 10% of rated are addressed in Section 4.4.4.2.1.

4.4.1.3.1.1 Minimum Critical Power Ratio

The onset of transition boiling results in a decrease in heat transfer from the cladding and, hence, an elevated cladding temperature and the possibility of fuel damage. However, the attainment of critical power, i.e., transition boiling, is not a directly observable event in an operating reactor. The margin to transition boiling

is calculated from plant operating parameters such as core power, core flow, feedwater temperature, and core power distribution. The margin for each fuel assembly is characterized by the critical power ratio (CPR), i.e., the ratio of the fuel assembly power which would produce onset of transition boiling divided by the actual fuel assembly power. The minimum (most limiting) value of this ratio among all fuel assemblies in the core is the minimum critical power ratio (MCPR).

4.4.1.3.1.2 Fuel Cladding Integrity Safety Limit MCPR

The fuel cladding is one of the physical barriers which separate radioactive materials from the environment. The integrity of this barrier is associated with its relative freedom from perforations or cracking. Although some corrosion or use-related cracking may occur during the life of the cladding, fission product migration from such cracking is incrementally cumulative and continuously measurable. Fuel cladding perforations, however, can result from thermal stresses which occur from reactor operation significantly above design conditions and protection system safety settings.

While fission product migration from thermally caused cladding perforations is just as measurable as that from use-related cracking, the occurrence of such cladding perforations signals a threshold beyond which still greater thermal stresses may cause gross, rather than incremental, cladding deterioration. Therefore, to prevent the possibility of sudden fuel damage, a fuel cladding integrity safety limit MCPR (or safety limit MCPR) is defined with margin to the conditions which would produce onset of transition boiling (MCPR of 1.0). These conditions significantly depart from the condition intended by design for planned operation.

The fuel cladding integrity safety limit MCPR is established such that no calculated fuel damage shall result from an anticipated operational occurrence (AOO). The basis of the values derived for this safety limit for each fuel type is documented in topical reports listed in the Technical Specifications.

Because fuel damage by overheating of cladding (defined in Section 4.2.1.1 as onset of transition boiling) is not directly observable, a step-back approach is used to establish this safety limit such that the MCPR for any AOO is no less than the fuel cladding integrity safety limit MCPR. The fuel cladding integrity safety limit MCPR is sufficiently conservative to assure that in the event of an AOO initiated from the normal operating condition, at least 99.9% of the fuel rods in the core would not experience transition boiling.

The margin between MCPR of 1.0 (onset of transition boiling) and the safety limit MCPR is derived from a detailed statistical analysis considering all uncertainties in monitoring the core operating state, including uncertainty in the critical power correlation. The critical power correlation is an empirical representation of the assembly coolant conditions at which transition boiling has been experimentally detected. Because the critical power correlation is based on a large quantity of full-scale test data, there is very high confidence that operation of a fuel assembly at the condition of MCPR equal to the fuel cladding integrity safety limit MCPR would not produce transition boiling.

Even if transition boiling were to occur, cladding perforation would not be expected. Significant test data accumulated by the NRC and private organizations indicate that BWR fuel can survive for an extended period in an environment of transition boiling.

If reactor pressure during normal power operation should ever exceed the limit of applicability of the critical power correlation, it would be assumed that the fuel cladding integrity safety limit MCPR was violated. This applicability pressure limit is higher than the pressure safety limit specified in the Technical Specifications.

4.4.1.3.1.3 Maximum Linear Heat Generation Rate

The MLHGR limits are steady state limits and have been defined to provide margin between the steady state operating conditions and any fuel damage condition to accommodate uncertainties and to assure that no fuel damage results even during the worst anticipated transient condition at any time in life.

4.4.1.3.2 Operating Basis

Based on the preceding design criteria, the operating basis for the thermal and hydraulic characteristics of the core design is to control the local power density to levels such that the fuel assembly powers are maintained within the critical power limits.

The basis of the steady-state MCPR and MLHGR limits is to provide sufficient margin to accommodate uncertainties and to ensure that the fuel damage limits would not be exceeded during transients caused by any reasonably expected single operator error or single equipment malfunction.

4.4.1.3.3 Operating Limits

The following operating limits are used during normal steady-state operation: the MCPR is maintained no less than the-, operating limits specified in the Core Operating Limits Report, and the linear heat generation rate (LHGR) is maintained no higher than the SLHGR for each fuel type stated in Section 4.2.3.1.2 (detailed curves are specified in the Core Operating Limits Report). Note that the above statement does not specify the operating power nor does it specify peaking factors; these parameters are controlled by the operator subject to a number of constraints, including the thermal limits given above.

4.4.2 Description of Thermal and Hydraulic Design of the Reactor Core

4.4.2.1 Fuel Cladding Integrity Safety Limit MCPR

The value of the fuel cladding integrity safety limit MCPR is generated by statistical analyses of the core near limiting conditions, as described in Section 4.4.4.1.1. This safety limit applies not only to core-wide transients but also conservatively to the localized rod withdrawal error transient.

Calculation of the operating limit MCPR (defined in Section 4.4.1.3.3) is addressed in Section 4.4.4.1.2.

4.4.2.2 Operating Limit Linear Heat Generation Rate

The MLHGRs for normal steady-state operation for various fuel types are discussed in Section 4.2.3.1.2 (detailed curves are specified in the Core Operating Limits Report which is in the Dresden Technical Requirements Manual).

4.4.3 Description of the Thermal and Hydraulic Design of the Reactor Coolant System

The Dresden reactor design employs variable recirculation flow control, which provides some degree of load following capability. The operating range is limited, however, by certain restrictions due to recirculation pump net positive suction head (NPSH), overall plant control characteristics, core thermal power limits, etc., as discussed in the following subsections.

4.4.3.1 Operating Map

The normal operating range for Dresden Units 2 and 3 under Extended Power Uprate conditions is shown schematically on a typical power-flow map in Figure 4.4-1. These figures are shown for illustrative purposes and are not necessarily accurate for the current operating cycles. Plant equipment, nuclear instrumentation, and reactor protection system, in conjunction with operating procedures, maintain operations within the allowable regions of this map for normal operating conditions. The boundaries, flow control lines (FCLs), and regions on this map are discussed in the following Sections 4.4.3.1.1 through 4.4.3.1.10.

4.4.3.1.1 Natural Circulation Line

The operating state for the reactor moves along the natural circulation line in the absence of recirculation pump operation.

4.4.3.1.2 Minimum Pump Speed Line

Startup of the unit is normally carried out with the recirculation pumps operating at minimum speed, or approximately 30% speed. The operating state for the reactor follows the minimum pump speed line for normal control rod withdrawal with the recirculation pumps held at minimum speed.

4.4.3.1.3 100% Flow Control Line

The 100% FCL passes through 100% power at 100% flow. The operating state for the reactor closely follows this line for rapid flow changes at a fixed control rod pattern that corresponds to 100% power at 100% flow. The line is based on constant xenon concentration.

4.4.3.1.4 Other Flow Control Lines

The other FCLs shown in Figure 4.4-1 represents part of a family of FCLs with control rod patterns corresponding to less than 100% power at 100% flow. During plant startup, a FCL is followed as the recirculation pump speed is increased above the minimum speed with a fixed control rod pattern.

4.4.3.1.5 APRM Rod Block Line

The APRM rod block line is established to limit the power increases due to possible inadvertent control rod withdrawal to values which avoid fuel damage. It is dependent on W_D, defined as the percentage of the drive flow required to produce a rated core flow of 98 Mlb/hr.

4.4.3.1.6 Constant Pump Speed Line

The Constant Pump Speed Line is not analyzed for EPU conditions.

4.4.3.1.7 Cavitation Interlock Line

The Cavitation Interlock Line results from the recirculation pump NPSH requirements. The static head alone does not provide sufficient NPSH for the recirculation pumps. However, during normal operation, the feedwater subcools the inlet flow to the recirculation pumps to prevent cavitation. Equipment automatically reduces the speeds of the recirculation pumps to the minimum speed when the feedwater flow drops below a preset level.

4.4.3.1.8 Extended Load Line Limit Analysis Region

The extended load line limit analysis (ELLLA) provides a basis to support plant normal operation in the region of the power-flow map above the 100% FCL and bounded by the APRM rod block line and the 100% rated power line. The ELLLA region provides operating flexibility to permit flow compensation for xenon buildup following startups and for fuel depletion later in the cycle and to improve the efficiency of achieving and maintaining 100% power.

All anticipated transient and loss-of-coolant accident (LOCA) analyses performed for cycle operation support operation in the ELLLA region. Note that the maximum allowed operating point on the APRM rod block line (highest thermal power allowed at a reduced core flow) is the point at 100% power and approximately 87% flow.

For operation with EPU, the ELLLA region has been extended to MELLLA.

4.4.3.1.9 Maximum Extended Load Line Limit Analysis Region

The maximum extended load line limit analysis (MELLLA) is applicable to Extended Power Uprate operation only, and is shown on power-flow Figure 4.4-1. MELLLA provides a basis to support plant normal operation in the region of the power-flow map above the 100% FCL and bounded by the MELLLA Upper Boundary and a rated power of 2957 MWt. The MELLLA region provides operating flexibility to permit flow compensation for xenon buildup following startups and for fuel depletion later in the cycle while improving the efficiency of achieving and maintaining 100% power.

All anticipated transient and loss-of-coolant accident (LOCA) analyses performed for cycle operation support operation in the MELLLA region.

4.4.3.1.10 Region of Potential Thermal-Hydraulic Instability

The region of potential thermal-hydraulic instability is evaluated every cycle and typically consists of a portion of the area above the 55% flow control line and less than 55% of rated core flow. Continuous operation in this region is not permitted because of the possibility of neutron flux oscillations.

4.4.3.2 Application of Thermal Hydraulic Design to Plant Operation

The following simplified description of operation of a BWR with recirculation flow control summarizes the principal steps of normal unit startup.

Assuming the unit to be in a hot standby condition, full power operation is ordinarily approached by increasing power with control rod withdrawal (with the recirculation pumps at minimum speed) until approximately 25% - 30% of rated core thermal power is reached. The initial power increase must be via control rod withdrawal, rather than recirculation pump speed increase, until the feedwater flow has reached approximately 20%. An interlock prevents low-power, high-recirculation flow combinations which can lead to recirculation pump NPSH problems.

Once greater than 20% feedwater flow is obtained, the operator is free to increase power by increasing recirculation pump speed as well as by further withdrawing control rods. Core flow is then increased in order to avoid the region with potentially less margin of stability. Control rod withdrawal is resumed until the desired FCL is reached. From this point, power is increased by increasing the core flow until rated core flow is reached. The recirculation pump speeds may be controlled individually or by using a master flow controller which controls both pumps simultaneously.

When recirculation pump speed is changed without rod motion, the power and flow follow one of a family of FCLs. These lines are not followed perfectly due to xenon buildup or burnout/decay in the core during power changes. Operation above the 100% FCL is permitted in the MELLLA region as shown in Figure 4.4-1 (see Section 4.4.3.1.9), which allows operators to anticipate and compensate for the effects of xenon buildup during power increases.

For SVEA-96 Optima2 reloads, the basis for coastdown operation is provided in the cycle-specific reload licensing report. The approval of Westinghouse BWR reload analysis methodology described in Reference 1 treats cycle extension strategies such as end-of-cycle coastdown operation as an operating flexibility option.

4.4.4 Evaluation

The following describes the methods for evaluating the design limits and operating limits. Section 4.4.4.1 describes the evaluation of the fuel cladding integrity safety limit MCPR and the operating limit MCPR. Section 4.4.4.2 describes the evaluations for other Technical Specification limits.

4.4.4.1 Fuel Cladding Integrity Safety Limit MCPR and Operating Limit MCPR Calculation Procedure

The following subsections describe the statistical methodology for calculating safety limit and operating limit MCPRs.

4.4.4.1.1 Safety Limit MCPR – Westinghouse Methods

Section 5.3.2 of Reference 1 provides the Westinghouse methodology for establishing the safety limit. The methodology is general and acceptable for design and licensing for all BWR cores containing Westinghouse fuel as well as for mixed cores containing both Westinghouse fuel and non-Westinghouse fuel assemblies. The safety limit MCPR (SLMCPR) is established to provide that at least 99.9% of the fuel rods avoid boiling transition. The SLMCPR for Westinghouse fuel, which is evaluated on a cycle-specific basis, is determined by statistically convoluting the uncertainties associated with the calculation of CPR. These uncertainties include core power, system pressure, inlet temperature, core flow, manufacturing tolerances of the fuel assembly components, assembly power, internal power distribution, the calculation of the core flow distribution, and the CPR correlation itself.

4.4.4.1.2 Operating Limit MCPR Calculation – Westinghouse Methods

Section 7.3.3 of Reference 1 provides the Westinghouse methodology for establishing the operating limit MCPR (OLMCPR). The cycle-specific OLMCPR is established to ensure that the SLMCPR is not exceeded for any moderate frequency event (anticipated operational occurrence). This limit is established by adding the maximum ΔCPR value for the most limiting transient postulated to occur from rated conditions to the SLMCPR.

4.4.4.1.3 MCPR Limit Calculation – GE Method

For GNF fuel GESTAR II (Reference 2) provides the basis for determining the safety limit and operating limit MCPR.

4.4.4.2 Additional Evaluation of Technical Specification Limits

The information in this section is intended to support the limits set forth in the Technical Specifications. This discussion demonstrates the margins existing between conditions of potential safety concern and conditions to which the unit is limited, either by nature or by protective device action.

4.4.4.2.1. Core Thermal Power Limit (Reactor Pressure At or Below 800 psia or Core Flow At or Below 10% of Rated)

At pressures at or below 800 psia, the core elevation pressure drop (zero power, zero flow) is greater than 4.56 psi. At low powers and flows this pressure differential is maintained in the bypass region of the core. Since the pressure drop in the bypass region is essentially all elevation head, the core pressure drop at low powers and flows will always be greater than 4.56 psi. Analyses show that with a fuel assembly flow of 28×10^3 lb/hr, fuel assembly pressure drop is nearly independent of fuel assembly power and has a value of 3.5 psi. Thus, the fuel assembly flow with a 4.56-psi driving head will be greater than 28×10^3 lb/hr.

Full-scale ATLAS test data taken at pressures from 14.7 psia to 800 psia indicate that the fuel assembly critical power at this flow is approximately 3.35 MWt. At 25% of rated thermal power, the peak powered fuel assembly would have to be operating at 3.84 times the average powered fuel assembly in order to achieve this assembly power. Thus, a core thermal power limit of 25% for reactor pressures at or below 800 psia is conservative.

4.4.4.2.2 Limiting Safety System Settings

The Technical Specifications include limiting safety system settings (LSSSs). The LSSSs related to the core thermal safety limit include the reactor high pressure scram and the high neutron flux (APRM) scram. The LSSSs that provide further conservative protection include the APRM rod block and the turbine stop valve closure anticipatory scram.

In the analyses for these LSSSs, the assigned trip values are intended for use in normal operation. They are not set to the maximum levels that would be allowed by the assumed safety limit.

The APRM scram trip setting is selected to provide adequate margin to the fuel cladding integrity safety limit MCPR and yet allow operating margin to reduce the possibility of unnecessary scrams. AOO analyses demonstrate that the scram trip setting, together with other reactor protection settings, protects against the violation of the MCPR safety limit. The high pressure scram is available as a backup protection to the high flux scram. These LSSSs are addressed in Section 7.2.

The APRM system provides a control rod block to prevent gross control rod withdrawal at any recirculation flowrate to provide protection against exceeding the fuel cladding integrity safety limit MCPR. This rod block trip setting, which is automatically varied with recirculation loop flowrate, prevents an increase in the reactor power level to excessive values due to control rod withdrawal. The flow variable trip setting provides substantial margin from fuel damage, assuming a steady-state operation at the trip setting, over the entire recirculation flow range. The APRM rod block maximum setting is addressed in Section 7.6.

The turbine stop valve closure scram trip anticipates the pressure, neutron flux, and heat flux increases that could result from the rapid closure of turbine stop valves. With the Technical Specification scram trip setting, the resultant increase in surface heat flux is limited such that the MCPR remains above the fuel cladding integrity safety limit MCPR even during the worst-case transient that assumes the turbine bypass is closed. This anticipatory scram is addressed in Section 7.2.

Both the reactor protection system and the reactor's inherent physical characteristics prevent exceeding safety limit conditions. Normal steady state and transient operating conditions do not exceed the operating limit MCPR, the LHGR, and the MAPLHGR specified in the Core Operating Limits Report. Slow increases in power would be terminated by the action of pressure scram, flux scram, or rod block (in the case of rod withdrawal).

4.4.4.2.3 Power Transient

During an operating transient, the heat flux lags behind the neutron flux due to the inherent heat transfer time constant of the fuel, which is 8 to 9 seconds. Also, the LSSSs are at values which do not allow the reactor to be operated above the safety limit during normal operation or during analyzed abnormal operating situations. For normal operating transients, the neutron flux transient is terminated by scram before a significant increase in surface heat flux occurs. Control rod scram times are checked as required by the Technical Specifications.

Analyses of normal turbine or generator trips, which are among the most severe normal operating transients expected, show that if a flux scram occurs such that the period of time when the neutron flux stays above the LSSS is less than 1.7 seconds, the safety limit will not be exceeded. These analyses show that even if the bypass system fails to operate, the design limit of MCPR equal to the fuel cladding integrity safety limit MCPR would not be exceeded.

During periods when the reactor is shut down, consideration must be given to water level requirements due to the effect of decay heat. If the reactor water level should drop below the top of the active fuel during this time, the ability to cool the core would be reduced, which could lead to excessive cladding temperatures and cladding perforation. The core would be cooled sufficiently to prevent clad melting should the water level be reduced to two-thirds the core height. Establishment of the safety limit at 12 inches above the top of the fuel provides adequate margin. This level is continuously monitored whenever the recirculation pumps are not operating.

During rapid power increases, the neutron flux may exceed the scram level by a considerable amount, but the resulting scram would be sufficiently fast that the heat flux would either decrease or exceed the initial value by only a small amount.

The potential transient events of BWRs have been reviewed by GNF/GE to determine the extent of analyses necessary for licensing the reload core. These events have been dispositioned as described in GESTAR (NEDE-24011-P-A). The events were dispositioned as not applicable, consequences of an event bounded by a different event, or analysis necessary for reload licensing.

The transients most likely to limit operation because of MCPR considerations are:

A. Turbine trips or generator load rejection without bypass (Section 15.2);

B. Loss of feedwater heating (Section 15.1.1) or inadvertent HPCI startup (Section 15.5.1);

C. Feedwater controller failure (to maximum demand) (Section 15.1.2);

D. Control rod withdrawal error (Section 15.4);

E. Fuel Bundle Loading error (Sections 15.4.7 and 15.4.8)

The analyses presented in these referenced sections show the capability of the protection system and the inherent reactor characteristics to prevent approach to the safety limit conditions. Practically, it is virtually impossible for the reactor to reach the assumed safety limit conditions.

4.4.4.2.4 Single-Loop Operation

For reactor operation with only one recirculation pump running (single-loop operation), the fuel cladding integrity safety limit MCPR is increased by an amount specified in the Technical Specifications. This increase accounts for increased uncertainties in core flow and transversing incore probe (TIP) instrumentation measurements for single-loop operations.

Analyses by GNF has demonstrated that transient events during single-loop operation are bounded by those at rated conditions. However, due to the increase in the fuel cladding integrity safety limit MCPR in single-loop operations, an equivalent adder must be uniformly applied to the operating limit MCPR to maintain the same margins to the safety limit MCPR.

During single-loop operation, the normal drive flow relationship during dual-loop operation is changed. This change is the result of reverse flow through the idle loop jet pumps when the active loop recirculation pump speed is above 40% of rated speed. Some of the active-loop flow is diverted from the core and backflows through the idle-loop jet pumps; hence, the core receives less flow than would be predicted based upon the dual-loop drive-flow-to-core-flow relationship. Therefore, the APRM flow-biased scram and rod block settings must be altered for single loop operation; otherwise, the new drive-flow-to-core-flow relationship would nonconservatively result in flow-biased trips occurring at neutron fluxes higher than normal for a given core flow.

4.4.5 Testing and Verification

Testing and verification were performed initially and are performed following each reload to confirm that the thermal and hydraulic characteristics of the core and the reactor coolant system are in accordance with design values and will remain within required limits throughout core lifetime. A description of startup testing is presented in Chapter 14.

4.4.6 Instrumentation Requirements

The functional requirements for the instrumentation employed in monitoring and measuring those thermal-hydraulic parameters important to safety are addressed in Sections 7.2, 7.5, and 7.6.

4.4.7 References

1. Reference Safety Report for Boiling Water Reactor Reload Fuel," Westinghouse Topical Report CENPD-300-P-A, July 1996.

2. Licensing Topical Report, "General Electric Standard Application for Reactor Fuel", NEDE-24011-P-A-14, June, 2000.

Tables 4.4-1 and 4.4-2

THESE TABLES HAVE BEEN DELETED INTENTIONALLY

4.5 REACTOR MATERIALS

4.5.1 Control Rod Drive System Materials

Control rod drive system materials are discussed in Section 4.6.

4.5.2 Reactor Internals Materials

The major internal components of the reactor include the control rod guide tubes; incore neutron monitors; shroud and other internal core support structures; steam separators; steam dryers; jet pumps; and the feedwater, core spray, and standby liquid control spargers and nozzles. This section does not cover the fuel assemblies, control rods, or incore neutron monitors; these components are discussed in Section 4.2, 4.6, and 7.6, respectively.

The following subsections describe the materials and welding methods used for reactor internals. A further description of reactor internals, including steam separators and steam dryers, is included in Section 3.9.5 and Section 6.1.

4.5.2.1 Structural Components

The materials used for the structural members of the reactor internals are listed below:

A. Shroud - Type 304 stainless steel
Shroud tie rod with spring stabilizers - 316/316L, XM-19 stainless steel and X-750 nickel base alloy,

B. Core top grid - Type 304 stainless steel,

C. Core bottom grid - Type 304 stainless steel,

D. Fuel support piece - Type 304 stainless steel,

E. Baffle plate - Inconel,

F. Baffle plate supports - Inconel,

G. Control rod guide tubes - stainless steel, and

H. Incore nuclear instrumentation tubes - stainless steel.

All reactor internal structural members located in high flux regions are constructed of Type 304 stainless steel.

The baffle plate and inner rim are made of Inconel to permit welding to the ferritic base metal of the reactor vessel. The welded joints that attach the baffle plate to the vessel wall were made in the vessel fabrication shop in a highly controlled operation. The bottom of the shroud is welded on top of the rim, which provides for the differential expansion between the ferritic, Inconel, and stainless steel

components. This welded joint was made in the field and was dye penetrant checked to ensure the weld integrity. Inconel legs welded at intervals around the baffle plate support it from the vessel bottom head.

4.5.2.2 Jet Pump Assemblies

The jet pump assemblies are made of Type 304 stainless steel except the following:

A. To accommodate the clamping loads generated in holding the inlet-throat subassembly in place, the beam is fabricated from Inconel X-750. Properly heat-treated, this high-strength, nickel-chromium-iron alloy exhibits good stress corrosion crack resistance in the reactor environment. As discussed in Section 5.4, jet pump parameters are monitored to detect integrity or operability problems which could indicate possible jet pump beam cracking.

B. The jet pump assembly contains one slip joint which permits removal of the inlet-throat subassembly. Both contacting surfaces utilize Stellite-6 with a minimum Rockwell hardness of RC-30 to prevent wear in the mating parts.

C. The spring used in the restrainer wedge device is Inconel X-750 which has the higher strength properties necessary for desirable spring forces.

D. Some stainless steel members which are threaded or otherwise bear against other stainless steel parts are surface hardened by nitriding to prevent galling. Nitriding, a process whereby nitrogen is diffused into the base material, provides a thin, wear-resistant layer (up to 0.007 inch thick) with a minimum hardness of 90 on the Rockwell 15 N scale.

The diffuser section of each jet pump is attached to the baffle plate by an adapter ring which is welded to the diffuser and to the baffle plate. The latter weld, a field weld, was dye penetrant checked on the first pass, halfway through the weld and on the finish surface weld to ensure its integrity. The seal ring is made of Inconel X.

4.5.2.3 Spargers and Spray Nozzles

The following sparger assemblies are part of reactor internals:

A. Core spray sparger

The spray sparger, spray nozzles, and the core structure supporting the spray spargers are all made of Type 304 stainless steel.

B. Feedwater sparger

Dresden Units 2 and 3 use General Electric triple-sleeve sparger assemblies. The materials are selected to optimize performance, to

minimize the potential for component failure, and to comply with the intent of Regulatory Guide 1.44, "Control of the Use of Sensitized Stainless Steel."

The sparger pipe, reduced tee, adapter, elbow, and orifice are all Type 304 stainless steel. The end plates and the extension on the reducing tee are Type 316L stainless steel. The sparger brackets are CF-3 cast stainless steel. Welding was done using 308L welding rod, and the whole assembly was solution-heat-treated after welding. The bracket pin and its stop are Type 304 stainless steel and were solution-heat-treated after machining. The brackets were welded to the end plates in the field to allow matching as-built dimensions. All field welds are made on 316L or CF-3 material.

The thermal sleeve is made of Inconel 600 and Type 316L stainless steel. The upstream portion which contacts the safe end is made of Inconel 600, which was purchased with a carbon limit of 0.1%. This portion of the thermal sleeve contains the mechanical grooves for the two seal rings. The coefficient of thermal expansion of Inconel 600 is close to that of the carbon steel safe end. Therefore, the use of Inconel 600 facilitates maintenance of an interference fit with the safe end and provides good corrosion resistance.

The triple-wall concentric sleeves are 316L stainless steel with a maximum limit of 0.02% carbon. Choice of this low-carbon alloy was made to prevent stress corrosion cracking, since solution-heat treatment was not feasible after assembly by welding.

Welds of Inconel 600 to Inconel 600 and Inconel 600 to Type 316L stainless steel are made with Inconel 82 welding material using the gas tungsten arc welding process. Welding of 316L to 316L components are done with 308L material.

The seal rings are made of Inconel 600, annealed at 2075 ± 25°F for optimum resistance to stress corrosion. They are machined from forged rings to ensure good dimensional control.

The backup springs used to increase the sealing pressure of the rings are made of Inconel X-750. The springs were initially stressed at 65,000 psi. This alloy was selected because of its high yield strength at 550°F of approximately 135,000 psi, permitting applied stress to be limited to 0.48 of yield.

C. Standby liquid control sparger

The standby liquid control sparger is made of stainless steel.

4.6 FUNCTIONAL DESIGN OF REACTIVITY CONTROL SYSTEMS

There are four elements of reactivity control: neutron-absorbing control rods; neutron-absorbing elements in the fuel; recirculation flow control; and standby liquid control system. The contribution of the standby liquid control system and recirculation flow control to reactivity control is partly discussed in Section 4.6.2, but other aspects of the systems are addressed in detail in sections 9.3.5 and 5.4.1, respectively. The fuel is addressed in Section 4.2. This section addresses the control rods and the control rod drive (CRD) system.

4.6.1 Design Bases

The control rod drive (CRD) system is designed to control reactor power and power changes during startup/shutdown and power operations by making gross power changes in core reactivity through incremental positioning of neutron absorbing control rods within the reactor core in response to manual control signals. The CRD system works in combination with the recirculation system to control overall reactor core reactivity.

The control rod drive system is designed to have adequate reactivity shutdown margin under normal operating conditions. (See Section 4.4.3.)

The CRD system will rapidly shut down the reactor (scram) in emergency situations by rapidly inserting withdrawn control rods into the core in response to a manual or automatic signal. The CRD system works in combination with the reactor protection system (RPS) which monitors reactor core parameters. If conditions cause these parameters to exceed predetermined limits, the RPS logic will initiate a scram.

The inherent reactor safety features described in Section 4.4 along with the control rod velocity limiters, control rod drive housing supports and the reactivity control system described in this section, assures that the consequences of a unplanned nuclear excursion, caused by any single component failure within the reactivity control system itself or operator error, will not damage the reactor primary coolant system.

4.6.2 Reactivity Control Methods

The control rods are used for flux shaping and for coarse reactivity control, such as startup, shutdown, and power changes. They are also used to compensate for reactivity changes caused by fuel and gadolinia depletion. The fuel rods contain a burnable neutron absorber (gadolinia) which is mixed with the fuel to aid in maintaining a consistent flux shape and to provide sufficient shutdown margin.

The recirculation flow control system modulates the void fraction, and accomplishes fine reactivity control with no control rod movement.

The standby liquid control system is a redundant shutdown method used in the unlikely event of a control rod system malfunction or in an anticipated transient without scram (ATWS).

4.6.2.1 Control Rods

4.6.2.1.1 Standard GE Control Blade

The standard GE control blade is shown in Figure 4.6-1. The original equipment manufacturer (OEM) supplied control blades are referred to as Duralife 100 (D-100) control blades. Duralife 120 (D-120) are OEM blades with improved tubing materials. Both are standard GE control blades. The cruciform-shaped control blades contain a number of vertical stainless steel tubes filled with boron carbide (B_4C) powder. Boron carbide is a preferable neutron absorber material because boron-10 (B-10) has a very large absorption cross section, approximately 3800 barns, in the thermal energy range. Boron carbide is also able to withstand high temperatures. The boron carbide powder is compacted to approximately 70% of theoretical density. A free volume of approximately 30% is provided in each tube as a plenum for helium from the B(n, α)Li reaction. Plugs are welded into the ends of the tubes to seal them.

The tubes are held in cruciform array by a stainless steel sheath extending the full length of the poison section. A cruciform-shaped top casting and handle aligns the tubes and provides structural rigidity at the top of the control blade. Rollers attached to the top casting maintain the spacing between the control blade and the fuel assembly channels. A similar connector casting which incorporates the blade velocity limiter is located at the bottom of the control blade and contains rollers to position the lower part of the control blade in the control rod guide tube located below the core. These bottom rollers always remain in the guide tube during operation. A coupling at the bottom of the control blade is connected and locked to the control rod drive (CRD) index tube by an expandable ball and socket joint.

4.6.2.1.2 General Electric Control Rod Assemblies

A cross section of the GE Hybrid I control rod (HICR) known as Duralife 160 (D-160) is shown in Figure 4.6-2. The HICR design configuration (e.g., upper handle, velocity limiter, and coupling socket) is similar to the standard GE control blade assembly (Figure 4.6-1). However, the HICR-type control blade has three solid uncladded hafnium neutron absorber rods in the tip position of each wing. Based on statistical analysis, the negative reactivity worth of the HICR-type control blade is equivalent to the standard GE all-B_4C control blade. Hafnium and its daughter products have a large absorption cross section for thermal neutrons and several large resonance cross sections at slightly higher energies. The capture of neutrons by hafnium-177 leads to the formation of hafnium-178, which leads to the formation of hafnium-179, and so on. Hafnium-177, 178, and 179 all have similar high absorption cross sections for thermal neutrons and, consequently , the worth of hafnium remains constant for a long time. Moreover, hafnium is less susceptible to swelling than B_4C due to its low thermal expansion coefficient and lack of internal helium pressure buildup (no B[n,α]Li reaction). When exposed to high temperatures, steam, and radiation, hafnium is not readily susceptible to corrosion.

The hafnium rods have a diameter of 0.188 inches and a length of 143 inches. The dimensions of the B_4C encapsulating tubes are similar to the tubes in the standard GE control blade. Since hafnium is a heaver material than B_4C, the sheath wall thickness is reduced from 0.056 inches to 0.045 inches to maintain the same weight as the standard GE control blade, approximately 218 pounds. Also, the overall blade width is reduced by 0.022 inches and, in turn, results in an increase in clearance. These factors ensure similar insertion times as the standard GE control blades during a scram. In addition, the roller and pin assemblies at the top and bottom end of the blades are made of noncobalt alloys. Therefore, the roller-and-pin assembly is less of an activation and radioactive waste concern than the standard GE control blades.

The Advanced Longer Life Control Rod design (ALLCR) (also known as the Duralife 190 control rod) is an extension of the HICR design. It is designed to increase control rod assembly life and to eliminate cracking of absorber tubes containing B_4C. This design is also compatible with reactor internals and existing site equipment. The ALLCR design differs from the HICR only in the following areas:

A. There is a 6-inch long hafnium plate in the top portion of each blade wing. The hafnium plate increases blade lifetime since the blade tip generally experiences the highest neutron flux.

B. There is a modified velocity limiter which weighs approximately 20 pounds less than the original design to compensate for the additional weight of the hafnium absorber plates. Scram and withdrawal performance, however, is maintained.

C. The overall weight is slightly less than the weight of either the standard GE blade or the HICR design due to the lighter velocity limiter. The reduction in weight does not adversely affect rod drop velocity or scram times. The new design results in average drop velocities of less than 2.78 ft/s at operating conditions which is bounded by the design basis value of 3.11 ft/s. Both velocities are bounded by the 3.11 ft/s drop velocity assumed in the rod drop accident analysis (see Section 15.4.10).

All other features of the HICR are retained, such as the high-purity, Type 304 stainless steel B_4C absorber rod tubing, the full-length hafnium rods in each wing, and the noncobalt pin-and-roller material.

A further advancement of the Duralife 190 control rod is the Duralife 230 control rod. These control rods are the same except the volume of absorber material (B_4C and Hafnium) is greater in the Duralife 230 control rod, extending the control rod life.

Another advancement in GE control blade design is the Marathon (Figure 4.6-3a). The primary difference between the Marathon control blade and the previously approved GE design is the use of externally-square tubes that are welded full length to each other to form the four wings. Each wing is comprised of 14 tubes with each tube acting as an individual chamber to hold the encapsulated B_4C and/or hafnium rods. The four wings are then welded to the tie rod to form the cruciform-shaped member of the control rod.

The square absorber tubes are circular inside and are loaded with either B_4C in thin-walled capsules or hafnium metal rods of varying lengths. Some of the square absorber tubes that contain B_4C capsules are also loaded with empty capsules to accommodate the helium release from B_4C. The square absorber tube material is high purity RAD RESIST 304S stainless-steel that is similar to the material used in previous GE designs except that two alloying components are added to provide additional resistance to irradiation-assisted corrosion cracking. These design features allow the Marathon to have an enhanced lifetime compared to the previous GE control blade designs.

The Marathon design is considered a matched in reactivity worth to the OEM control blades design, which means that the reactivity is within 5% of the original equipment design and thus no additional consideration need to be applied in core design or analysis.

The velocity limiter on the Marathon control blades is composed of a cast vane section and matched/welded parts. This configuration maintains critical parameters to ensure compliance with the drop speed limit of 3.11 ft/s assumed in the rod drop accident analysis (Section 15.4.10).

4.6.2.1.3 ASEA-ATOM Control Blade

The Westinghouse ATOM AB, formerly ASEA ATOM, manufactured control blades (Figure 4.6-3) are very similar to standard GE control blades. The cruciform absorber section is formed by four solid stainless steel sheets intermittently welded together at the center. The intermittent center weld-joint ensures straightness and required stiffness while permitting 28 cutout sections which result in significant weight savings. The blade

wings are 0.317 inches thick. Each wing has 454 horizontally drilled holes which are 0.236 inches in diameter and are spaced at a pitch of 0.315 inches.

There are five types of ASEA-ATOM blades. Type 1 contains only B_4C powder as the absorber material in holes 4.055 inches deep. Type 2 is very similar to Type 1 except that the holes in the upper 6 inches contain hafnium metal rods instead of B_4C powder. Types 3 and 4 are very similar to Type 2 except that the absorber holes are 3.583 inches and 3.425 inches in depth, respectively, resulting in a reactivity worth closely matched to that of the standard GE control blade. The horizontal holes of the control blades, except the top 6 inches of the hafnium-tipped control blades, are filled with B_4C powder by vibratory compaction to a packing density of 70% of the theoretical density. The holes are closed at the outer blade edge by a stainless steel cover bar but are connected through a narrow slot. This slot allows He gas pressure equalization between the absorber holes without any significant displacement of the B_4C powder. The horizontal holes also minimize the effect of any further B_4C densification after initial filling. Type 5 blades are identical to the Type 2 blades with the exception that the top 6 inches of the stainless steel cover bar is replaced with a stainless-steel-clad hafnium-filled bar. The hafnium-filled cover bar provides better reactivity matching with the standard GE control blade.

The total weight of the ASEA-ATOM control blades is calculated to be 213 pounds for the Type 1 blades; 218 pounds for the Type 2, 4, and 5 blades; and 222 pounds for the Type 3 blades. The standard design control blade weighs about 218 pounds. The ASEA-ATOM blades yield equal or better scram insertion times than the standard GE blades. The ASEA-ATOM blades are mechanically compatible with the reactor and rod drive components in that the coupling and velocity limiter section is identical to the standard GE control blades. Blade span, blade thickness, and handle features are also similar to those for the standard GE blades. The dimensional tolerance envelope of the ASEA-ATOM blade is well within that currently required.

A lifting handle, which is cut from the same material as the blade wings, is welded to the top end of the absorber section. This handle is designed to fit the grapple used for installing the blades. At the top end of the blade are guide pads, one on each wing, which prevent direct contact between the blades and the adjacent fuel channels. The blade absorber section and velocity limiter are welded together.

4.6.2.1.4 Mechanical Design of Control Rods

Design stress intensity limits for control blade tubes in the standard GE control blades are given in Table 4.6-1.

A stress analysis was performed for a control blade similar to those used at Dresden. It was assumed that all control blade neutron absorptions were in B-10. Based on experimental data a value of 18% was used for the fraction of helium gas generated by the $B(n,\alpha)Li$ reaction which was released from the B_4C to cause the internal pressure within the poison tubes. When the end of design life due to the depletion of B-10 was reached, the internal pressure in the most highly exposed poison tube was 13,000 psi, and the resultant maximum general primary membrane stress was less than 50,000 psi compared to a design limit of 51,500 psi for irradiated material.

The tubes in the HICR- and ALLCR-type control blades are made of a high-purity, Type 304 stainless steel, resulting in these control blades being less susceptible to intergranular stress corrosion cracking than the standard GE control blades. These control blades experience lower gas pressure buildup since there is no gaseous release from the hafnium.

Operating experience shows that the materials used in the control blades are not susceptible to dimensional distortion in service.

Control blade absorber tubing is supported within the control blade assembly and can withstand external pressures far in excess of those experienced under accident conditions.

The design internal pressure and design external pressure for the ASEA-ATOM blades were set at 2175 psi and 1375 psi, respectively. Results from a stress analysis indicated that a maximum internal pressure and maximum external pressure of 2030 psi and 3190 psi, respectively, would not exceed ASME Section III criteria. The design internal pressure (2175 psi) was achieved by tightening manufacturing tolerances in order to increase minimum wall thickness. These control blades are expected to withstand external pressures that may be experienced under accident conditions.

4.6.2.1.5 Control Blade Life

The end of control blade life is defined as either the exposure when any quarter segment of a control blade reaches a 10% reduction in worth relative to a new original equipment control blade, or a mechanical (structural) limit. The reduction in control blade worth is due to a combination of B-10 depletion, transmutation of hafnium isotopes and the B_4C loss resulting from the cracking of the absorber tubes, commonly known as wash-out. B-10 depletion occurs when a B-10 atom captures a neutron to form helium and lithium (i.e., $^{10}B + {}^{1}n \rightarrow {}^{7}Li + {}^{4}He$). Thus, for each B-10 neutron capture, the number of B-10 atoms is reduced. In control blades utilizing hafnium, hafnium transmutation is expressed in terms of B-10 equivalent depletion. Washout has been observed in original equipment control blades irradiated to exposures greater than 50% of the B-10 depletion lifetime criteria. The B_4C in original equipment control blades is in a powder form packed in stainless steel tubes. At high exposures in the reactor, these tubes have been observed to crack thereby allowing the reactor coolant to wash-out the local B_4C. Therefore, an acceleration term is used in determining the recommended lifetime for original equipment control blades. The end of control blade life (i.e., 10% reduction in relative worth) for the different control rod designs is provided in the appropriate lifetime documents.[4,5]

The on-line core monitoring code calculates control blade exposure across the axial height of each control blade. These control blade exposures are then compared to appropriate lifetime limits for the various control blade types in the core.

4.6.2.2 Burnable Neutron Absorbers

See Section 4.2 for information on the use of gadolinium in the fuel.

4.6.2.3 Recirculation Flow Control

The recirculation flow control system is discussed in Section 7.7.

4.6.2.4 Standby Liquid Control

The standby liquid control system is described in Section 9.3.5.

4.6.3 Information for Control Rod Drive System

4.6.3.1 Control Rod Drive System Design

The reactivity control system provides the means to regulate core excess reactivity under normal operating conditions. Moveable control rods are used to control the fission rate and fission density. The control rods are capable of being positioned in 6-inch steps, more commonly called notches, corresponding to the CRD index tube, to control neutron flux distribution in the reactor core. They can be moved only individually at an average rate of approximately 3 in./s once system differential pressures and flows have been established. The movement of control rods does not perturb the reactor beyond the capability of an operator to respond to the disturbance. This requirement prevents unnecessary operation of the reactor protection system. The maximum rate at which the rods can be moved and the incremental distance between control drive notches is such that under normal operating conditions a single notch increment of control rod withdrawn at the maximum withdrawal rate results in a reactor period of not less than 20 seconds.

4.6.3.2 Control Rod Drive

The control rod drives are of the locking-piston-type. The CRD as described here is the same as used on all General Electric BWRs. The CRD hydraulic system piping and instrumentation drawing is shown in Drawings M-34 and M-365. Figure 4.6-6 shows the basic CRD hydraulic system flow path. An assembly drawing of the CRD is shown in Figure 4.6-7. The CRDs are mounted vertically in housings which are welded into the reactor bottom head penetrations. The low end of each housing terminates in a special flange which contains ports for attaching the hydraulic system lines and a machined face which mates with a corresponding flange at the lower end of the drive.

At the top end of the drive index tube (the moveable element), a coupling is provided which engages and locks into a socket at the base of the control rod (Figure 4.6-8). The weight of the control rod alone engages and locks this coupling. Once locked, the drive and rod form an integral unit which must be manually unlocked by specific procedures before a drive or rod can be removed from the reactor. These procedures are established to prevent accidental separation of the control rod from the CRD.

The CRDs position the control rods in 6-inch increments of stroke and hold them in these discrete latch positions until actuated for movement to a new position by the hydraulic system. Visible indication of the position of each drive is displayed in the control room by means of illuminated numerals which correspond with the respective latched positions.

In addition, indication is provided that shows insert and withdraw travel limits of the drive when an overtravel withdraw limit on the drive has been reached. Control rod seating at the lower end of the stroke prevents the overtravel withdraw limit from being reached unless the control rod is uncoupled from the drive. This allows the coupling to be checked. These indicators and those for the incore monitors are grouped together and displayed on the control panel and arranged on the board to correspond to relative rod and incore monitor positions in the core.

Movements of the control rods when the reactor is critical or near critical cause changes in the neutron flux. Rod coupling is verified by observing the neutron flux changes during rod movement.

Originally BWR/3-type CRDs were installed at Dresden Station. Since May 1987, BWR/6-type CRDs have been used to replace BWR/3-type CRDs requiring maintenance. The BWR/6-type CRD performs the same function as and is a one-for-one changeout for the BWR/3-type CRD.

The functional operation of the BWR/6-type CRD is identical to BWR/3 CRD. The CRD accumulator pressure and operating principles remain unchanged. The failure modes are the same. These failures could result in a control rod drop accident (CRDA) and severance of drive housing. The CRDA is analyzed in Section 15.4.10. All various scram conditions resulting in hydraulic loading of the BWR/6-type CRDs are enveloped by the original design of the CRD system.

The following list of BWR/6-type CRD components vary from the original BWR/3-type CRD:

A. Piston tube,

B. Index tube,

C. Buffer assembly,

D. Spud and cylinder,

E. Inner filter,

F. Uncoupling rod,

G. Cooling water orifice ,

H. Nut, and

I. Drive piston assembly.

The BWR/6 CRD design, which incorporates a new hydraulic buffer configuration, utilizes the higher strength material and implements the latest design improvements. These BWR/6-type features provide improved operating availability and reduced maintenance. The BWR/6-type design was previously installed in a BWR/4-type plant at a different utility. This installation was for one operating cycle and served as part of the demonstration/verification test for this new design. The design has been recommended and reviewed by General Electric Company. General Electric has also provided a safety evaluation report and a stress analysis report.[2]

4.6.3.3 Control Rod Drive Hydraulic System

4.6.3.3.1 Design Bases

The control rod drive hydraulic system is designed to achieve the following objectives:

A. Provide a water source at a pressure of nominally 1380-1510 psig for charging the scram accumulators;

B. Provide a water source at a constant pressure of nominally 250-280 psi above reactor pressure to supply water for normal drive operation;

C. Provide a water source at a constant pressure above reactor pressure to supply cooling water for each control rod drive mechanism, and

D. Provide a source of clean high pressure reactor recirculating pump seal purge flow.

E. Provide a continuous source of water to backfill the reference-leg piping of the Reactor Vessel Water Level Instrumentation System.

4.6.3.3.2 System Description

Under normal operation, the hydraulic control system uses condensate as the working fluid to accomplish hydraulic positioning of the control rod drives and their attached control rods. Drive water pressure is set to achieve the desired control rod velocity during control rod positioning. The desired rate of control rod motion is obtained by supplying a set quantity of water to the drive which moves the drive by displacing water on the other side of the drive piston. Manual valves are set to provide the desired water flowrate at the established drive water pressure thereby controlling the control rod speed. Pressure and flow for fast insertion (scram) of the control rods is supplied by stored energy in the scram accumulators or by reactor pressure.

The system, shown in Drawings M-34 and M-365, is made up of supply pumps, filters, strainers, control valves and associated instrumentation and controllers. The CRD system normally draws suction from the condensate reject line which is downstream of the condensate demineralizers. This system can also draw suction from the condensate storage tank. The CRD system provides water for the reactor recirculation pump seals, CRD accumulator charging, drive water for normal CRD insert/withdraw operations, CRD drive cooling water and the RVWLIS Backfill System. Flow control and drive water pressure control stations are connected in series and provide pressure regulation for the various requirements. The highest pressure, nominally 1500 psig, is provided to the scram subsystem for charging the scram accumulators and to purge the reactor recirculation pump seals. The next highest pressure is regulated to maintain 250-280 psi above reactor pressure and supplies water for normal CRD drive operations. The third water source is above reactor pressure and provides cooling water to the drive mechanisms. These pressures vary directly with reactor pressure changes, and are controlled by using valves which develop constant pressure drops due to the constant flow from the flow control station. These three water supplies plus the exhaust water header are the four operating pressures of the control rod drive hydraulic system. A crosstie of the Unit 2 and Unit 3 CRD hydraulic systems is provided on the discharges of the CRD pumps.

The CRD hydraulic line, which penetrates primary containment at Unit 2 Penetration X-139B, is used during reactor shutdowns to test the Reactor Recirculation Pump Seals. During normal reactor operations, this line is isolated by containment isolation valves. The heatup of the drywell during a postulated loss-of-coolant-accident could, in turn, heat up the volume of liquid trapped between the containment isolation valves. Heatup of this trapped volume could overpressurize and fail the associated piping, creating a bypass path for the primary containment. To prevent the potential overpressurization of this piping, a relief valve has been installed between the containment isolation valves to protect against the consequences of thermal expansion of the trapped fluid.

The CRD hydraulic lines which penetrated primary containment at Penetration X-139B (Unit 2) and X139C (Unit 3) are used during reactor shutdowns to test the Reactor Recirculation Pump seals. During normal reactor operation, these lines are isolated by containment isolation valves. The heatup of the drywell during a postulated loss-of-coolant-accident could, in turn, heat up the volume of liquid trapped between the containment isolation valves. Heatup of this trapped volume could overpressurize and fail the associated piping, creating a bypass path for the primary containment. To prevent the potential overpressurization of this piping, a relief valve has been installed between the containment isolation valves to protect against the consequences of thermal expansion of the trapped fluid.

The CRD hydraulic system is also identified as an alternate reactor coolant supply during an accident as directed by the Emergency Operating Procedures.

4.6.3.3.2.1 Supply Pump

The supply pump pressurizes the system. The spare pump is a 100% capacity standby unit. Changeover from one unit to the other is manual. Each pump is installed with a suction strainer and appropriate isolation valves to permit pump maintenance. The pump is designed to operate at the required pressure. The pump discharge pressure is indicated at the pump by a pressure gauge.

A minimum-flow bypass connection between the discharge of the pump and the contaminated condensate storage tanks prevents the pump from overheating if the pump discharge valve is inadvertently closed. A separate minimum flow bypass line is provided from the common pump discharge header to the condensate header used to supply the CRD pumps. The bypass line regulates flow through the pump(s) to maintain high pump efficiency. The CRD piping is routed from the CRD pumps in the turbine building through the feedwater heater bay to the reactor building and the drive water filters. A line taps off to provide water to the reactor recirculation pump seals.

The CRD pump discharge valves are motor-operated stop-check valves. The power source for each motor operator is the same as that of the associated CRD pump. The power and control cables for the motor operators are routed as balance-of-plant cables with separate routings provided to enhance the reliability of the design.

Two parallel filters are provided on the suction side of the pump to remove foreign material larger than 25 microns from the hydraulic system water. Discharge filters utilize a 50 micron material. Either filter can be drained, cleaned, and vented for reuse while the other is in service. A differential pressure indicator and an alarm monitor the discharge filter elements as they collect foreign material. Strainers in the filter discharge lines guard the hydraulic system in the event of a filter element failure.

4.6.3.3.2.2 Accumulator Charging Pressure

The accumulator charging pressure is established by pump head and the flow control station and is independent of reactor pressure. The accumulator charging header taps off the outlet of the drive water filters downstream of the system flow-sensing element but before the flow control station. The CRD accumulator charging water pressure is considered the first stage pressure in a three-stage pressure control system. On a scram, the scram inlet valves open causing the accumulators to discharge to the area below the drive pistons. The scram outlet valves allow water above the pistons to discharge to the scram discharge headers. The accumulators automatically recharge by CRD system flow when the scram signal is cleared and the inlet and outlet scram valves close.

Since the accumulators discharge during a scram, the CRD supply pumps provide maximum flow to try to recharge the accumulators. The high charging line flow is sensed by the flow element closing the flow control valve during a scram to force the water to the accumulators. Once the accumulators are recharged, the flow control station is restored to its normal flow control operation.

The accumulator charging pressure in the header is monitored in the control room with a pressure indicator and low pressure alarm.

4.6.3.3.2.3 Flow Control Station

Downstream of the accumulator charging line is a flow control station which consists of air-operated flow control valves. Two parallel valves are provided, one being a spare to permit valve maintenance. The CRD flow-indicating programmable controller works in conjunction with the flow sensor located upstream of the accumulator charging line to maintain a constant flow through the flow control valves. The pressure in the charging line header is monitored in the control room with a pressure indicator and a low pressure alarm. (See Section 4.6.3.3.2.2 for a description of the flow control station during a scram.)

4.6.3.3.2.4 Drive Water Pressure Control Station

The second stage pressure is maintained at approximately 250-280 psi above the reactor vessel pressure. A motor-operated drive water pressure control valve, which is remotely adjusted from the main control room, is used in conjunction with the CRD stabilizing valves to adjust CRD drive water flow. Two stabilizing valve stations are provided, each containing one insert and one withdraw stabilizing valve. These normally open valves provide bypass flow around the drive water pressure control valves to the cooling water header. This flow helps maintain constant CRD drive pressure when making CRD position changes by compensating for the flow needed to reposition the CRD. Whenever an insert signal is given, the insert stabilizing valve closes to provide the required CRD insert flow (approximately 4 gal/min). Whenever a withdraw signal is given, the withdraw stabilizing valve closes to provide the required CRD withdraw flow (approximately 2 gal/min). The variation in flow requirements between drives is small enough that the corresponding pressure variation is within acceptable limits.

Filters are installed before the stabilizing bypass valves to prevent fouling. Isolation valves are provided for maintenance. A flow element and an indicator are installed for measuring the flow through the stabilizing bypass valves so that they can be adjusted to provide the required flow for normal drive operation.

The drive water header flow element and indicator are used to measure flow to the drives for adjustment and testing. Differential pressure indication in the main control room and in the reactor building shows the differential pressure between the reactor vessel and the drive water header. This pressure indicator is used when adjusting the second stage pressure with the motor-operated drive pressure control valve.

The CRD drive water pressure control valve control switch is a spring-return-to-center-position-type switch and is located in the main control room on the 902(3)-5 panel.

4.6.3.3.2.5 Cooling Water Header

The CRD cooling water header pressure is greater than reactor pressure. The CRD cooling water supplies the CRD drives. This pressure is controlled from the control room and maintained by the combination of the upstream flow control station and the drive water pressure control station.

The CRD cooling water system is made up of the cooling water header, an individual line for each drive and a ball check valve at the CRD. This system admits water to the underside of the drive piston. Although the drive can function without cooling water, the life of the graphitar seals and elastomer O-rings is shortened by exposure to reactor temperatures; therefore, cooling water is provided to protect these components. The ball check valve opens to admit cooling water when the drive is stationary. When a drive is in motion, the pressure under the piston is higher than the cooling water pressure, and the ball check valve closes.

The cooling water is monitored by a flow indicator located in the main control room. A differential pressure indicator indicates the difference between reactor pressure and cooling water pressure. Control rod drive temperatures are recorded in the control room.

4.6.3.3.2.6 Exhaust Header

The exhaust header receives water discharged by the drives during repositioning and returns this water to the reactor through the CRDs by way of the cooling water header and back lifting of other "121" valves. The piping is sized to maintain a low differential (approximately 5 psi) above reactor pressure in this header. A check valve prevents backflow through the exhaust header.

4.6.3.3.2.7 Hydraulic Control Unit

One hydraulic control unit (HCU) serves each individual CRD and contains all actuating valves and other components required for the normal or scram operation of that CRD. Figures 4.6-9 and 4.6-10 provide an overall view of an HCU. The 177 HCUs are installed in roughly equal numbers in eight rows divided into two banks, one bank on the east side and one bank on the west side of the reactor building at ground level, as shown on Drawing M-4. Each bank consists of four rows of HCUs arranged back-to-back forming two row-pairs. Principal components of the HCUs are described below.

4.6.3.3.2.7.1 Accumulator

The accumulator in each HCU is an independent source of stored energy for the scram function of the associated drive.

To assure that it is always capable of producing a scram, the accumulator is continuously monitored for water leakage and for nitrogen pressure. A float-type level switch actuates an alarm if water leaks past the nitrogen-water barrier and collects in the bottom of the HCU instrument block. A pressure indicator and a pressure switch are connected to the accumulator to monitor nitrogen pressure. A decrease in nitrogen pressure actuates the pressure switch and sounds an alarm in the control room. An isolation valve allows the accumulator instruments to be isolated and serviced.

4.6.3.3.2.7.2 Scram Pilot Valves

During normal operation, each of the two parallel branches of the RPS energizes one of the two 3-way solenoid scram pilot valves associated with each HCU. During normal operation, these pilot valves are energized and supply instrument air to the operators of both the scram inlet valve and the scram outlet valve, holding both scram valves closed. During a full scram, both of the RPS branches are deenergized and both pilot valves open, venting the scram valve operators and allowing the scram valves to open. To protect against spurious scrams, the pilot valves are interconnected so that both pilot valves must be deenergized to vent the scram valve operators. On the other hand, either loss of electric power to both solenoids or loss of instrument air produces a scram. The pilot valves are selected based on simplicity of design, a minimum of moving parts, fast opening time (approximately 0.050 seconds) and satisfactory statistical operating history on similar units.

For added protection, the instrument air header to all the pilot valves has a pair of backup scram valves. When energized, the backup scram valves isolate and vent the instrument air header to the scram valves and insert all drives should any of the scram pilot valves fail to vent.

4.6.3.3.2.7.3 Inlet/Outlet Scram Valves

The scram inlet valve is a globe valve which opens by the force of an internal spring and closes when air pressure is applied to the top of the diaphragm operator. The opening force of the spring is approximately 700 pounds. Each valve has a position indicator switch. The inlet and outlet scram valve position indicator switches energize a light in the control room as soon as both valves start to open. The scram inlet valve was selected based on high operating force, fast opening time (approximately 0.1 seconds) and satisfactory operating history on similar units.

The scram outlet valve is identical to the scram inlet valve. By design it must open first to prevent damage to the CRD, therefore the scram outlet valve spring is set at a higher tension.

4.6.3.3.2.7.4 Directional Control Valves

Four solenoid directional control valves are used for switching the drive water header and the exhaust header to the two drive ports of the CRD. By energizing and opening two valves at a time, the drive water header can be connected under or over the control rod drive piston while the exhaust header is connected to the opposite side. Two of these directional control valves, which include speed control valves, are connected so that they always pass the flow to or from the underside of the piston. The normal drive speed is 3 in./s. The maximum control rod drive withdrawal speed is 5.14 inches/second when the Operating Limit MCPR established in the Core Operating Limits Report (COLR) is set greater than or equal to the value corresponding to a Rod Withdrawal Error (RWE) – at Power analysis for an “unblocked” condition. See subsection 15.4.2.

The balance of forces in the drive mechanism is such that the differential pressure under the piston is approximately 80 psi whenever the drive is either inserting or withdrawing.

Proper speed for control rod insertion is obtained when the speed control valve is set so that a flow of 4 gal/min through the valve produces a pressure drop of 200 psi (from 280 psi in the drive water header to 80 psi under the piston). Similarly, for control rod withdrawal, the speed control valve is set so that 3 gal/min produces a pressure drop of 75 psi (from 80 psi under the drive piston to 5 psi in the exhaust header). The directional control valves are protected from dirt by filters.

The cooling, control, and scram flow paths for each drive use common piping to the drive. The two directional control valves connected to the drive water header could be caused to open when subjected to this higher pressure during a scram on their outlet ports. The check valve prevents significant loss of water to the drive water header during scram.

4.6.3.3.2.8 Scram Discharge Volume

The scram discharge volume (SDV) is used to limit the loss of, and contain, the reactor vessel water from all the drives during a scram. During normal operation, the SDV is empty, with its drain and vent valves open. These valves operate very much like the HCU scram valves. With a scram signal, the RPS is deenergized and the two SDV pilot valves vent the discharge volume valve operators, causing them to close. Position indicator switches on the main valves indicate the position of the vent and drain valves.

The SDV consists of a separate, nonconnected volume for each of the two banks of CRDs. For each bank of CRDs, the SDV consists of four 4-inch and two 8-inch diameter pipes mounted horizontally over the CRD HCUs, a 20-inch diameter tank located nearby, and a 6-inch header connecting the pipes and tank. Each tank on Unit 3 is instrumented with level sensors. Each tank on Unit 2 has 4 moisture detection switches and 2 dP-type switches. One level switch provides a high-level alarm, and one a rod block. The other four level switches provide a scram function in the RPS. These level switches also guard against the SDV being filled such that it cannot accommodate the water discharge during a scram. Should the SDV start to fill with water, an alarm would sound, a rod block would be activated, and if filling were to continue, the reactor would automatically scram. Each tank is also provided with a vent and drain. The Unit 2 vent goes to a vent header routed to the RBEDT, while the drain goes to the equipment drain header. The Unit 3 vent goes to a floor drain while the drain is piped directly to the RBEDT.

During a scram, the SDV partly fills with the water from above the drives. While scrammed, the control rod drive seal leakage continues to flow to the SDV until the SDV pressure equals reactor vessel pressure or until the scram valves are reset. When scram signals are no longer present, the scram logic can be reset to allow the scram valves to reclose. This allows the SDV isolation valves to reopen and allow the SDV to be drained. A control system interlock does not allow the drives to be withdrawn until the SDV is emptied to below the rod block point.

A test pilot valve allows the SDV valves to be tested without disturbing the RPS.

4.6.3.3.2.9 Alternate Rod Insertion Valves

The alternate rod insertion (ARI) scram valves provide an alternate means of initiating control rod insertion during an anticipated transient without scram (ATWS) event. The ARI system and other ATWS related systems are described in Section 7.8.

4.6.3.4 Control Rod Drive System Operation

4.6.3.4.1 Insertion and Withdrawal

As described in preceding paragraphs, insert motion is obtained by opening the proper pair of valves. In order to unload the collet so it can be unlocked to allow withdrawal, this pair of valves is also opened for approximately ½-second during a withdrawal operation. After the collet is unlocked, the pair of withdrawal valves are opened. When the withdrawal mode of operation is selected by the operator, the proper pair of valves is energized electrically long enough to allow the drive to move to the next notch position, at which time the valves are automatically deenergized even if the operator continues to hold the withdraw switch in the withdraw position. This feature relieves the operator of having to estimate the time required to accomplish a single notch withdrawal.

If all four directional control valves are closed while the drive is in a position between notches, water displaced by the drive piston must leak past the drive seals in order for the drive to settle into latched position. With normal seals this settling speed is a fraction of normal withdrawal speed. To speed up the settling and latching of a drive following an insert or withdrawal movement, the closing of the valve is delayed for several seconds to facilitate the displacement of water from the drive. This allows the drive to settle at about one-half normal speed to the next latch position.

Normal withdrawal speed is determined by differential pressures at the drive and is set for a nominal value of 3 in./s. The characteristics of the pressure regulating system are such that this speed is maintained independent of reactor pressure. Tests have determined that accidental opening of the speed control valve to the full open position produces a velocity of approximately 6 in./s. Should this system fail, producing maximum available pump pressure (1750 psig) to the drive system while reactor pressure is 0 psig, the hydraulic resistances in the system would limit the withdrawal velocity to 2 ft/s. The maximum control rod drive withdrawal speed is 5.14 inches/second when the Operating Limit MCPR established in the Core Operating Limits Report (COLR) is set greater than or equal to the value corresponding to a Rod Withdrawal Error (RWE) – at Power analysis for an “unblocked” condition. See subsection 15.4.2.

The allowable operating limits on withdrawal and insertion speed are determined by requirements for the insert-before-withdrawal motion and for jogging. These limits are lower than those which might be set by considerations of maximum allowable reactivity variations. The jog withdrawal operation of the drive is an excellent test of the correctness of the speed setting: the drive generally fails to withdraw if the speed is incorrectly adjusted. A pressure of approximately 60 psi higher than reactor pressure must be maintained above the main drive piston in order to keep the collet unlocked which corresponds to a pressure greater than 60 psi above reactor pressure over the main piston. Any malfunction which allows the

pressure to drop below this value, a condition necessary for higher withdrawal speeds, results in collet locking.

During reactor shutdown and with fuel loaded into the core all control rods are normally inserted. Interlocks are provided which prevent the inadvertent withdrawal of more than one control rod with the mode switch in the refuel position.

4.6.3.4.1.1 Operational Reliability

Each drive mechanism has its own complete set of electrically operated directional control valves, which are closed when deenergized. The correct operation of all four valves in the correct sequence is required to cause the drive to withdraw. Consequently, the probability of multiple simultaneous independent valve failures that could cause accidental multiple rod withdrawal is extremely small. The electrical system which actuates the directional control valves is designed to prevent any credible failure from producing accidental movement of more than one control rod.

High operational reliability contributes generally to overall safety by minimizing the occasions when abnormal operating conditions are encountered. High operational reliability is the objective of the following features of the CRD hydraulic system:

A. Components in the hydraulic system are picked based on established reliability. A spare pump and control valves are provided for reliability. Operating valves are accessible for maintenance while the reactor is in operation.

B. Provisions are made to operate with a reasonable amount of foreign material in the reactor water and in the water supplied to the hydraulic system. Filters and strainers are incorporated in the drive mechanism in passages through which water is drawn into the drive mechanism.

C. The CRD housing has the capacity to resist buckling under the design loads and reduces the potential consequences in the event that it did buckle. Using conservative assumptions (housing at outer edge of pattern, full length of housing thin wall, extreme tolerances, and no support by housing support structure) the housing can support a load of 66,500 pounds. The maximum applied load occurs when the control rod is scrammed and is reaching its fully inserted position. The maximum column loading on the CRD housing during this instant is 17,100 pounds. A safety factor of nearly 4 exists. This maximum loading occurs at the end of the control rod insertion; therefore, if the control rod housing were to buckle, the control rod would remain inserted and could not be withdrawn.

Instrumentation and alarms monitor operation of flow and pressure regulation to assure availability of drive water and cooling water. Operation of drive control, scram, and scram pilot valves are observed during periodic testing of CRD operation and during scram tests.

4.6.3.4.2 Scram Operation

Rapid shutdown of the reactor is accomplished through automatic or manual actuation of the RPS which opens the scram valves and permits water under pressure to be applied to the drive mechanism. The action exerts a pressure on CRD piston mechanisms and causes all rods to be fully inserted into the core. Pressure for rod insertion is also available from the reactor, as noted previously.

The scram inlet and outlet valves open during a scram, admitting the pressure in the accumulator under the main drive piston and venting the area over this piston to the SDV. The large differential pressure (initially about 1400 psi and always several hundred psi, depending on reactor pressure) produces a large upward force on the index tube and control rod, giving the rod a high initial acceleration and providing a large margin of force to overcome any possible friction or binding. This initial scram force is a maximum of 5600 pounds under cold reactor conditions and 2800 pounds when the reactor is at operating pressure and greatly exceeds the insert/withdraw force of approximately 360 pounds.

The characteristics of the hydraulic system are such that after initial acceleration (less than 30 milliseconds after start of motion) the desired scram velocity of about 5 ft/s is achieved and the drive travels at a fairly constant velocity. This characteristic provides a high initial rod insertion rate and a high operating force margin. As the drive piston nears the top of its stroke, velocity is reduced by the CRD scram buffer. Actual methods for reducing velocity differ between the BWR/3- and BWR/6-type drive mechanisms. Each drive requires about 2.5 gallons of water during the scram stroke.

There is adequate water capacity in each drive's accumulator to complete a scram in the required time at low reactor pressures. At higher reactor pressures, the accumulator is assisted by reactor pressure reaching the drive through a ball check valve located in the drive itself. As water is drawn from the accumulator, the accumulator discharge pressure falls below reactor pressure. This causes the check valve to open which admits reactor pressure to below the drive piston. Thus, reactor pressure supplements the force needed to complete the scram stroke at higher reactor pressures, while the accumulator alone can accommodate the low-pressure scrams. When the reactor is up to full operating pressure, the accumulator is not required to meet scram time requirements.

4.6.3.4.2.1 Rate of Scram Response

Under conditions of expected abnormal reactor system disturbances, the reactivity control system provides a sufficient rate of negative reactivity insertion, upon a signal of the RPS, to prevent fuel damage. Expected abnormal reactivity disturbances and resulting power transients in the core can derive from any of the following three sources:

A. Reactor system inducing disturbances of core parameters, such as coolant flow or pressure;

B. Single operator errors or procedural violations; or

C. Single equipment malfunctions.

The RPS described in Section 7.2 senses the disturbances and, under certain specified conditions, initiates a scram signal. Upon receipt of a scram signal, the reactivity control system is required to render the reactor subcritical at a rate sufficient to prevent the initiating disturbance from causing fuel damage. An extensive program has been conducted to determine the characteristics of the CRD system for a BWR. Part of this program has been the measurement of rod position versus time after pilot valve actuation. Many drives have been tested and the data has been treated statistically to arrive at a position versus time curve which is based on 95% confidence that 99.5% of all scram times are less than that confidence level line. In addition a design specification has been written which is more stringent than the confidence level line. The specification for rod insertion on scram is as follows:

The average elapsed time after the opening of the main scram contact required for all operable drives to reach the percent insertions shown below shall not be exceeded:

A. 5% insertion in 0.375 seconds maximum,

B. 20% insertion in 0.90 seconds maximum,

C. 50% insertion in 2.0 seconds maximum, and

D. 90% insertion in 3.5 seconds maximum.

The above requirements do not include any delays due to instrumentation or scram circuitry. The actual reactivity inserted during scram would correspond to the mean of the data which shows better characteristics than the specifications.

4.6.3.4.2.2 Scram Reliability

High scram reliability is the object of a number of features in the system, such as the following:

A. There are two sources of scram energy (accumulator and reactor pressure) for each drive whenever the reactor is operating.

B. Each drive mechanism has its own scram valves and pilots so that only one drive can be affected by a scram valve failure to open. A separate backup pilot valve is provided to scram all drives (after some time delay) should this failure occur.

C. Under scram conditions the drive mechanism develops from 5600 pounds (at zero reactor pressure) to 2500 pounds (at rated pressure) of force, a large margin to overcome possible friction.

D. The scram system and drive mechanism are designed so that the scram signal and mode of operation override all others.

E. The scram valves fail open on loss of either air or electrical power. Hence, failure of the valves, air system, or electric system would produce, rather than prevent, a scram. All components used in the scram hydraulic system are selected either after an extensive testing program or after many millions of accumulated operating hours in service.

F. The ARI system provides an alternate path for reactor shutdown in the event that the normal scram path cannot be initiated by RPS. The ARI system is diverse and independent from RPS. The ARI system is further described in Section 7.8.3.

4.6.3.5 Control Rod Drive Housing Supports

4.6.3.5.1 Design Bases

Control rod drive housing supports are provided to prevent ejection of a control rod from the reactor core in the event a CRD housing should fail. The reactivity addition associated with a sudden control rod ejection exceeds the threshold of fuel cladding rupture. To obtain a margin of safety, there must not be a failure of a CRD housing associated with the drive mechanism which would permit a significant movement of the rod and its drive at high velocities. To achieve this margin, the housing support design was based upon permitting less than 3-inches of total control rod motion - less than a normal withdrawal increment.

4.6.3.5.2 System Design

The support system consists of structural members, rods, grid plates, support bars, and disk springs.

Figure 4.6-12 presents a cutaway view of the support system to illustrate the various components. The structural members are placed between the rows of housing, immediately below the bottom head of the reactor vessel. These members are supported on the reinforced concrete pedestal which supports the reactor vessel.

The grid plates are located under the drive flanges. These plates are attached to the rods which are supported from the structural members. A stack of disk springs is provided on each rod. The support system, therefore, is an elastic structure which is capable of absorbing the energy resulting from the assumed failure. This system also limits the magnitude of the resulting dynamic forces on the supports. Turning moments on the rods are prevented by the support bars.

4.6.3.6 Control Rod Velocity Limiters

A rod velocity limiter is provided on each control rod. The limiter is a hydraulic piston on the bottom of the control rod which adds substantial drag against

downward control rod movement. This device limits the rod drop velocity to 3.11 ft/s maximum.

A description and evaluation of the control rod velocity limiter has been submitted separately to the NRC under APED-5446, "Control Rod Velocity Limiter."[1]

4.6.3.6.1 Design Bases

The purpose of the control rod velocity limiter is to reduce the consequences in the event a high-worth control rod became detached from its rod drive and dropped out of the reactor core (a control rod drop accident). To accomplish this purpose the velocity limiter was designed using the following bases:

A. The control rod free fall velocity shall be less than 3.11 ft/s;

B. A minimum impedance of the control rod scram time or positioning ability will be maintained; and

C. The velocity limiter will be integrally attached to the control rod structure.

4.6.3.6.2 System Design

The original GE velocity limiter assembly consists of a single, Type 304 stainless steel casting in the shape of two nearly mated conical elements. These elements are separated from one another by four radial spacers. The separated surfaces of the upper and lower conical elements differ by 15□, with the peripheral separation less than the central separation.

The velocity limiter assembly, shown in Figure 4.6-13 with its associated components, acts within a cylindrical guide tube. The annulus between the guide and the velocity limiter assembly permits the free passage of water over the smooth surface of the cone when the control rod is scrammed in the upward direction. In the opposite direction, however, water is trapped by the lower cone and discharged through the interface between the two conical sections. Because this water is jetted in a partially reversed direction into water flowing upward in the annulus, a severe turbulence is created, thereby slowing the descent of the control rod and limiter assembly.

The Duralife 190 and 230 control rods include a new velocity limiter. This lighter weight velocity limiter compensates for the added weight of the hafnium metal incorporated into the control rod design. This velocity limiter is also a more efficient design such that increased drag is created in the drop direction without an increase flow resistance in the scram direction. The configuration incorporates an optimized twin reverse jet which has reduced weight and a drop velocity below 3.11 ft/sec. All the interfacing dimensions between the velocity limiter and the guide tube and CRDs are the same as the present design. Therefore, the new velocity limiter is interchangeable with the original design.

The Marathon control blades include a fabricast velocity limiter which has the same critical features as the previous designs; therefore, the testing done to verify the performance of the original velocity limiter is applicable to the fabricast design.

The guide tubes are 10-inch, Schedule 10, Type 304 stainless steel pipe. Each guide tube has a backseat on the lower end which rests on the control rod drive thimble. This seat restricts water flow out of the tube during a velocity limiter free fall; the seat also restricts water flow into the interior of the guide tube during normal reactor operation to prevent coolant bypass of the fuel elements.

4.6.3.6.3 Design Evaluation

During the development of the original GE velocity limiter, sensitivity tests were performed to assess the effect of manufacturing tolerances in the following items on the velocity limiter performance: limiter and guide tube diametral tolerance; nozzle (interfacial gap between cones) gap; top cone thickness; limiter/guide tube eccentricity; and surface finish. These tests and the optimization of the velocity limiter design are described in detail in APED-5446, "Control Rod Velocity Limiter."[1] The results of these tests are summarized as follows:

A. Dropout Velocities

1. Cold reactor 2.46 ft/s

2. Hot reactor 2.86 ft/s

B. Scram Times

1. 10% of full insertion 0.33 s

2. 90% of full insertion 3.05 s

Since the new velocity limiter is interchangeable with the original GE velocity limiter, the operational characteristics are bounded by the original velocity limiter design. This was confirmed by extensive testing performed at both room and operating temperatures and pressures to confirm that drop velocities and scram performance are within the design bases of the original velocity limiters. During these tests, the velocity limiter and control rod were subjected to the worst case scram loads, including failed CRD buffer conditions, with no degradation of structural integrity.

4.6.4 Evaluation of the Control Rod Drive System

4.6.4.1 Scram Effect

The approved ODYN computer code, used by GNF/GE to perform transient analyses, contains a one-dimensional reactor kinetics model. 'The scram reactivity is calculated using one of the two options, A and B, the ODYN code provides. An option is selected based on whether scram times have been statistically evaluated. If statistical compliance with the scram time basis is not demonstrated at the plant, then Option A, based on measured scram times, applies. Under ODYN Option B, statistically evaluated scram times are used.

The response of the RPS, in combination with the size, heat transfer features, and inherent dynamic response characteristics of the core, prevent fuel damage resulting from a reactivity insertion accident due to any single equipment malfunction or single operator error.

4.6.4.2 Control Rod Drive Uncoupling and Control Rod Drop

The coupling mechanism connecting each control rod to its CRD, which allows for removal of either component for maintenance or replacement, creates the potential for accidental decoupling of a control rod from its CRD and subsequent drop of a control rod from the active core region.

The consequences of a postulated control rod drop accident (CRDA) are ultimately mitigated by the control rod velocity limiters, discussed in Section 4.6.3.6. The use of planned control rod withdrawal sequence, enforced by the rod worth minimizer (addressed in Section 7.7) or an independent verifier, further lessens the potential consequences of certain CRDA events. The CRDA is addressed in Section 15.4.10.

4.6.4.3 Control Rod Drive Ejection

The design of the CRD housing support is based on the assumption that despite the conservatism employed in the design of the CRD housing, any one housing could experience instantaneous circumferential failure with the reactor vessel at a pressure of 1250 psig.

All structural components of the CRD housing supports are designed for a load combination of dead load, accident jet force (which is equal to the reactor pressure vessel design pressure times the area of the support housing), and impact force. For this once-in-a-lifetime load condition the design stresses are 150% of the AISC normal allowable stresses. The deflection is limited to a maximum of 3 inches, which is about one half of one CRD notch movement.

When the supporting system is installed, a gap of about 1-inch is provided between the lower grid clamps and the contact surface on the CRD flanges. During system heatup, this gap is reduced due to a net downward expansion of the housings with respect to the grid clamps. In the hot operating condition, the gap is approximately ¼-inch.

The downward travel of the housing following the assumed housing failure is the sum of the initial gap, plus the elastic deflection of the supporting structure under dynamic loading. The support system limits the total downward movement of the drive and housing to 3 inches under the worst case conditions assuming an initial gap of approximately 1 inch. The total deflection would normally be substantially less than 3 inches because an operating gap of ¼-inch exists between the lower support plates and the contact surface on the control drive flange. Thus, the drive movement following a housing failure, is always less than one normal drive notch position.

Impact is factored in the design of the structure by multiplying the applied vertical load consisting of accident, jet, and dead loads by the impact factor of 3. The resulting force is then treated as a static load in designing formulas.

The vertical seismic load was determined by applying a static coefficient of 0.10 to the total dead load of the CRD housing and support components. This vertical load, due to seismic, is less than 1% of the total design load. The impact factor of 3 was determined by using a standard impact factor formula:

$$\frac{\Delta}{\Delta_S} = 1 + \sqrt{1 + 2\frac{\eta}{\Delta_S}}$$

A number of different arrangements regarding the size of the rods, the number of springs, and the stiffness of the support beams and plates were investigated to determine the optimum design for this system. The design stresses for the CRD housing support structure components were limited to 90% or less of the yield strength of the materials. The stress criteria was selected to provide a system that is as elastic as possible and which can be considered adequate for the loading condition.

The number and placement of disk springs is determined by the load and deflection requirements. The load requires 1 stack of 2 disk springs while the deflection requires 24 stacks of 2 disk springs. Therefore, the improper placement of 1 stack of disk springs affects only the impact factor applied to the support structure. A reduced deflection of the disk spring stack would not increase the impact factor beyond the design impact factor of 3 because during the hot operating condition the maximum gap between the housing and the housing support structure is only ¼-inch rather than 1 inch, as was assumed in arriving at the design impact factor of 3.

Procedural controls are used to ensure correct reassembly and reinstallation of the housing support following CRD maintenance, so that the support will perform as originally designed.

One of the procedural requirements for support structure reassembling is that the design gap between the housing flange and support structure be obtained. The only way to obtain the required gap is by adjustment of the two nuts on the hangar rod. This adjustment is additional assurance that the nuts would be in place when the unit is put into operation.

Failure of the support bar, grid clamp, or grid to function as a structure depends upon its ability to carry the design load. Since all of the stresses in the structural component are below the yield stresses of the material (150% of ASIC allowable), the component cannot fail structurally.

4.6.4.4 Scram Discharge Volume Pipe Break

The probability of an SDV pipe rupture resulting in a loss-of-coolant accident is of such a small magnitude that the event is beyond the range of a credible occurrence.

This is based on the results of two independent studies performed on SDV piping systems and on the low probability that all scram outlet valves would fail simultaneously with the pipe break.

The first of these studies was performed by GE and documented in report NEDO-24342.[3] In this generic evaluation report regarding BWR scram system pipe breaks, the probability of an SDV pipe break per scram was calculated to be less than 5×10^{-6} per reactor year.

In addition to the GE report, a plant-specific pipe fracture analysis was performed on the SDV system piping installed at LaSalle Station Unit 1. As a result of this study, the probability of an SDV pipe break was conservatively calculated to be 7×10^{-6} per reactor year. The SDV system piping at LaSalle Station is similar to the SDV system piping found at Dresden.

The SDV pipe break scenario can result in a loss-of-coolant accident only when the postulated pipe break occurs simultaneously with a failure of all scram outlet valves to close. Conservatively assuming that the probability of all scram outlet valves failing to close is 1×10^{-1} per reactor year, the combined events result in a probability of 10^{-7} per reactor year or less. Therefore, the frequency of occurrence is beyond the range of probabilities which needs to be taken into account in the design of a nuclear facility.

The results of the two independent studies combined with the positive results of the SDV piping hydrostatic tests and the unlikely failure of all scram outlet valves to close all provide sufficient assurance that the probability of an SDV pipe break occurrence resulting in fuel failure does not merit further review.

4.6.4.5 Scram Failure Modes

The hydraulic control system is arranged so that the equipment common to each drive can be packaged in modular form (Figure 4.6-9), one module (HCU) for each drive. Any failure of the scram system within a particular module would affect only its associated drive. Areas which are necessary to the scram system and common to all modules include the accumulator charging header, the scram discharge header, and the SDV.

If for any reason the accumulator charging header supply pressure were to fail (this failure would be alarmed), the stop-check valves supplying pressure to the accumulator in each module would close and hold the charged pressure so that scram capability would not be lost.

The SDV receives water from the drives during a scram. SDV problems have included accumulation of water in the SDV (which can hamper a scram), failure of level indication or high-level alarm, and plugging of drain or vent lines.

The only common point in the system where an accident, such as a plugged line, could affect the scram time of more than one drive would be in the SDV itself. Since the 4-inch lines are much larger than the individual ¾-inch lines feeding into them, it is extremely unlikely that the volume could become plugged. Furthermore, the action of the drive during a scram is such that it will develop a pressure in excess of 2000 psig if its discharge is restricted. This pressure should

be capable of expelling any conceivable line restrictions. The system is designed to accommodate such pressures.

Also, because of the unique design of the locking-piston drive, an automatic scram occurs if both drive lines or only the outlet line is severed at any point with the reactor at pressure.

4.6.4.6 Potential Release Path Through the CRD Hydraulic System

An issue raised by the NRC in IE Notice 90-78 identified the CRD system as a potential containment bypass pathway. This issue combines a loss-of-coolant accident (LOCA) with a loss of the CRD pumps potentially resulting in primary system fluid back leakage through the CRD system outside containment. An evaluation was performed of the Dresden design to assess the risk to the public and the plant operators during such an event. The potential pathways are from the reactor through the CRD hydraulic control units and from the reactor recirculation pumps through the seal purge lines. It was determined that this pathway could result in primary system fluid flowing to the condenser via the CRD pump discharge sample line, the Contaminated Condensate Storage Tank (CCST) level sandpipe via the CRD pump miniflow lines, and the CCST's via the CRD pump suction lines and CCST level standpipe line. As a result, testable check valves were added to the CRD header within the Reactor Building for each unit, to limit the potential back leakage through the CRD system in this event. These check valves are leak rate tested as part of the IST program. Consequently, no significant increase in control room, exclusion area, or low population zone doses will result from this pathway following a LOCA.

4.6.5 Testing and Verification of the CRD System

4.6.5.1 Control Rods and Control Rod Drives

Testing and inspecting of the control rod velocity limiter is not required following installation of the control rod assembly. In addition to close surveillance during the fabrication of the rod velocity limiter and control rod assembly manufacture, random control rod assemblies were shop-tested (which included rod drop tests). Each velocity limiter was visually inspected and gauged prior to assembly. Preoperational tests confirm the operation of the individual control rod assemblies for normal operation and scram conditions.

During production, control rods are statistically tested for dimensions. After installation, all rods and drive mechanisms are tested full stroke for operability.

During reactor operation, individual drive mechanisms can be actuated to demonstrate functional performance. Each time a control rod is withdrawn a notch, the operator observes the incore monitors' indications to verify that the control rod is following the drive mechanism.

When the operator withdraws a control rod fully out of the core, the coupling integrity is tested by trying to withdraw the rod drive mechanism to the overtravel position. Failure of the drive to overtravel demonstrates rod-to-drive coupling integrity.

During reactor shutdown, the shutdown margin can be verified by withdrawing a maximum worth rod and demonstrating that the reactor is substantially subcritical. During a refueling outage, each control rod is fully withdrawn and inserted to test for operability. The scram time for each control rod is tested as required by the technical specifications.

During normal rebuilding of drive mechanisms, a pull test is performed on the inner filter to insure proper installation. Loose inner filters had been identified as contributing to control rod to drive uncoupling events. The pull test is performed to significantly reduce the potential for a loose inner filter to cause control rod uncoupling.

4.6.5.2 Control Rod Drive Housing Supports

Sections of the CRD housing support may be removed to permit maintenance on control rods. Any time maintenance or other work on the CRD system has been performed, the support structure is inspected to assure proper installation before the reactor is returned to operation.

4.6.6 References

1. General Electric, "Control Rod Velocity Limiter," APED-5446 (March 1967).

2. General Electric letter to E.D. Eenigenburg, G-EBO-7-18, dated January 9, 1987.

3. "GE Evaluation in Response to NRC Request Regarding BWR Scram System Pipe Breaks," NEDO-24342, April 1981.

4. "GE BWR Control Rod Lifetime," NEDE-30931.

5. "ABB-ATOM Control Rods for BWR 2/3/4/5/6 Service Life Limits Recommendations," UR 87-102, Revision 1, April 15, 1987.

6. GE Marathon Control Rod Assembly “NEDE-31758 P-A October 1991.

7. “Fabricast Velocity Limiter for Duralife and Marathon Control Blades” WLM-CR-9808 Rev. 0, September 1998.

Table 4.6-1

NEUTRON ABSORBER TUBE STRESS INTENSITY LIMITS

Categories	Stress Intensity Limits in Terms of: Yield Strength (S_y)	Ultimate Strength (S_u)
General Primary Membrane Stress Intensity	0.667 S_y	0.5 S_u
Local Primary Membrane Stress Intensity	S_y	0.75 S_u
Primary Membrane plus Bending Stress Intensity	S_y	0.75 S_u
Primary plus Secondary Stress Intensity	2 S_y	1.5 S_u

Figures 4.2-1 through 4.2-3a have been deleted intentionally.

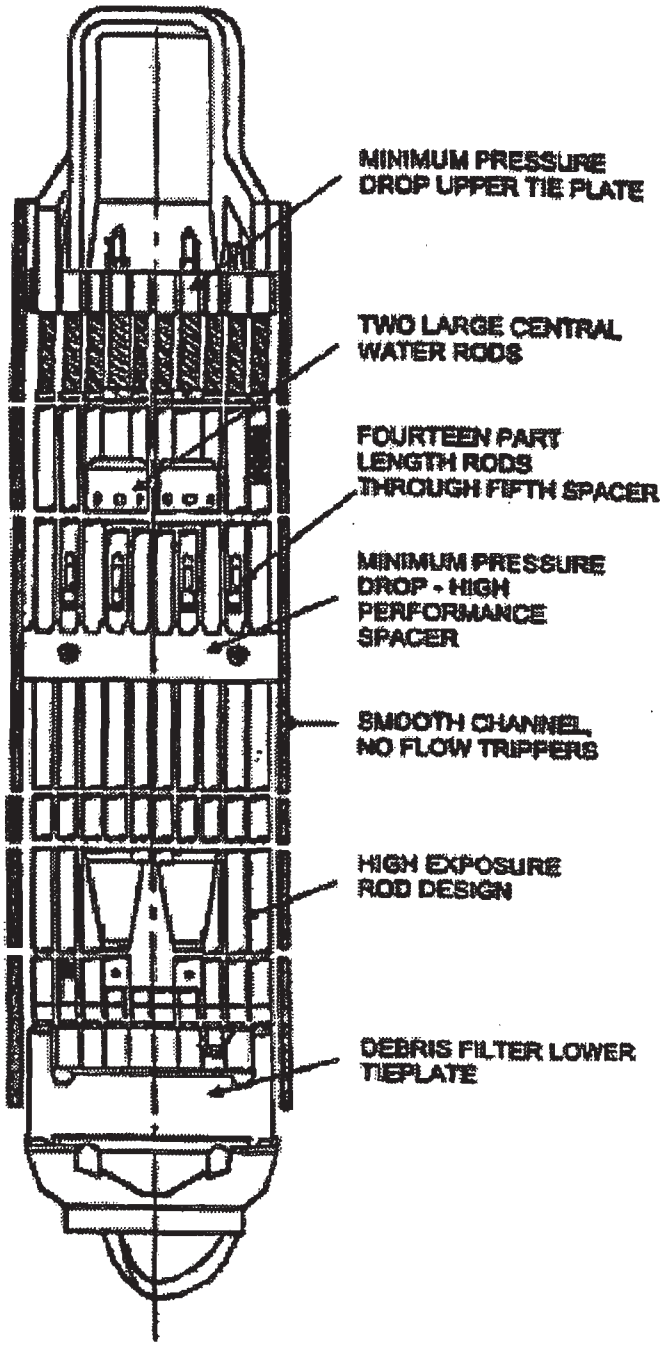

DRESDEN STATION
UNITS 2 & 3

GNF GE14C FUEL BUNDLE

FIGURE 4.2-4

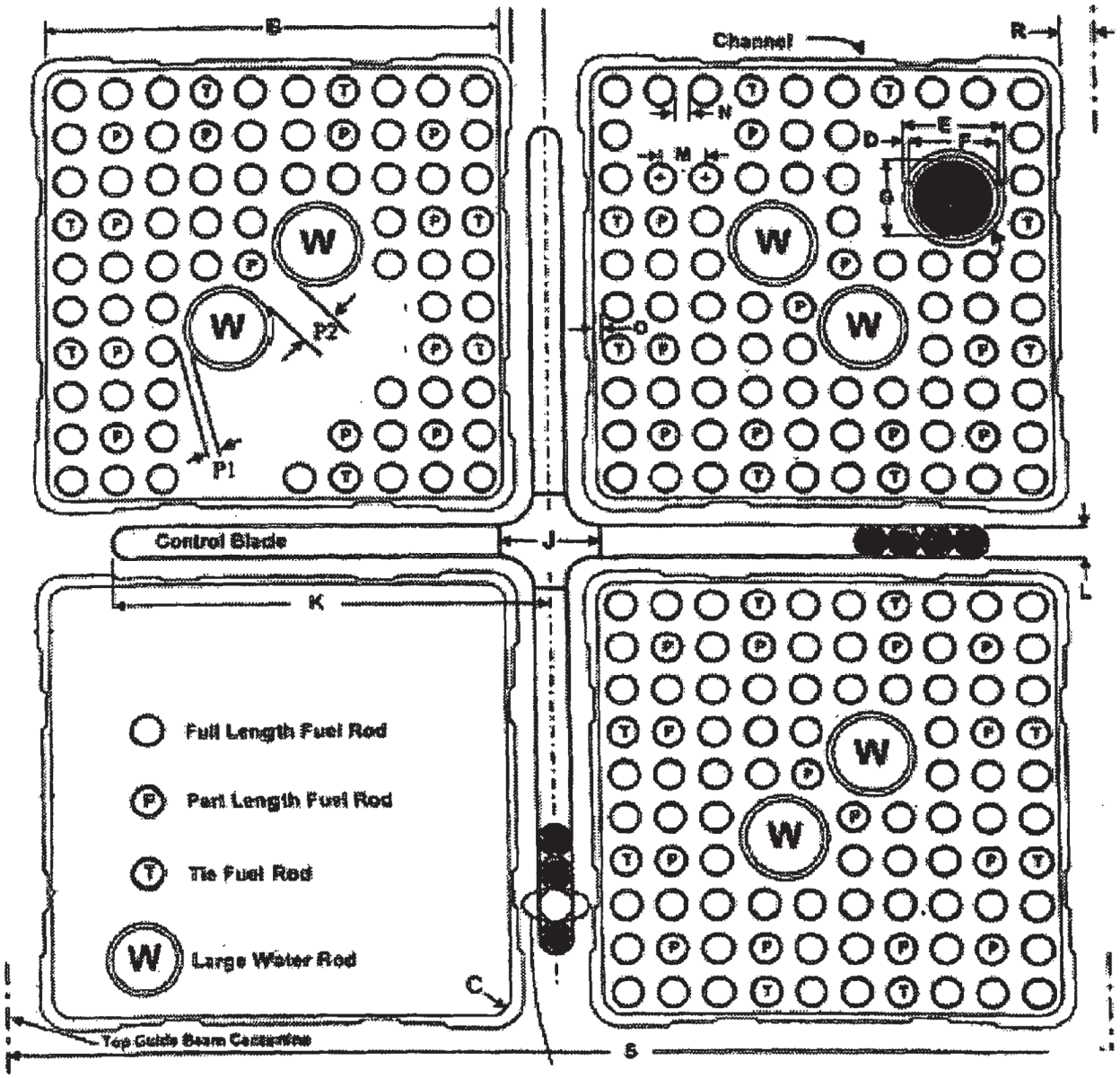

DRESDEN STATION UNITS 2 & 3
TYPICAL GE14C LATTICE DESIGN
FIGURE 4.2-5

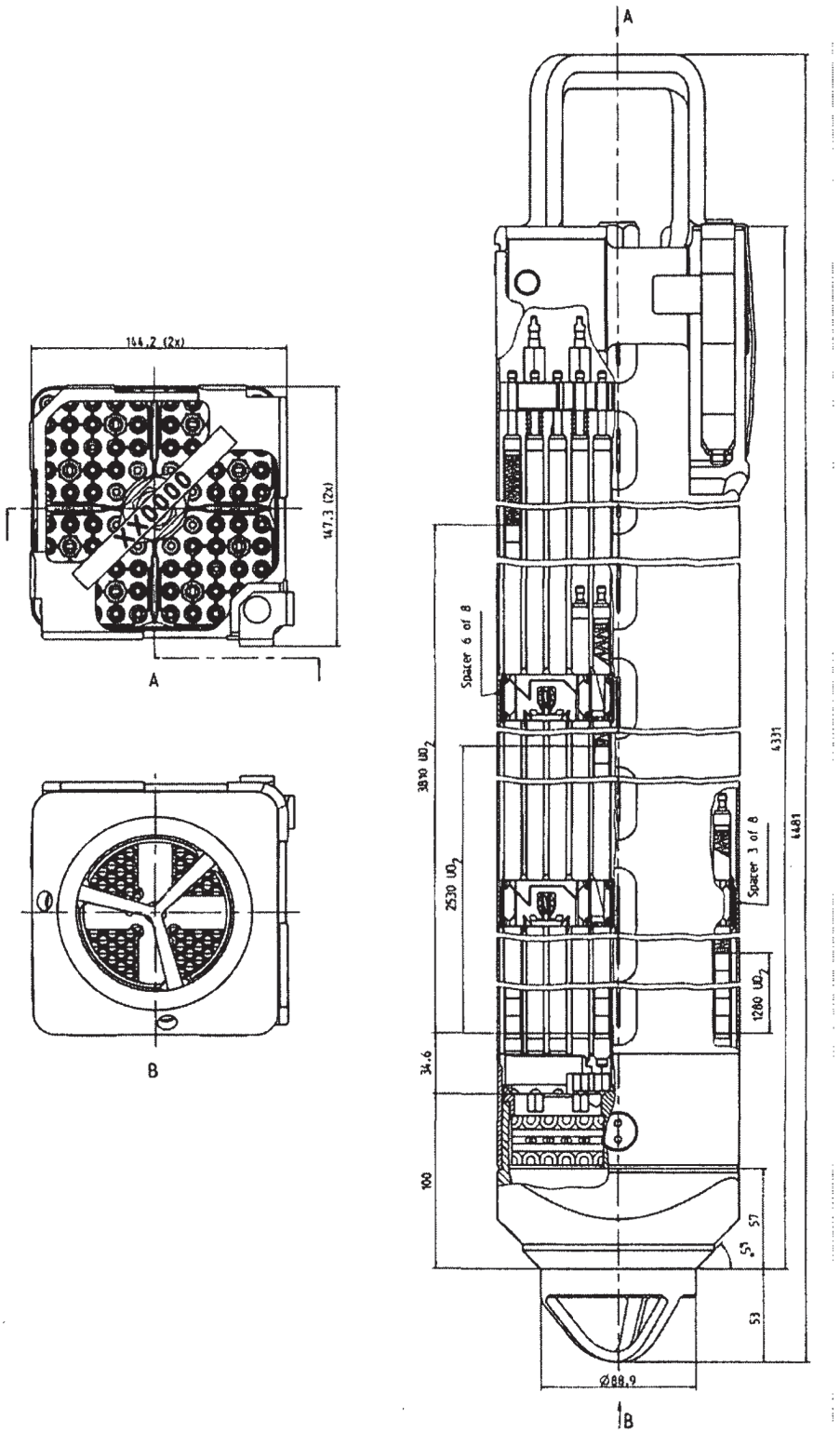

Dresden Station Units 2&3
WEC SVEA-96 Optima 2 Fuel Assembly
Figure 4.2-6

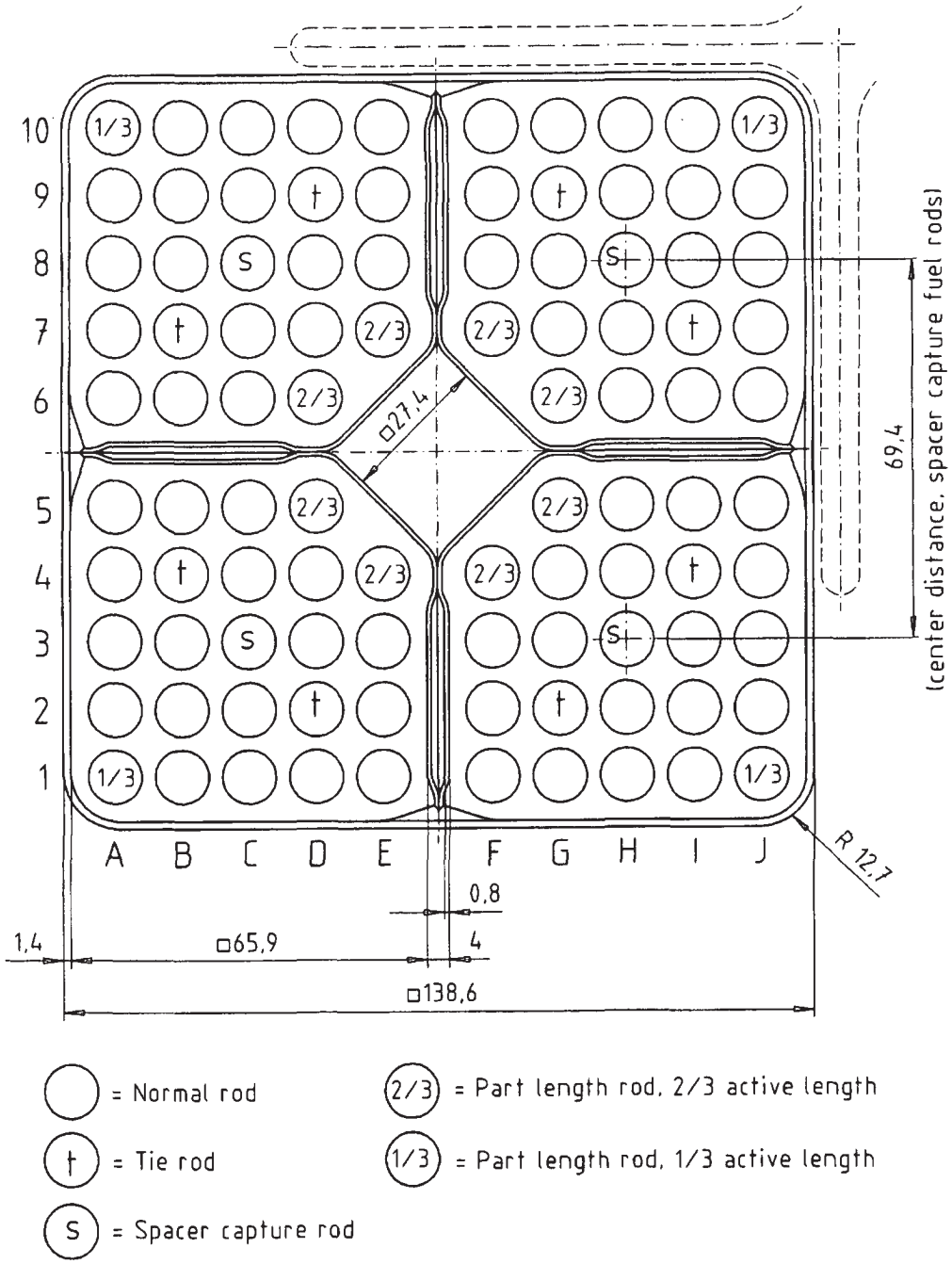

Dresden Station Units 2&3
WEC SVEA-96 Optima 2 Typical Lattice
Figure 4.2-7

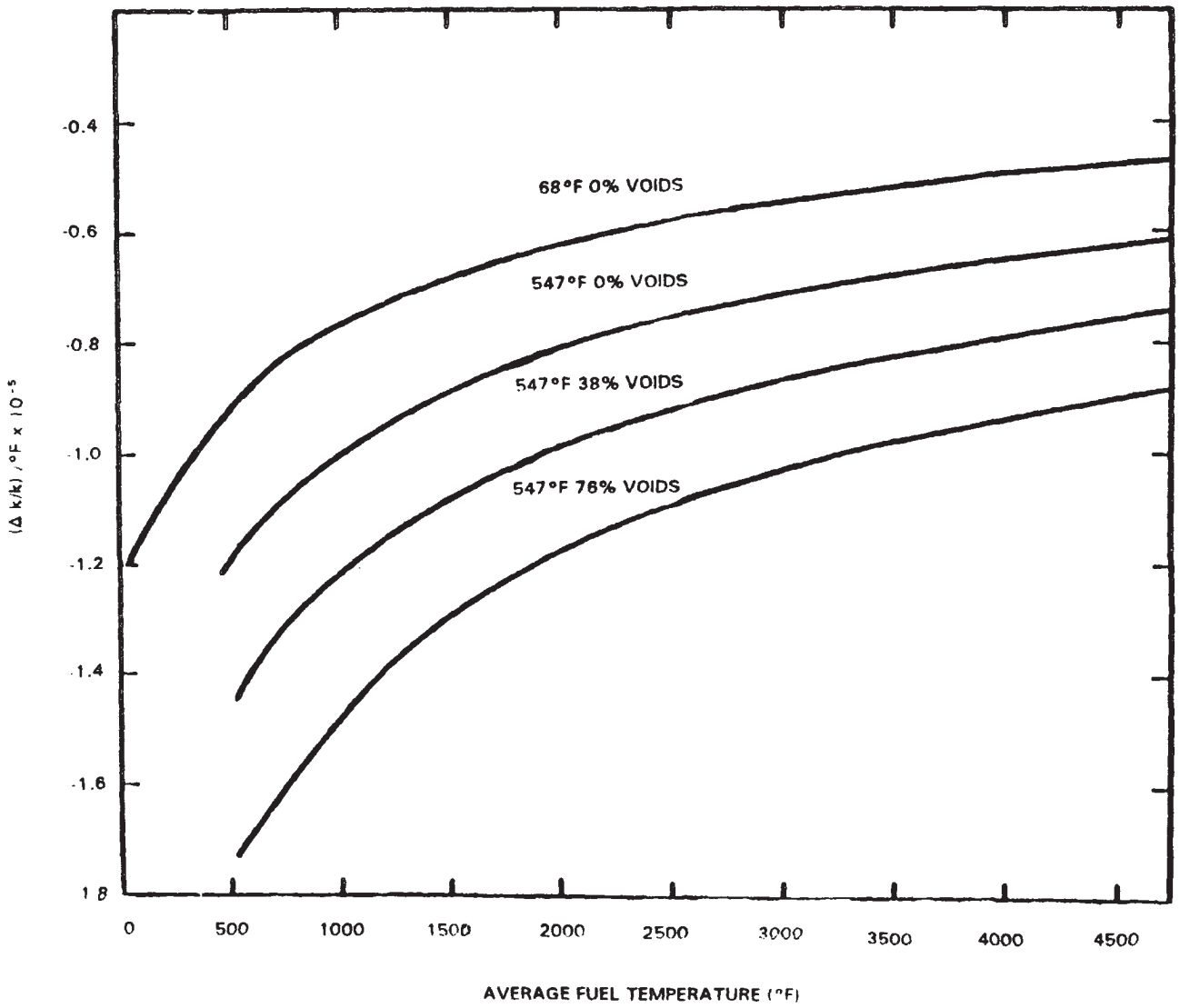

DRESDEN STATION
UNITS 2 & 3

DOPPLER COEFFICIENT OF REACTIVITY

FIGURE 4.3-1

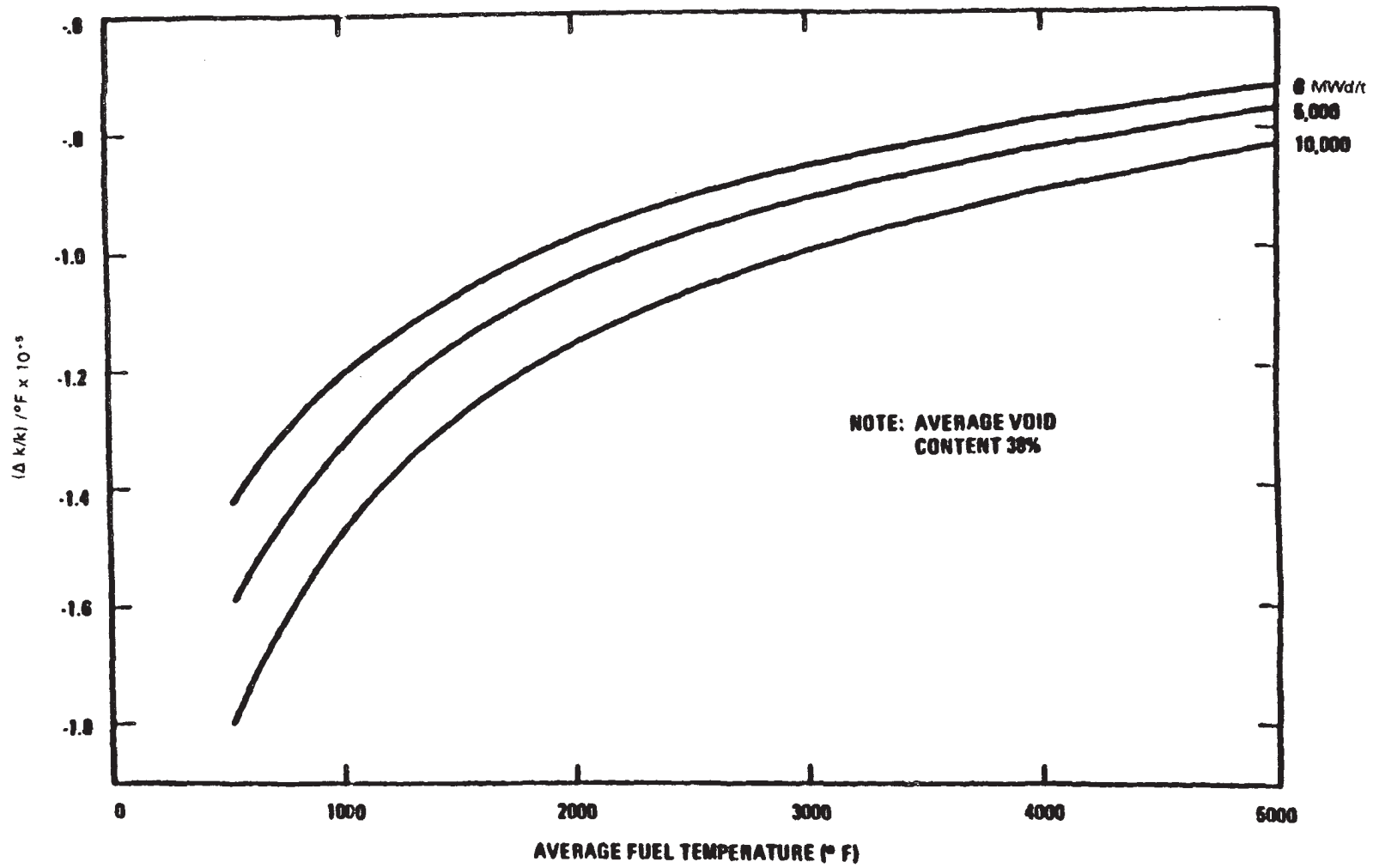

DRESDEN STATION UNITS 2 & 3
DOPPLER COEFFICIENT AS FUNCTION OF FUEL EXPOSURE
FIGURE 4.3-2

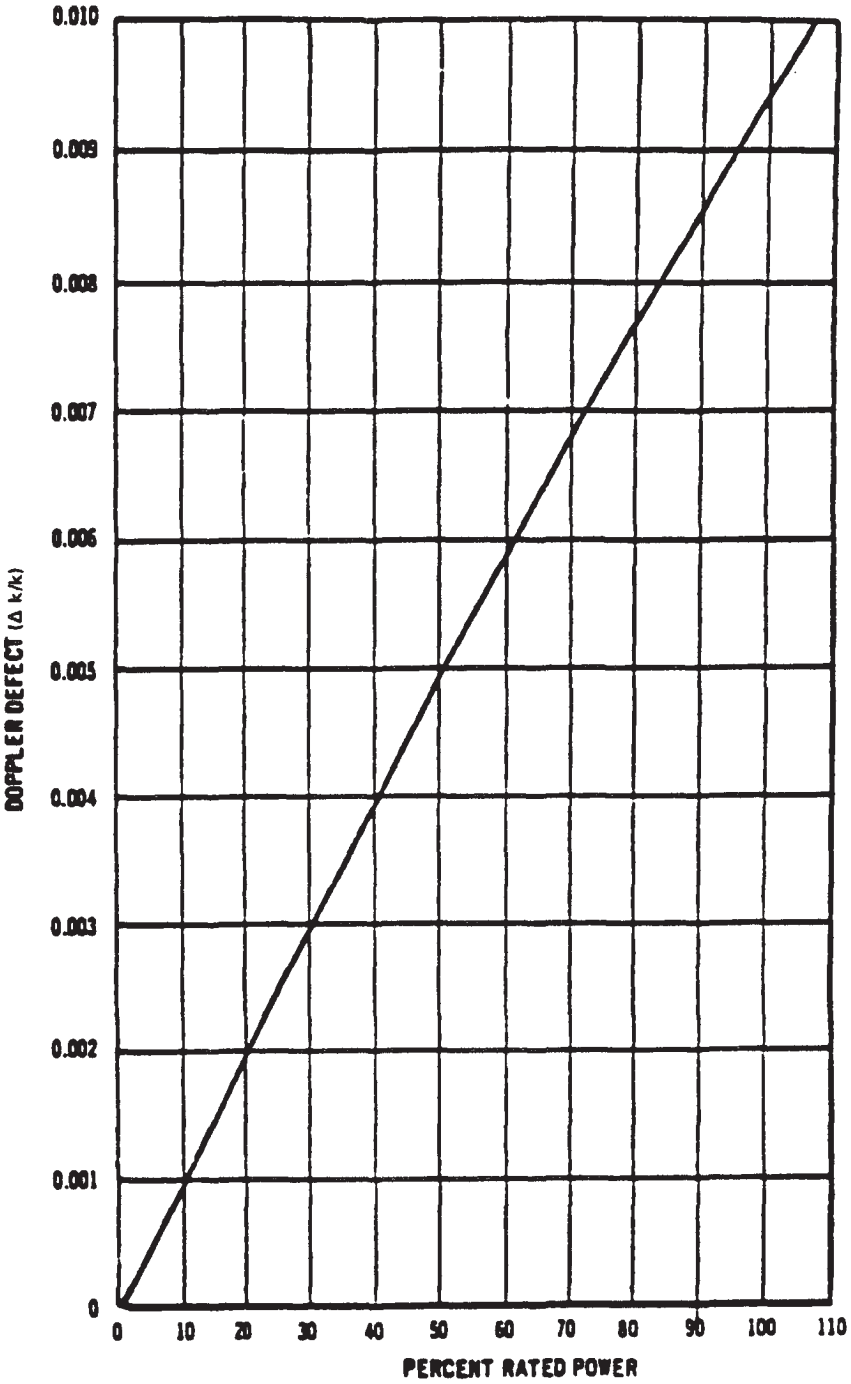

DRESDEN STATION UNITS 2 & 3
CORE AVERAGE DOPPLER DEFECT VS. POWER LEVEL
FIGURE 4.3-3

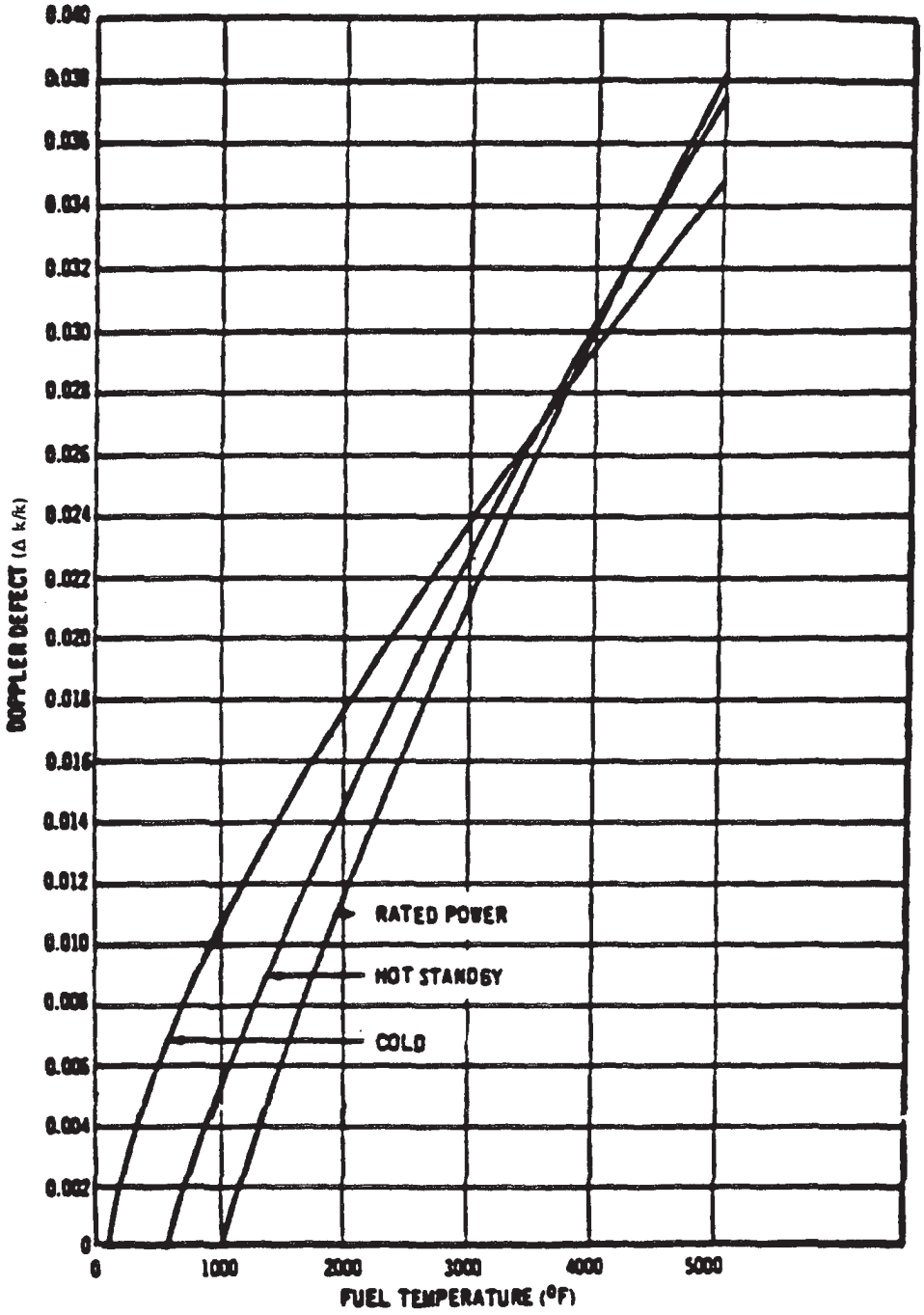

DRESDEN STATION UNITS 2 & 3
DOPPLER DEFECT VS. FUEL TEMPERATURE
FIGURE 4.3-4

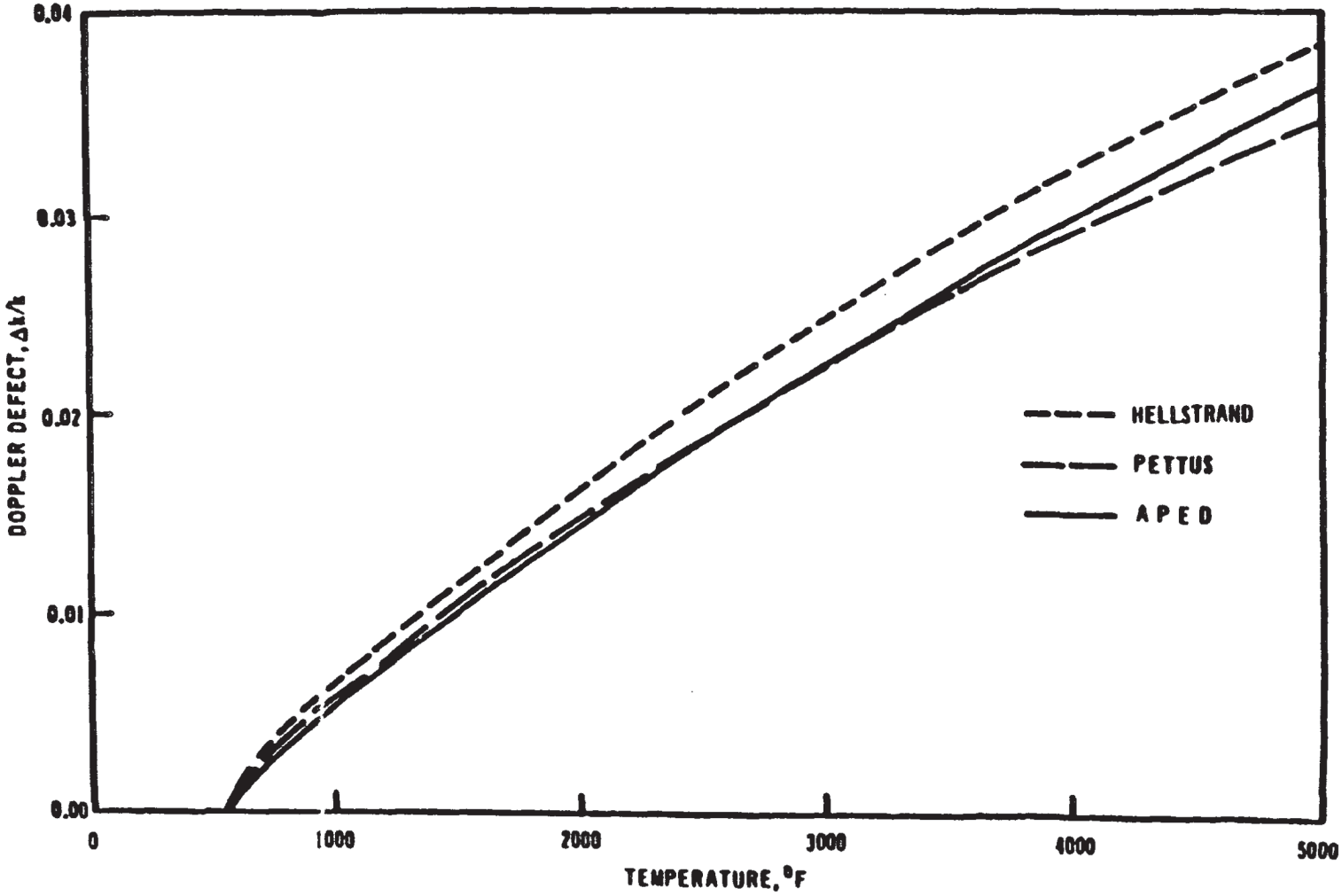

DRESDEN STATION UNITS 2 & 3
DOPPLER MODEL COMPARISON
FIGURE 4.3-5

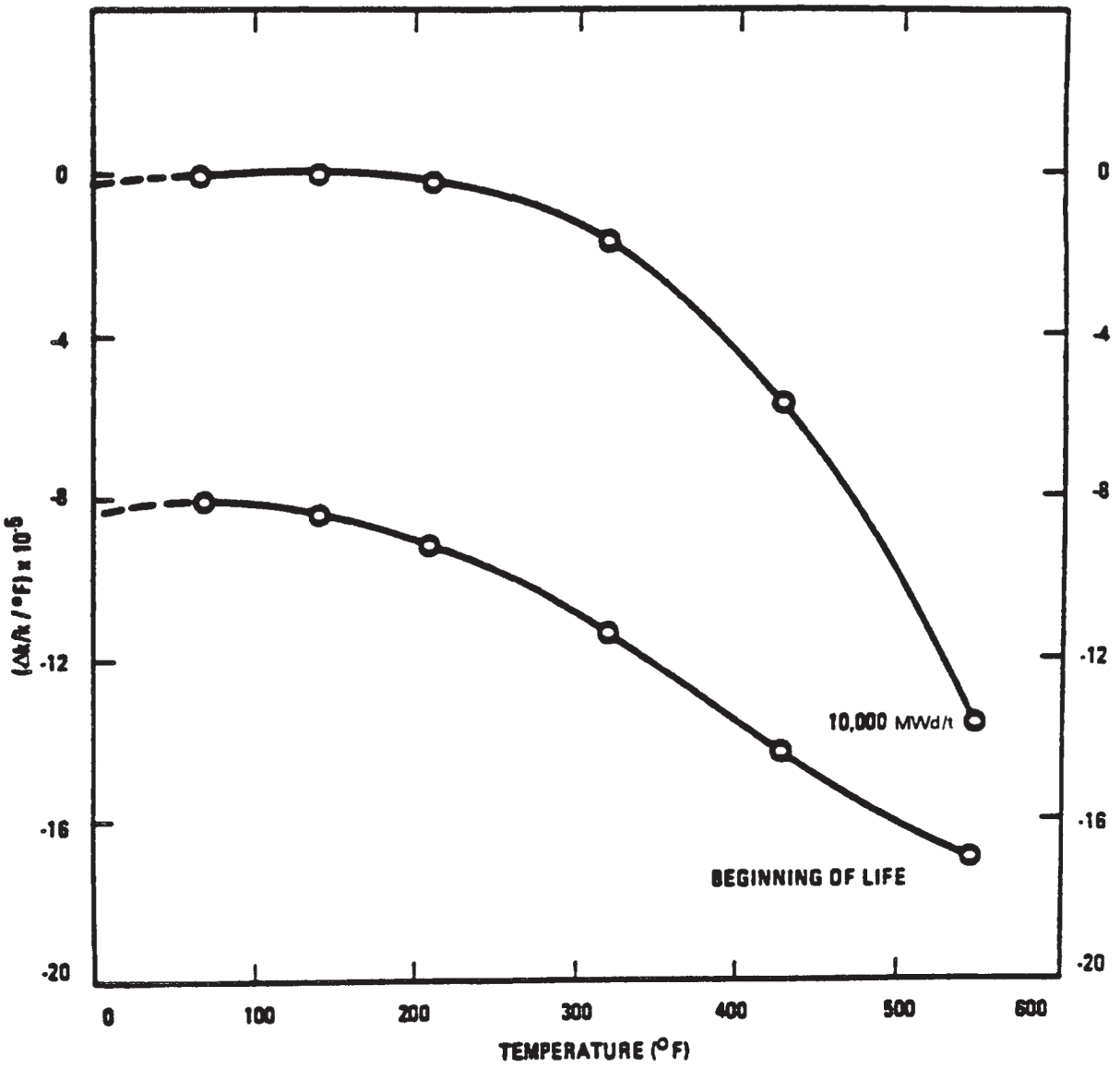

DRESDEN STATION UNITS 2 & 3
MODERATOR TEMPERATURE COEFFICIENT OF REACTIVITY
FIGURE 4.3-6

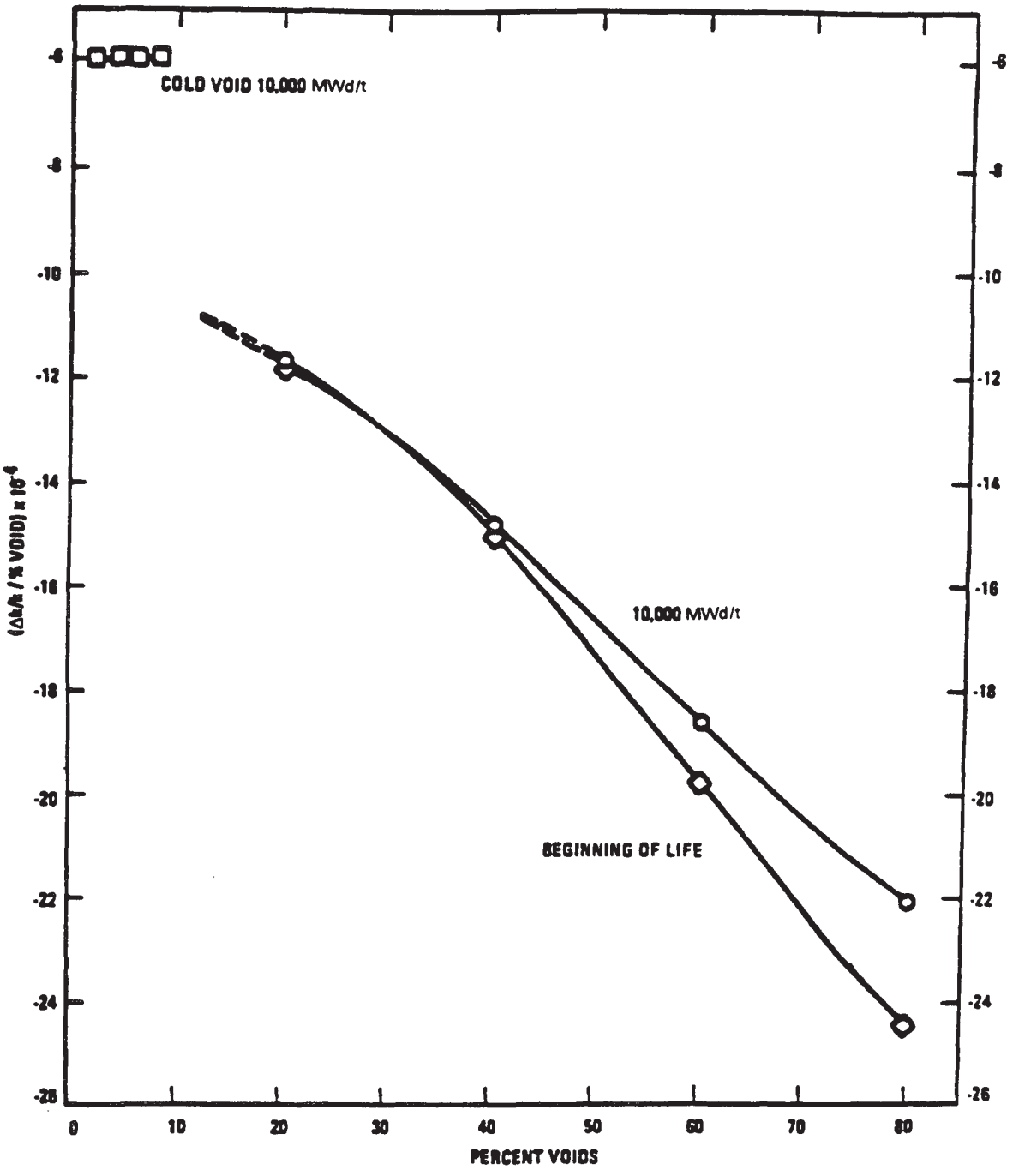

DRESDEN STATION UNITS 2 & 3
MODERATOR VOID COEFFICIENT OF REACTIVITY
FIGURE 4.3-7

Figures 4.3-8 through 4.3-37 have been deleted intentionally.

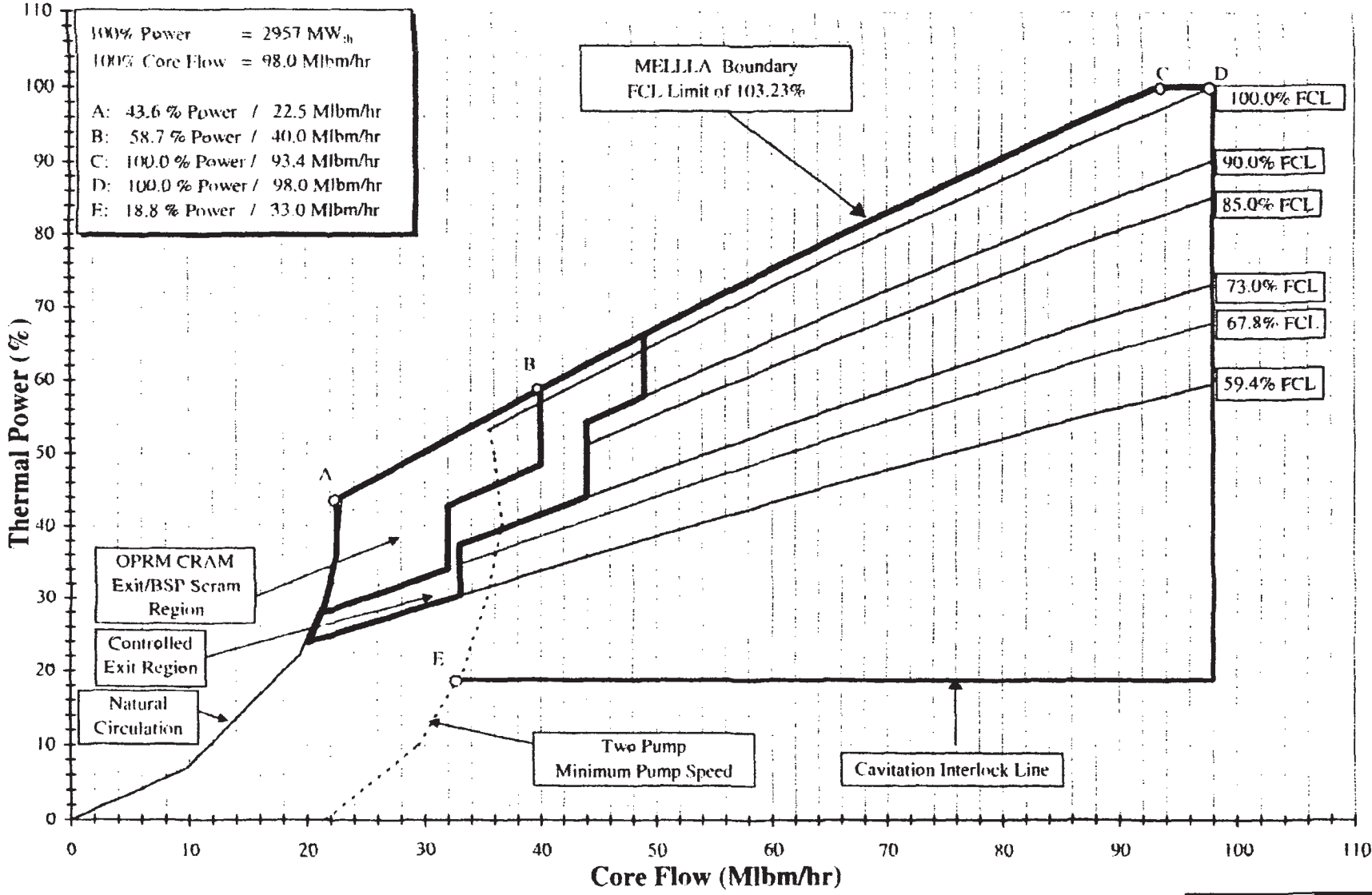

UFSAR REVISION 7, JUNE 2007
DRESDEN STATION UNITS 2 & 3
TYPICAL POWER – FLOW MAP
FIGURE 4.4.1

Figures 4.4-2 through 4.4-5 have been deleted intentionally.

REVISION 5
JANUARY 2003

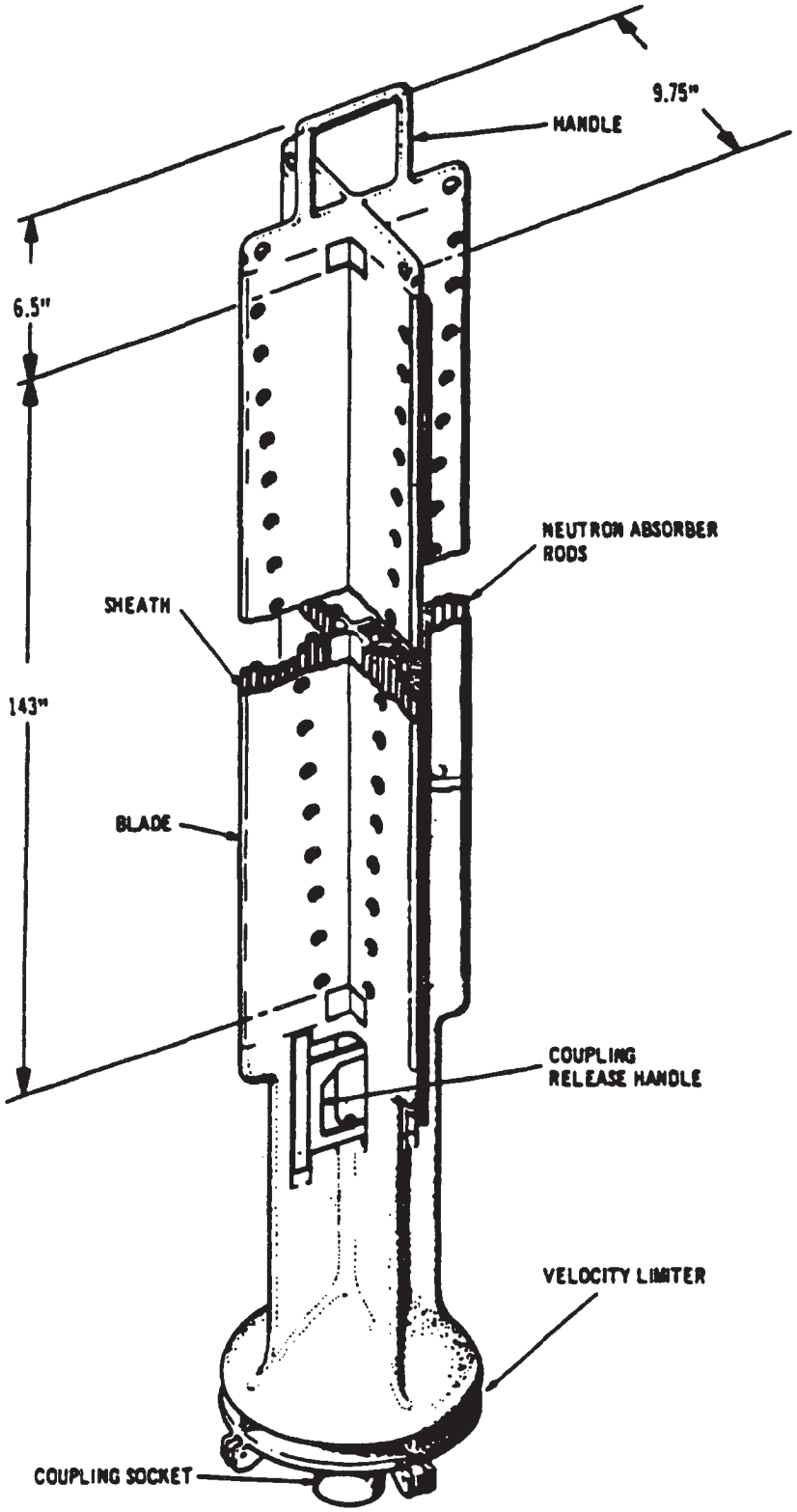

DRESDEN STATION
UNITS 2 & 3

ORIGINAL EQUIPMENT
CONTROL BLADE ISOMETRIC
(D-100, D-120)

FIGURE 4.6-1

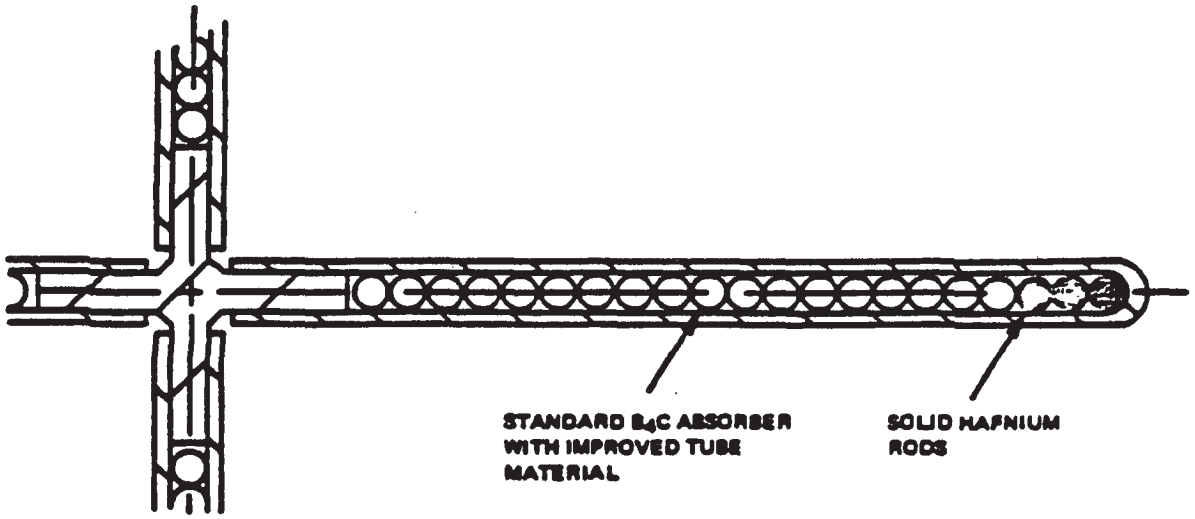

DRESDEN STATION
UNITS 2 & 3

GE HYBRID I CONTROL ROD TYPE
CONTROL BLADE

FIGURE 4.6-2

REVISION 5
JANUARY 2003

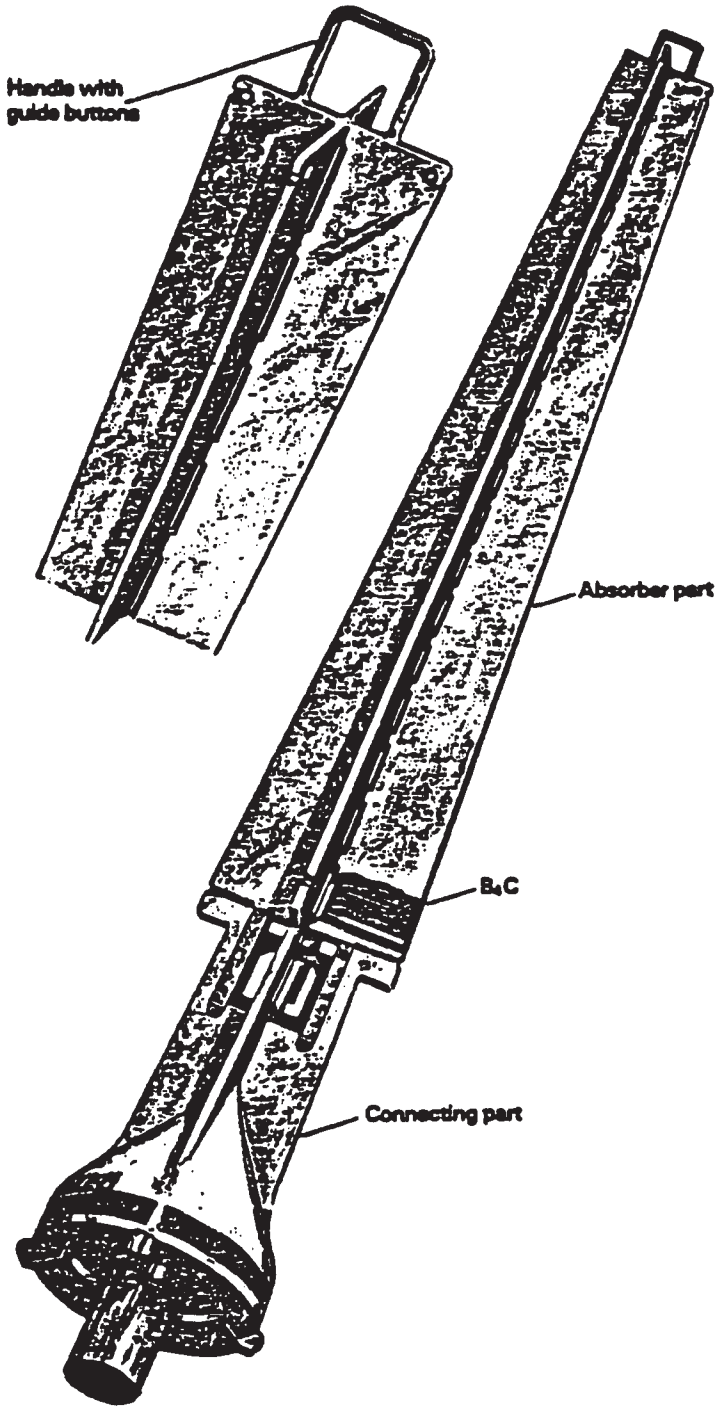

DRESDEN STATION
UNITS 2 & 3

WESTINGHOUSE ATOM AB
CONTROL BLADE ISOMETRIC

FIGURE 4.6-3

REVISION 5
JANUARY 2003

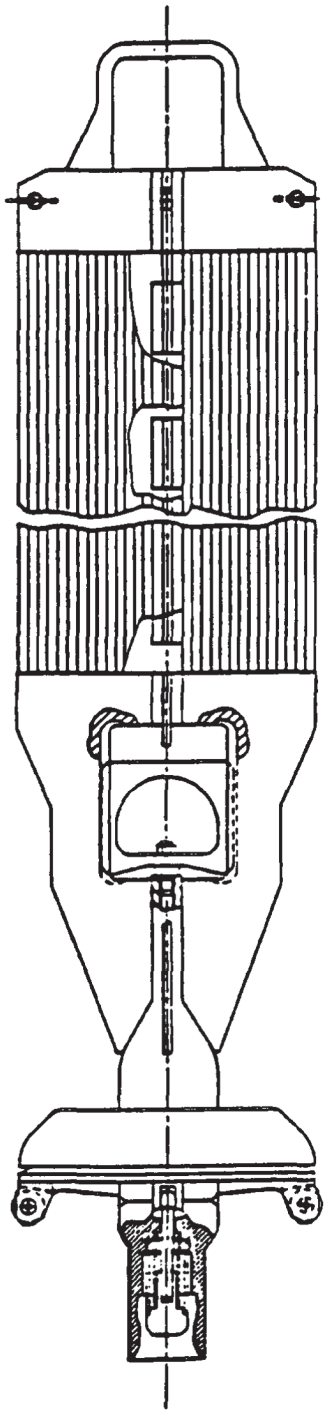

DRESDEN STATION
UNITS 2 & 3

GE MARATHON
CONTROL BLADE ISOMETRIC

FIGURE 4.6-3A

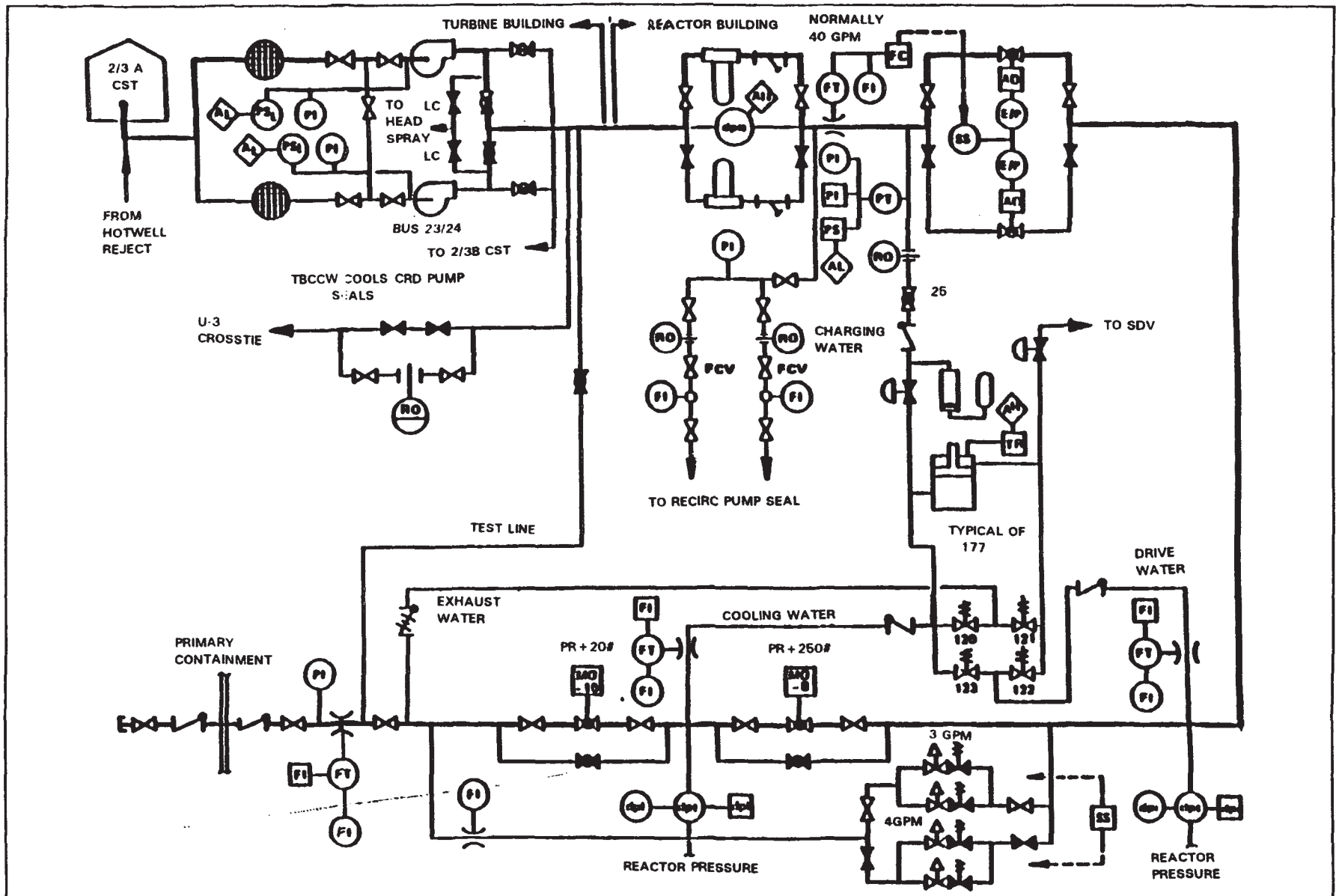

DRESDEN STATION
UNITS 2 & 3

CRD HYDAULIC SYSTEM (BASIC FLOWPATH)

FIGURE 4.6-6

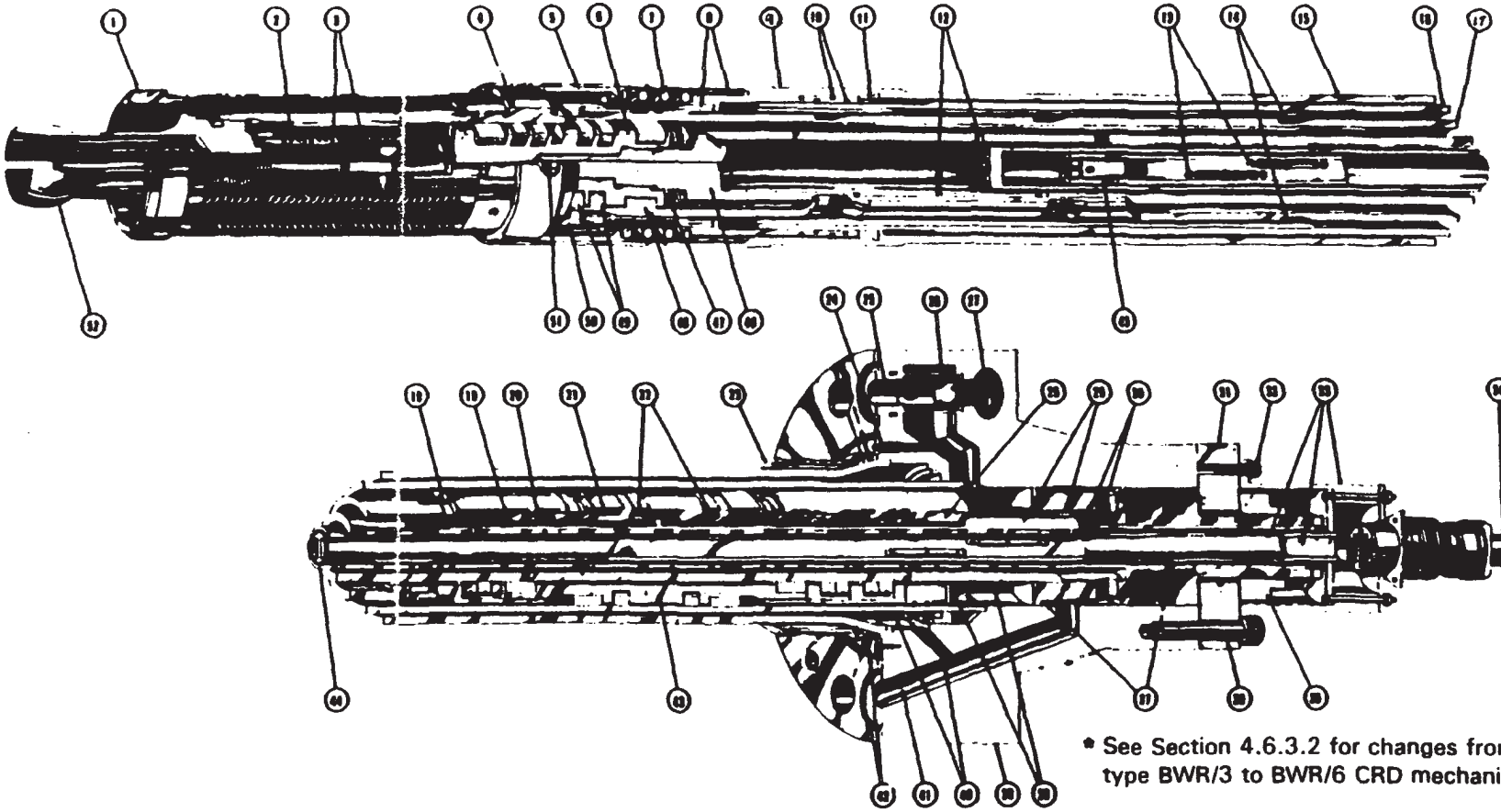

* See Section 4.6.3.2 for changes from type BWR/3 to BWR/6 CRD mechanisms.

1. EXTERNAL FILTER ASSEMBLY
2. INTERNAL FILTER ASSEMBLY
3. UNCOUPLING ROD ASSEMBLY
4. GUIDE CAP
5. BARREL
6. STOP PISTON
7. COLLET SPRING
8. COLLET AND COLLET PISTON
9. COLLET HOUSING (Part of cylinder, tube and flange)
10. COLLET PISTON SEALS
11. SPACER (Part of cylinder, tube, and flange)
12. BUFFER ORIFICES (Typical)
13. POSITION INDICATOR SWITCHES (Typical)
14. LOCKING GROOVE (Typical)
15. OUTER TUBE (Part of cylinder, tube, and flange)
16. CYLINDER TUBE
17. INDEX TUBE
18. LOCKING BAND (Typical)
19. INTERNAL PISTON SEAL RINGS (Typical)
20. INTERNAL PISTON BUSHINGS (Typical)
21. EXTERNAL PISTON BUSHINGS
22. EXTERNAL PISTON SEALS
23. STRAINER
24. COOLING WATER ORIFICE
25. DRIVE-INSERT WATER INLET (Normal and scram; drive-withdrawal outlet)
26. BALL-SHUTTLE VALVE
27. REACTOR WATER INLET (Through drive housing)
28. SWITCH-ACTUATING MAGNET (Part of drive piston)
29. PISTON TUBE ASSEMBLY
30. DRIVE-WITHDRAW PORTS AND ANNULUS (Also scram outlet)
31. RING FLANGE
32. MACHINE SCREW (Typical)
33. POSITION INDICATOR PROBE
34. POSITION INDICATOR CABLE
35. PISTON TUBE NUT
36. CAP SCREW (Typical)
37. O-RING SEALS
38. DRIVE-INSERT PORTS AND ANNULUS
39. DRIVE FLANGE (Part of cylinder, tube, and flange)
40. UNLOCKING PORT AND ANNULUS (Withdraw pressure to collet piston)
41. DRIVE-WITHDRAW WATER INLET (Also outlet for scram water)
42. METAL O-RING SEAL (Drive to housing)
43. DRIVE PISTON
44. INDICATOR TUBE (Part of piston tube)
45. THERMOCOUPLE (Part of position indicator probe)
46. STUD (Part of piston tube)
47. SPRING WASHERS
48. STOP PISTON BUSHINGS (Typical)
49. STOP PISTON SEAL RINGS (Typical)
50. COLLET FINGER (Typical)
51. COTTER PIN
52. COUPLING SPUD

DRESDEN STATION
UNITS 2 & 3

CONTROL ROD DRIVE - CUTAWAY

FIGURE 4.6-7

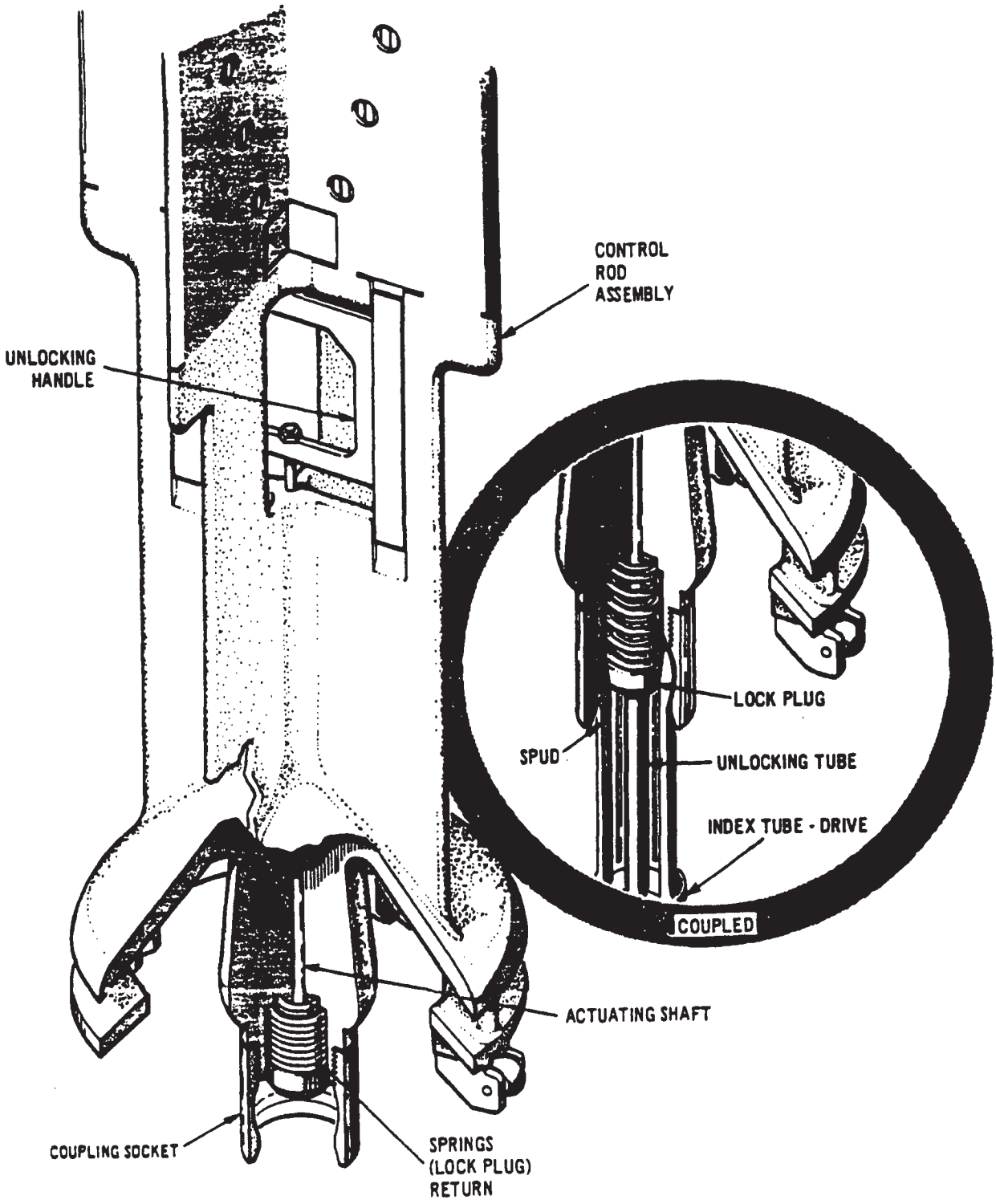

DRESDEN STATION UNITS 2 & 3
CONTROL ROD-TO-DRIVE COUPLING ISOMETRIC
FIGURE 4.6-8

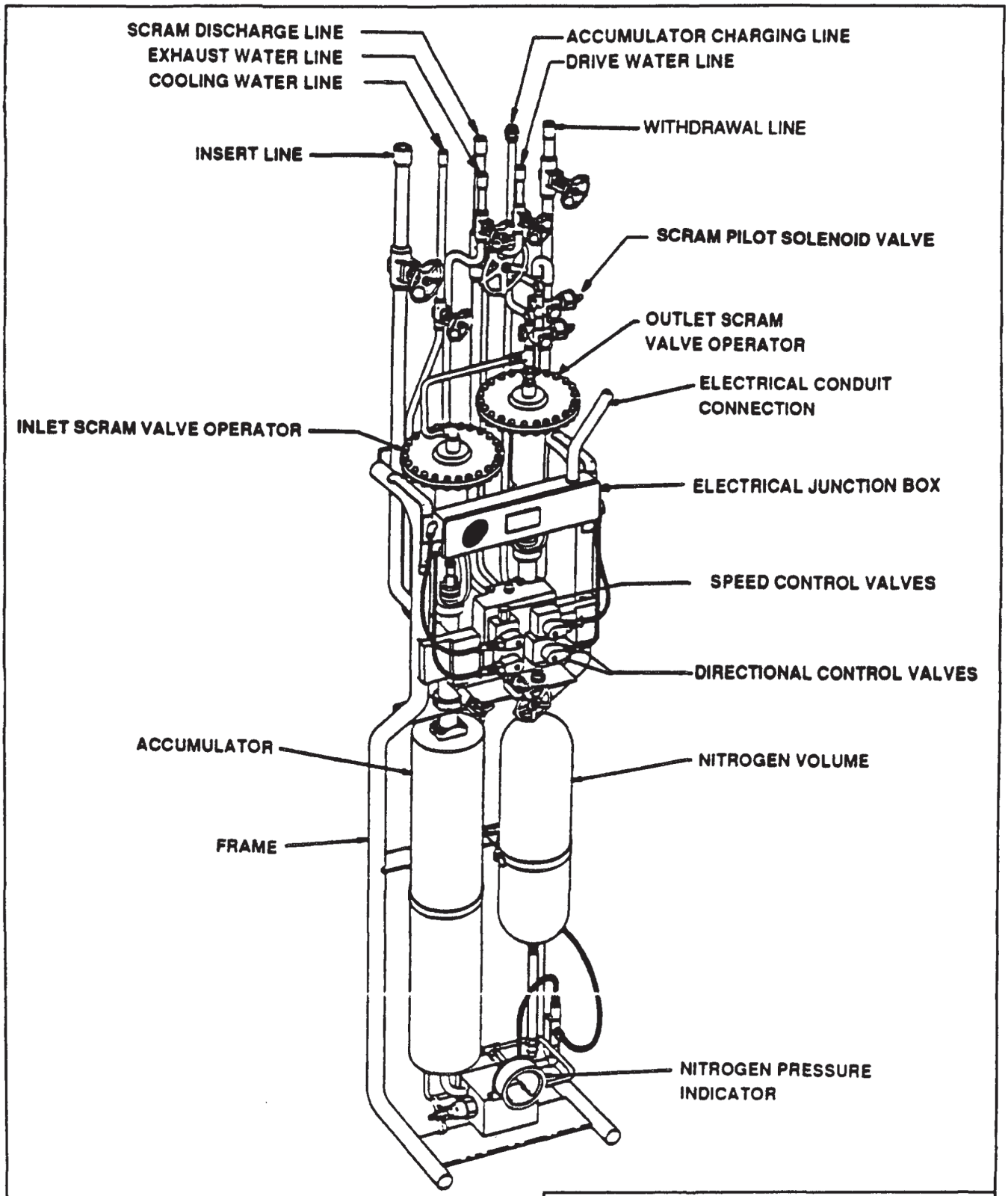

DRESDEN STATION UNITS 2 & 3
CONTROL ROD DRIVE HYDRAULIC CONTROL UNIT ISOMETRIC
FIGURE 4.6-9

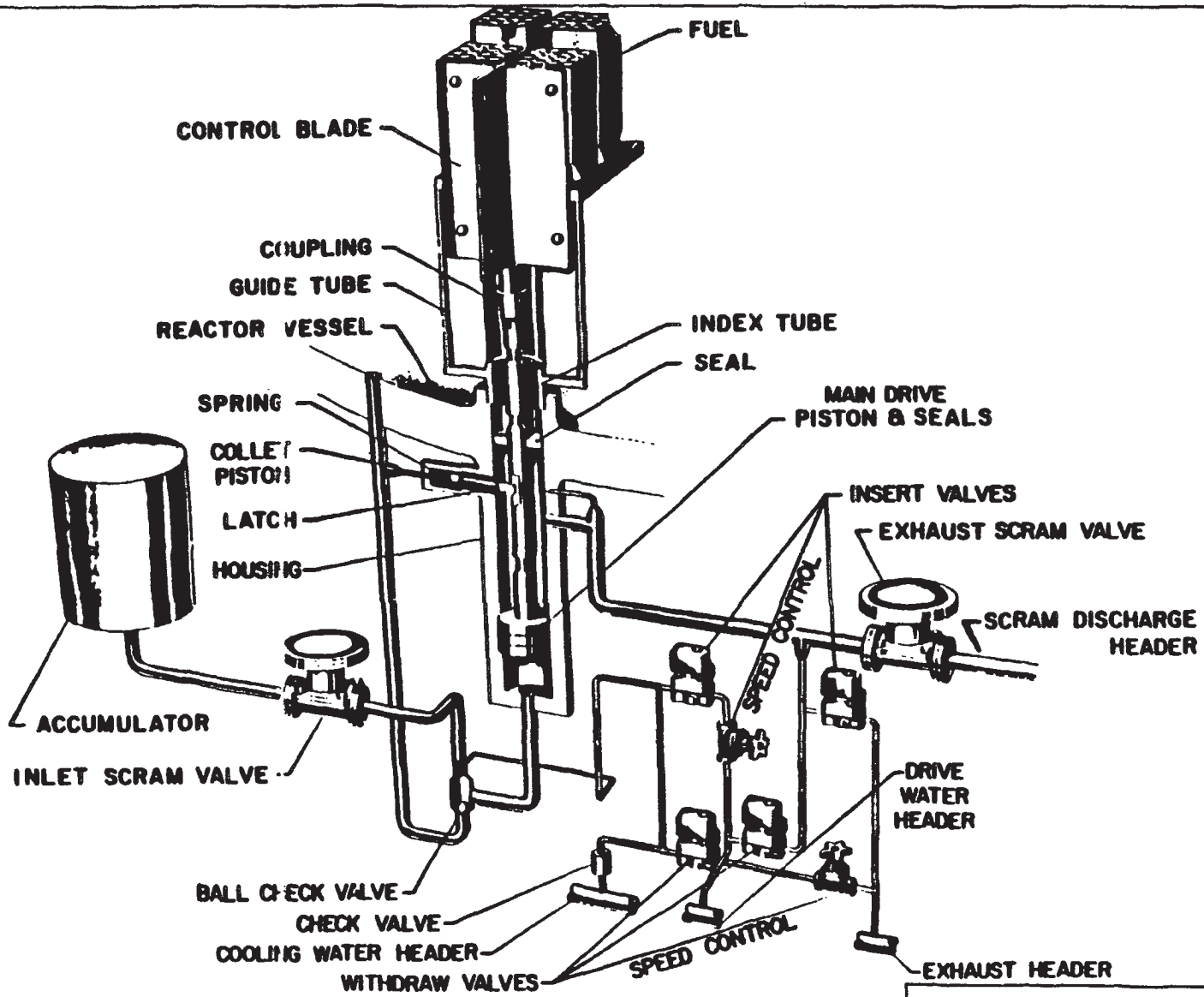

DRESDEN STATION
UNITS 2 & 3

CONTROL ROD DRIVE
HYDRAULIC CONTROL UNIT -
SIMPLIFIED COMPONENT ILLUSTRATION

FIGURE 4.6-10

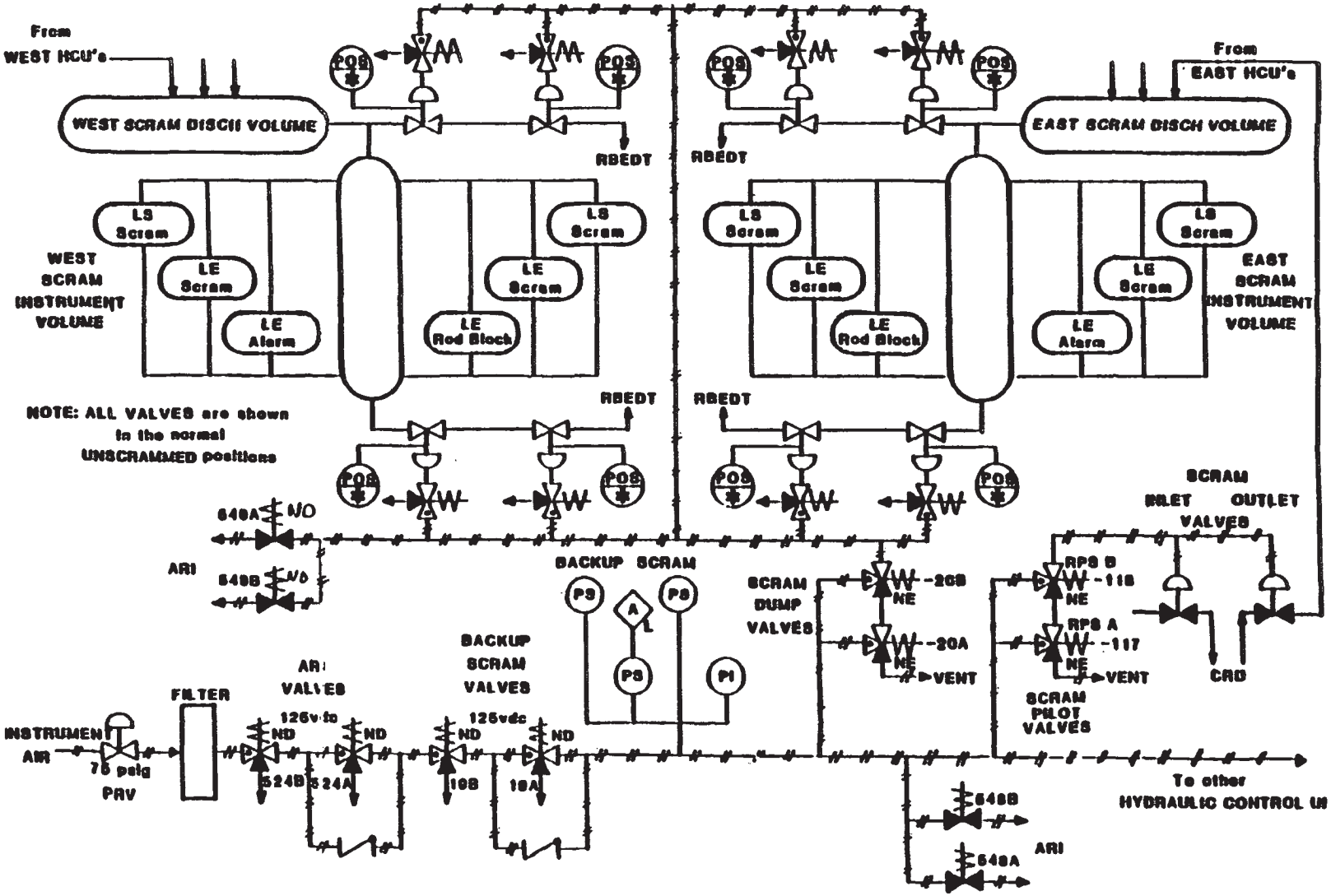

DRESDEN STATION UNITS 2 & 3
SCRAM DISCHARGE VOLUME (SDV)
FIGURE 4.6-11

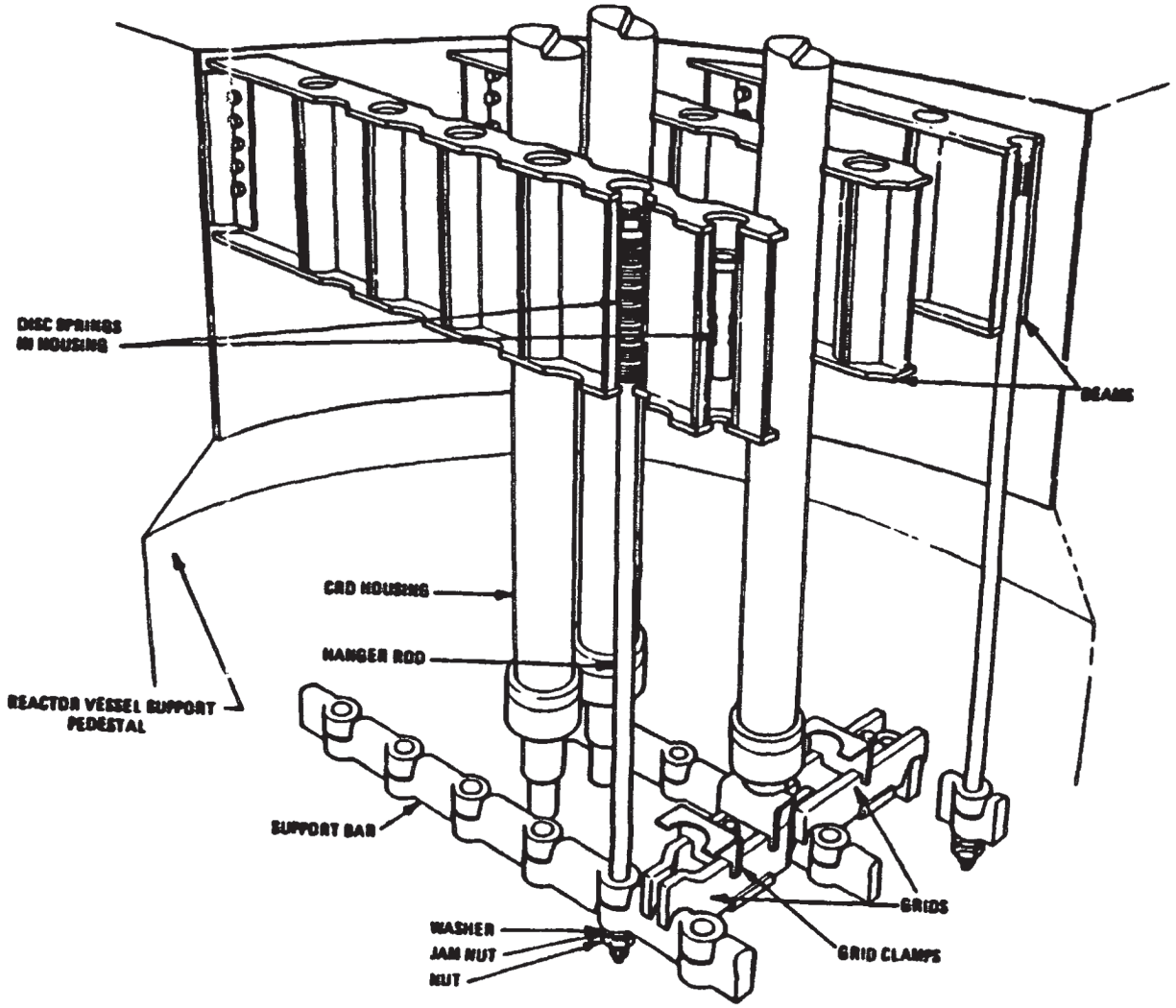

DRESDEN STATION
UNITS 2 & 3

CONTROL ROD HOUSING SUPPORT
ISOMETRIC

FIGURE 4.6-12

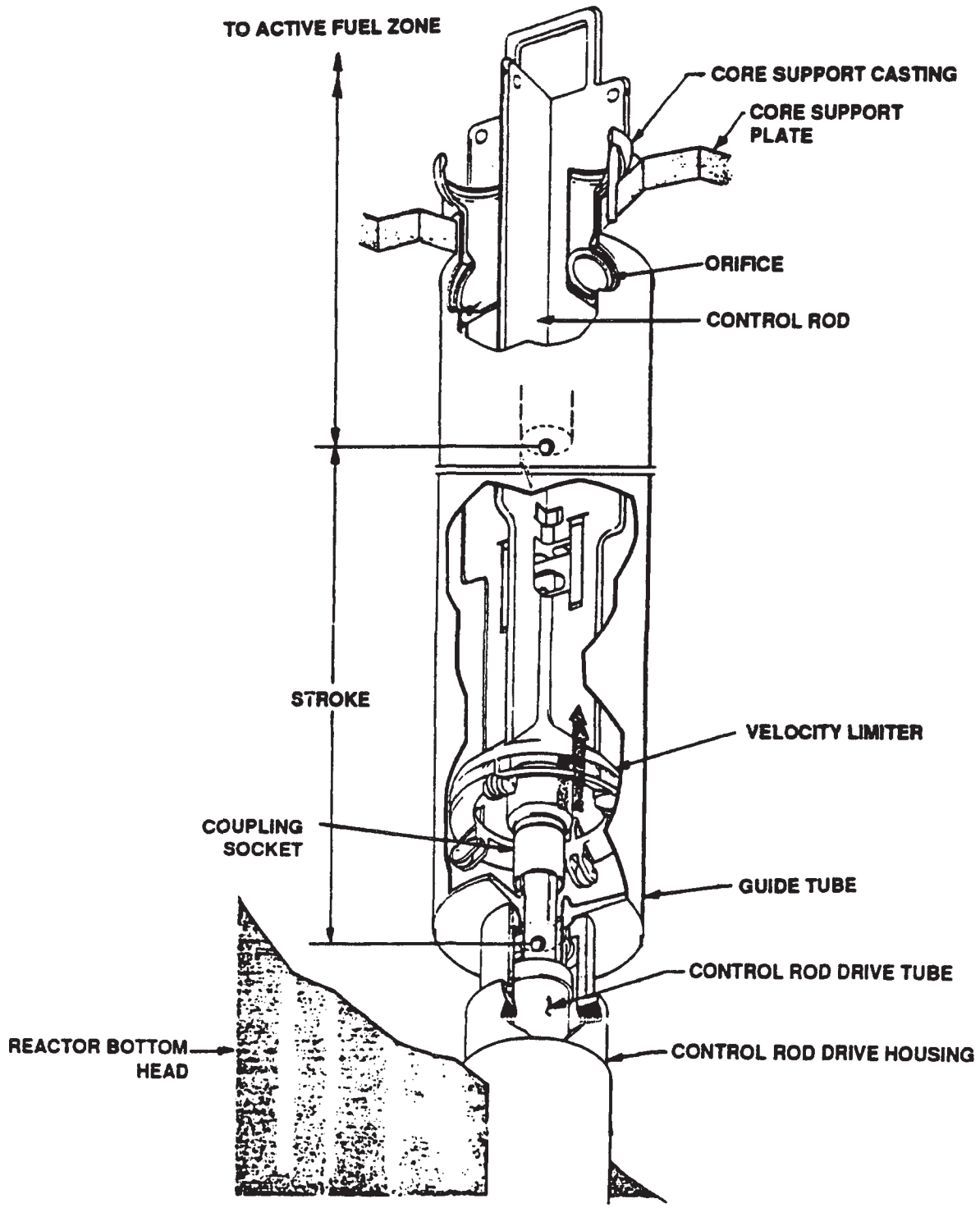

DRESDEN STATION
UNITS 2 & 3

CONTROL ROD VELOCITY LIMITER
ISOMETRIC

FIGURE 4.6-13